

The Messenger



No. 131 – March 2008

Testing adaptive optics for ALMA
The outburst of V1647 Orionis
FLAMES survey of massive stars
ESO users feedback campaign



Advanced Calibration Techniques for Astronomical Spectrographs

Paul Bristow¹
 Florian Kerber¹
 Michael R. Rosa^{2,3}

¹ ESO

² Space Telescope European
 Coordinating Facility, ESO

³ Affiliated to the Science Operations and
 Data Systems Division, Science Depart-
 ment, European Space Agency

ESO's Calibration and Model Support Group is involved in a variety of activities related to the calibration and physical description of instruments, with the objective of supporting the reduction of science data and facilitating operations. Here we describe the construction, optimisation and application to scientific data reduction of physical instrument models. Such models have been implemented for the HST STIS spectrograph and form an integral part of the data reduction pipelines for CRIRES and X-shooter. These models are supported by validated physical data of the instrumental components and calibration reference data.

The life cycle of an instrument can be described as follows:

1. Science Requirements
 2. Optical Design (Code V/Zemax)
 3. Engineering Expertise
-
4. Testing and Commissioning
 5. Operation and Data Flow
 6. Calibration of Instrument
 7. Scientific Data and Archive

Experience shows that it is difficult to ensure that the know-how and expertise that went into designing and building the instrument (steps 1–3) is brought to full use in the instrument calibration and scientific operations (steps 6 and 7).

A case in point is the wavelength calibration, in which well-understood physics is employed to design a spectrograph with an optimal format while during operations the dispersion solution is then derived over and over again in a purely empirical manner by, for example, fitting polynomials to a sparse calibration line spectrum.

One way to ensure that the engineering data propagates from instrument building to operations is to capture all the engineering information in a physical model-based description of the instrument.

This model accompanies the instrument throughout its life cycle and is used to drive the science data reduction pipeline. In our concept the model is combined with validated physical data of the instrumental components and calibration reference data.

Implementation and application of an instrument physical model

Our approach comprises an instrument-specific model kernel and associated software to optimise the model parameters and to apply the model's predictive power to the calibration of science data.

Model kernel

First of all a streamlined model of the dispersive optics, that enables a rapid evaluation of where any photon entering the instrument arrives on the detector array, is constructed. Though based upon the optical design, it is no substitute for the fully-fledged optical (e.g. Zemax/Code V) models developed by the designers.

Clearly this model kernel is specific to each instrument, but the following sub-components and associated parameters are typical:

- Entrance slit and collimator
 - Relative position and orientation of the slit
 - Focal length of collimator
- Pre-disperser (e.g. Prism)
 - Orientation of entrance surface
 - Orientation of exit surface
 - Temperature
 - Refractive index as a function of wavelength and temperature
- Main disperser (e.g. reflection grating)
 - Orientation
 - Grating constant
- Camera and detector array
 - Focal length of focusing optics
 - Orientation of detectors
 - Relative positions of detectors
 - Dimensions of pixel grid

We follow the prescription of Ballester and Rosa (1997) in constructing this model.

Most of the computations involve rotation matrices to represent the change of orientation of the optical ray at the surfaces of the components. For example, the matrix representation of the order m transformation performed by an echelle grating with constant σ_E at off-blaze angle θ , operates on a 4D vector with components (λ, x, y, z) representing a ray of wavelength λ . Here θ and σ_E are amongst the physical model parameters for this instrument.

Hence there is a complete set of parameters that describe the passage of a photon through the spectrograph. These parameters are physical quantities (angles, distances, temperatures, etc.) and describe the actual status of components. They can always be adjusted to match the observed behaviour of the instrument or to predict the effects of tilting/modifying a component. For example, adjusting the camera focal length will change the scale on the detector.

Optimisation

The model parameter set can be optimised to reflect the performance of the operational instrument with suitable calibration data, in a similar way that a polynomial dispersion solution would be fit. The difference is that the parameters optimised here have physical meaning and represent the actual configuration of the instrument. There are essentially two scenarios in which one needs to perform the optimisation.

Before the instrument is actually built, the only parameters available are those from the instrument design. Inevitably, once the instrument has been built, it will differ from the design predictions, so it is necessary to establish the true values. This may also be the case after a major maintenance intervention, upgrade to the instrument or even an earthquake, resulting in a physical change in the instrument. In this situation a comprehensive and uniform set of robustly identified calibration features from dedicated calibration exposures is required. The core model function is then iteratively called for the identified calibration wavelengths and the results of each iteration are compared with the centroids for these wave-

well as recovering the predictive power of the physical model for calibration applications, this process also gives us some insight into which parameters need to be modified in order to match the changing spectral format. In this case we found that the grating and associated focusing optics were the parameters responsible.

Calibration

The principal purpose of the physical modelling approach is to provide accurate wavelength calibration for spectroscopic science data. Once the physical model parameter set is optimised to match the instrument reality and, where necessary, fine tuned to match the actual operating conditions, it is trivial to recover the wavelength corresponding to each pixel in the 2D detector array or each bin in extracted 1D spectra. For CRIRES and X-shooter this is incorporated in the standard data reduction software (DRS) pipeline.

The application to the Space Telescope Imaging Spectrograph (STIS) provided encouraging verification of the validity of wavelength calibration using this technique. Many spectral features occur in adjacent spectral orders in cross-dispersed echelle spectrograms. An accurate dispersion solution should assign identical wavelengths to these features regardless of which spectral order they are measured from. Figure 3 is a histogram of the wavelength offset between wavelengths assigned to line positions on adjacent orders. The blue histogram is that found for the standard STIS data reduction software, *calstis*. Note that STIS is arguably one of the best empirically calibrated modern astronomical spectrographs. The red histogram is what we obtain with the physical model approach. The goodness of the latter dispersion solution is even more impressive if one recalls that it is a global solution across the entire 2D dispersion map, while the 2D polynomials of the canonical *calstis* pipeline are matched locally (per order).

The physical model can also be used to drive the extraction of 1D spectra from 2D data since it will predict the locus on the detector array of wavelengths entering

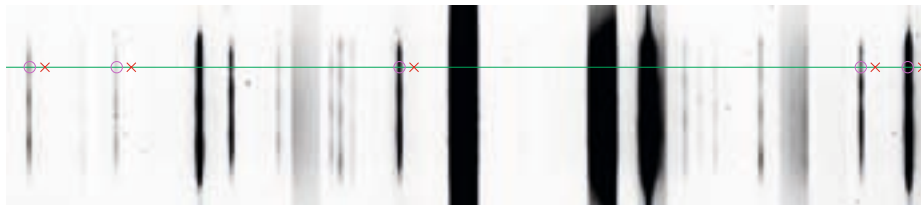


Figure 2: A CRRES full slit Th-Ar Hollow Cathode Lamp exposure used to discover the change in spectral format. The green line is the locus of a chosen entrance slit position on the detector array. Red crosses mark the predicted positions of isolated spectral features according to the baseline model parameter configuration. Purple circles mark the actual position of these features after a shift in spectral format.

at a given entrance slit position. A further possibility, which has not yet been fully exploited, is to use a physical model to fully map flux in the 2D detector pixel array plane back to the slit position/wavelength plane.

Simulation tools

Such an instrument model can also be used to simulate spectroscopic data. In addition to the geometric capabilities of the physical model, basic photometric simulation is also implemented. Blaze efficiency can be computed directly from the model parameter set, whilst other throughput issues such as quantum efficiency, dichroic transmission, etc. are incorporated through reference data for the materials used.

In order to produce a simulated 2D exposure of a given spectrum, the model kernel is then called iteratively for photons in the given spectral energy distribution with a realistic distribution on the entrance slit. If so required, one can generate a stochastic and probabilistic observational result model. The pixel that would be illuminated on the detector array is recorded, and a 2D array describing where the flux arrives on the detector is built up. Before the instrument is even built we are able to provide simulated 2D data (flat fields, arc lamp exposures or astronomical objects) that can be used in the development of the data reduction software or can be used as an aid when aligning the instrument in the laboratory (e.g. Vernet et al. 2007).

Figure 4a shows a section of a Th-Ar hollow cathode lamp X-shooter VIS exposure made using a nine-pinhole mask, while 4b shows the equivalent section from a model based simulation. Figure 5 shows a 2D simulation of an observation of the Orion nebula on the UVB and VIS detectors of X-shooter.

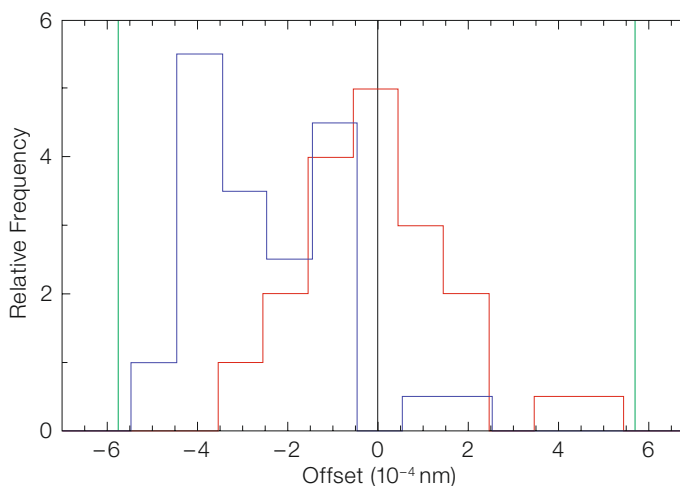


Figure 3: Histograms of the discrepancy in the wavelength assigned to features appearing in adjacent orders in STIS E140H exposures by the standard STIS DRS (blue) or the physical model derived dispersion solution (red). The green bars indicate the size of one STIS pixel.

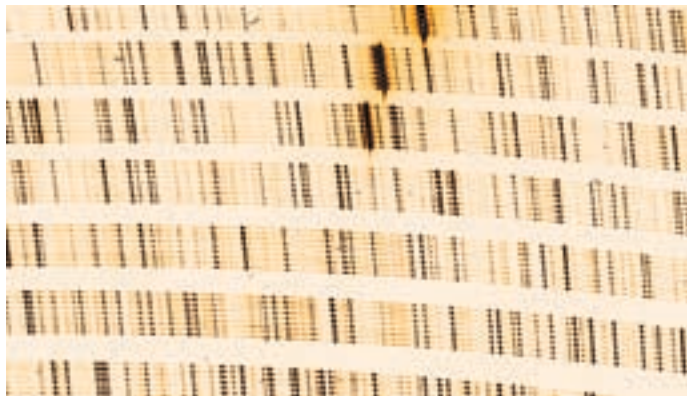
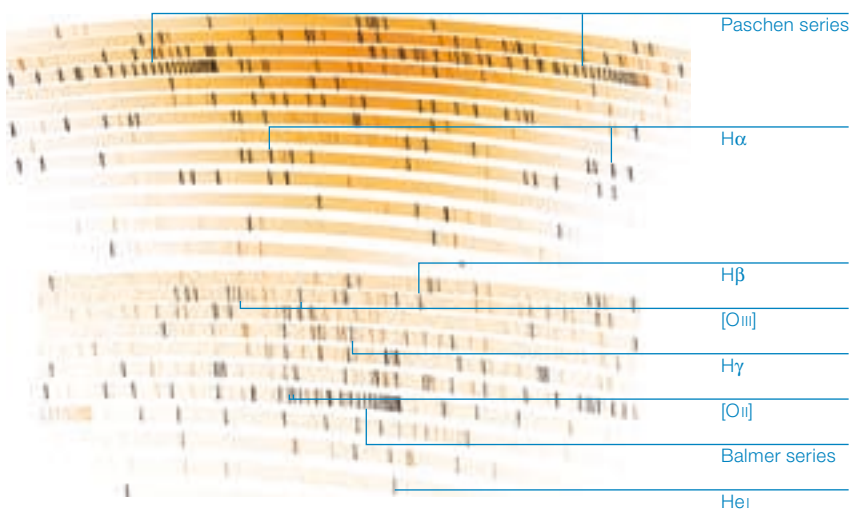


Figure 4 (above): Left: Section of an X-shooter VIS 180 s exposure of a Th-Ar HCL through a nine-pin-hole mask obtained in the laboratory. Right: Physical model based simulation of the above left image.

Figure 5 (left): Simulated 2D echellogram exposures with the X-shooter UVB arm (below) and VIS arm (above) of the Orion nebula. Some familiar emission lines are indicated.



of wavelength calibration for CRIRES up to 2 500 nm (Kerber et al. 2008). For longer wavelengths, gas cells (N₂O and OCS) are being established as calibration sources by using NIST reference data and laboratory measurements with ESO's Fourier Transform Spectrometer to characterise the gas cells as a function of fill gas pressure and temperature.

With these developments wavelength calibration in the near-IR will become very similar to the UV-visible region, and it is possible to support high accuracy absolute wavelength calibration without having to rely on atmospheric features. In an earlier very similar effort, a multitude of additional lines were measured in the spectrum of Pt/Cr-Ne lamps as used onboard STIS (Sansonetti et al. 2004). The STIS Calibration Enhancement effort using a physical model in combination with these data was recognised by a NASA Group achievement award in 2006 (see The Messenger 126, page 54). For future E-ELT instruments the group has already started a project to study various elements spectroscopically in order to identify the best near-IR calibration sources as a function of spectral resolution. Similarly, improved spectro-photometric standard stars for the near-IR are being established for use with X-shooter (Vernet et al. 2008) and future IR spectrographs.

Calibration Reference Data and Model Support

The Calibration and Modelling Support Group performs several activities that are aimed at obtaining data that will ensure optimum calibration of the science instruments at ESO.

Properties of physical materials

A realistic description of an instrument requires data describing the physical properties of critical components. For example, in CRIRES a ZnSe prism is used as a pre-disperser making it essential to quantitatively know the properties of ZnSe at CRIRES' cryogenic operating temperature. Since no such data were available in the literature, new laboratory measurements, taken at NASA's CHARMS facility (Kerber et al. 2006), were included in the model. The validity of the model in this respect was verified by comparing

it with data taken during a temperature ramp during testing.

Wavelength standards

Like any other approach to wavelength calibration, the use of instrument physical models requires high quality reference data traceable to laboratory standards, such as the wavelength standards emitted by calibration lamps. For CRIRES, ESO, in collaboration with the the Space Telescope European Co-ordinating Facility (ST-ECF) and the US National Institute of Standards and Technology (NIST), embarked on a project to establish Th-Ar wavelength standards in the 950–5 000 nm operating range of CRIRES. Through dedicated laboratory measurements at NIST, a catalogue of about 2 400 lines between 750 and 4 800 nm with highly accurate wavelengths (accuracy 0.001 cm⁻¹ for strong lines) was obtained. This now forms the backbone

Optimising calibration systems

The combination of laboratory measurements with a physical instrument model is a very powerful tool for assessing the predicted performance of an instrument or its calibration subsystem. For the selection of the best-suited wavelength calibration sources for the near-IR arm of X-shooter, we did an in-depth analysis (Kerber et al. 2007). As a result we have been able to identify a combination of the noble gases Ne, Ar and Kr as the best three-lamp combination. Our analysis provides a quantitative order-by-order prediction about the number of lines available from a given source, their relative intensities – including the effect of the blaze function – and an estimate of the line blending between sources.

We have recently extended this concept to develop a technique to customise calibration source line catalogues according to the instrument, mode and operating conditions. By creating a 2D simulation with a given set of physical model parameters, and extracting a 1D spectrum from the simulation, one obtains a realistic flux distribution for the spectral features to which, if desired, a noise level appropriate to the exposure time of calibration observations can be added. This spectrum will include potential blending from neighbouring features and, for some spectrographs, order overlap, an effect that would normally be difficult to evaluate. By measuring centroids in the simulated data and comparing to the known centroids we can determine which features will potentially be blended or poorly resolved and thus not useful for auto-

mated wavelength calibration. In the event of a major change in spectral format (intervention, earthquake, etc.), this procedure enables us to identify calibration features that will always be isolated within a window of a size that reflects the uncertainty, hence reducing the chance of false matches.

Summary and outlook

We have developed streamlined physical models for a variety of astronomical spectrographs that are characterised by a model kernel with an associated set of parameters; each parameter has a clear physical meaning. In addition we have implemented the tools necessary to optimise the parameter sets to match the actual configuration of the real instruments using dedicated calibration observations.

Once optimised, the physical model drives the wavelength calibration inside the data reduction pipeline. This is already an option for CRIFRES and is being realised for X-shooter. We have also produced a suite of software to simulate 1D and 2D spectroscopic data using such models. These simulations aid the initial alignment of the instrument in the laboratory, the development of the DRS and, potentially, the planning of observations.

Calibration reference data traceable to laboratory standards provide the ground truth needed for quantitative calibration. A combination of the modelling techniques and calibration reference data can

be used to optimise instrument performance throughout all phases of the life cycle of an instrument: design, manufacture, testing and operations.

Key to success and to achieving the best science product is an integrated approach that combines the development of physical instrument models, application of and feedback from these models during instrument integration, testing, commissioning and science verification and their integration in the data reduction software.

Second-generation VLT instruments and E-ELT instruments clearly stand to benefit from this approach.

Acknowledgements

We would like to thank our CRIFRES and X-shooter project colleagues for their support and co-operation and Gillian Nave and Craig Sansonetti at NIST for fruitful collaboration. Special thanks also to Yves Jung for his sterling effort (and patience) interfacing the physical model code with the CRIFRES DRS.

References

- Ballester P. and Rosa M. R. 1997, *A&A Supp.* 563, 126
- Carter E. 2001, <http://www.taygeta.com/annealing/simanneal.html>
- Kerber F. et al. 2006, *SPIE* 6269, 42
- Kerber F., Saitta F. and Bristow P. 2007, *The Messenger* 129, 21
- Kerber F. et al. 2008, *ApJ Supp.*, submitted
- Sansonetti C. J. et al. 2004, *ApJS* 153, 555
- Vernet J. et al. 2007, *The Messenger* 130, 5
- Vernet J. et al. 2008, in "2007 ESO Instrument Calibration Workshop, Proceedings of the ESO Workshop held in Garching, Germany, 23–26 January 2007", eds. A. Kaufer and F. Kerber, Springer



Photo: H. H. Heyer, ESO

VISTA's 67-Mpixel near-infrared camera (black and silver) is shown in the Instrument Preparation Room at VISTA on its blue handling carrier. An auto-guider test source is fitted across the camera window. Primary Mirror polishing is close to completion and first light is expected later this year. See <http://www.vista.ac.uk/> for more details.

Laser Guide Star Adaptive Optics without Tip-tilt

Richard Davies¹
 Sebastian Rabien¹
 Chris Lidman²
 Miska Le Louarn²
 Markus Kasper²
 Natascha M. Förster Schreiber¹
 Veronica Roccatagliata³
 Nancy Ageorges¹
 Paola Amico²
 Christoph Dumas²
 Filippo Mannucci⁴

¹ Max-Planck-Institut für Extraterrestrische Physik, Garching, Germany

² ESO

³ Max-Planck-Institut für Astronomie, Heidelberg, Germany

⁴ INAF-Istituto di Radioastronomia, Firenze, Italy

Adaptive optics (AO) systems allow a telescope to reach its diffraction limit at near-infrared wavelengths, but a bright natural guide star (NGS) is needed for the wavefront sensing, severely limiting the fraction of the sky over which AO can be used. To some extent this can be overcome with a laser guide star (LGS). While the laser can be pointed anywhere in the sky, one still needs to have a natural star, albeit fainter, reasonably close to correct the image motion (tip-tilt) to which laser guide stars are insensitive. There are in fact many astronomical targets without suitable tip-tilt stars, but for which the enhanced resolution obtained with the Laser Guide Star Facility (LGSF) would still be very beneficial. This article explores what adaptive optics performance one might expect if one dispenses with the tip-tilt star, and in what situations this mode of observing might be needed.

To find a star, or not

The constraints for adaptive optics with a natural guide star mean that very few astronomical targets are suited to this technique: to get the best performance it has to be brighter than $V \sim 13$ mag and within $15\text{--}20''$. With a laser guide star these restrictions are very much relaxed; but even with an LGS, one still needs to find a natural guide star for the tip-tilt correction. At the VLT this tip-tilt star must

be brighter than $V \sim 17$ mag within about $60''$. While this vastly increases the number of targets to which adaptive optics can be applied, there are still important cases that slip through the net. Perhaps the most obvious of these are the so-called “deep fields” (such as the GOODS-CDFS) which are currently extensively surveyed at all accessible wavelengths to study galaxy formation and evolution out to very high redshift. But galaxies at high redshift are typically 1 arcsec or less across, so such work would benefit enormously from adaptive optics techniques that enable the galaxies to be resolved. Yet these fields are barely accessible to AO because one of their prime selection criteria is to contain as few bright stars as possible to avoid saturation in long exposures. Even when survey fields sometimes do inevitably include bright stars (e.g. VVDS), galaxies near these stars are rarely selected for follow-up spectroscopy, hampering the use of AO. For deep fields, and in many other cases, it would be a significant gain if LGS-AO without a tip-tilt star allowed one to achieve a resolution better than the seeing limit.

A quantitative example of the advantage – in terms of number of sources accessible – has been given by Mannucci (2007). He selected sources from the survey of about 1000 Lyman Break Galaxies, based on whether there is a nearby star and if the source is at a redshift conducive to near-infrared observations. The result he finds is that none of the galaxies can be observed profitably with NGS-AO, and only about 10 with LGS-AO. But by dispensing with the tip-tilt star, one can find nearly 50 suitable targets.

This increase in number of sources available is actually the same effect that can be seen in figures of the sky coverage as a function of Strehl ratio for NGS- and LGS-AO, which have been published in numerous places. Such figures demonstrate first that sky coverage with LGS-AO is much higher than with NGS-AO. But they also show that the sky coverage increases as the acceptable/achievable Strehl decreases. Fortunately, for LGS-AO, a low Strehl is not necessarily bad. The reason is that the flux in the core of the PSF (which depends on the high-order correction from the LGS) is independent of the tip-tilt star. Instead,

the low Strehl is due to a slight broadening of the PSF core, although its FWHM remains much better than the seeing limit. The cause is the residual image motion (tip-tilt jitter) from the natural tip-tilt star which may be faint and far off-axis. Using a tip-tilt star that is faint and/or far off-axis is nearly the same as not using one at all. The big advantage of dispensing with tip-tilt completely is, of course, that one has fully 100% sky coverage.

Performance simulations and measurements

Based on estimates of atmospheric tip-tilt (direction of arrival statistics) in typical conditions, one might expect image motion – and hence the resultant resolution – to be of order $0.4''$ independent of wavelength. However, simulations suggest one should do rather better than this. The simulations presented here have been set up specifically for the 7×7 lenslet array of NAOS on the VLT, assuming $0.8''$ seeing (at 500 nm). The noise level was adjusted so that with full LGS-AO and perfect tip-tilt correction, one achieves about 35% Strehl in the K -band and a FWHM of about 70 mas. This corresponds well to the better measurements made with NACO (Kasper et al. 2007). As expected, one then finds that as the number of photons available for tip-tilt correction decreases, so does the predicted Strehl ratio. In the limit of no photons (i.e. no tip-tilt correction), the Strehl is about 11%, corresponding to a FWHM of about 120 mas. In both cases, these values correspond well to measurements that have actually been made with NACO (Figure 1). If one considers encircled energy, then the price to pay for dispensing with tip-tilt appears very affordable. The simulations indicate that both with and without tip-tilt, 50% of the flux – twice that for the seeing limited case – remains within a $0.3'' \times 0.3''$ aperture (Figure 2).

In fact this is not the full story. The simulations do not include wind shake and other vibrational effects that are responsible for a significant amount of jitter, and which might strongly limit the resolution on these scales. Without a tip-tilt star these will not be corrected. However, the stabilisation provided by the actuation of

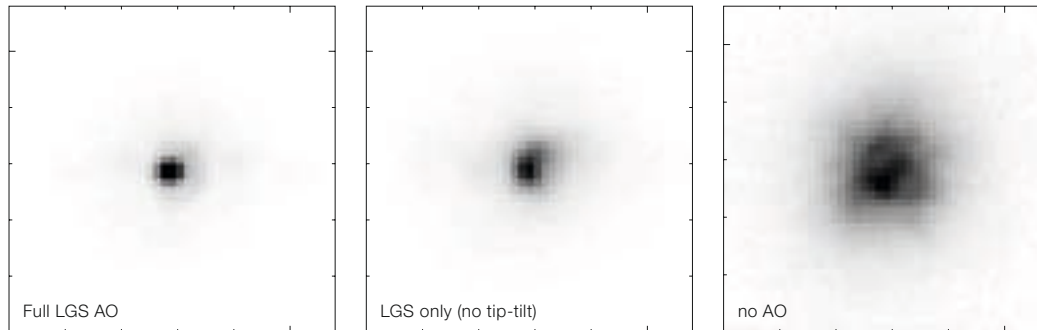


Figure 1: NAOS performance measured on CONICA in the *K*-band for full LGS-AO (left), and without tip-tilt (centre). The seeing limited PSF (right) is shown for reference. With full LGS-AO, the Strehl ratio was 22 % and the FWHM ~ 85 mas. Without tip-tilt, the Strehl ratio was reduced to 10 % and the FWHM increased to 130 mas. For comparison, the *K*-band FWHM without AO is 300 mas.

the secondary mirror of the VLT, which can run with a measurement frequency of up to 30 Hz, acts as a 'hidden' tip-tilt correction which is going on all the time. As such it takes care of most of these effects without limiting the sky coverage and allows one to reach resolutions that are better than otherwise expected, and close to the predictions above.

Astronomical applications

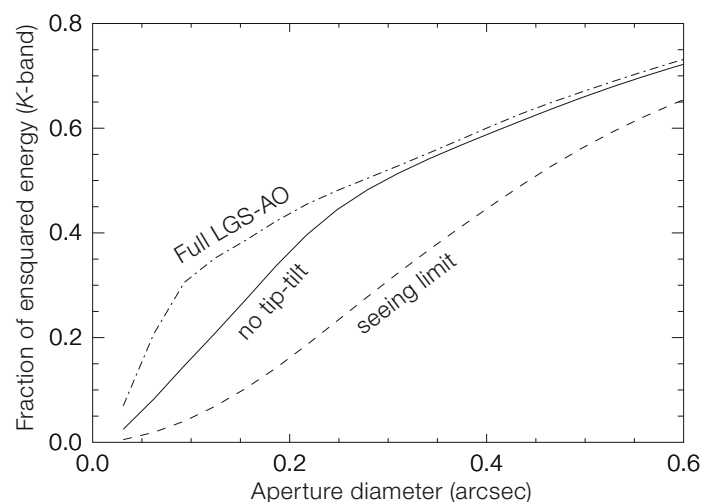
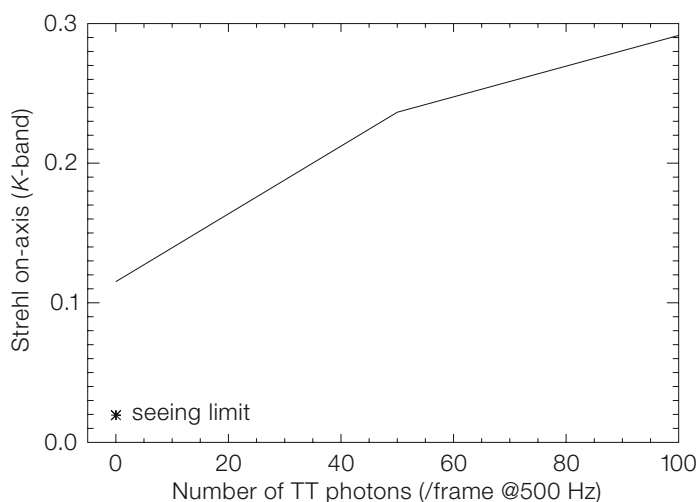
There are two adaptive optics instruments on UT4 which are able to make use of the Laser Guide Star Facility. The near-infrared integral field spectrometer SINFONI, and the imaging spectrometer NACO. This section describes observations made with both of these instruments, that demonstrate a few science cases where the seeing enhancement afforded by LGS-AO without tip-tilt is beneficial, and outlines some of the reasons why one might want to consider using it.

One object was already observed using this mode accidentally during the early phases of commissioning, when the tip-tilt loop failed to close but the integration continued (a feature which was quickly corrected). It was the ultraluminous infrared galaxy IRAS 11095-0238 (Figure 3), which was easily resolved into two close nuclei separated by only $0.53''$. This corresponds to 1.8 kpc at the galaxy's redshift of $z = 0.107$, indicating that these two nuclei are in the final stages of merging. Earlier optical observations with HST (Bushouse et al. 2002) had also resolved the two bright spots, but it was not clear whether it was instead a single nucleus crossed by a dust lane. These NACO *K*-band adaptive optics data rule out that possibility.

A young star cluster in NGC 1313 was also observed during LGS commissioning. NGC 1313 is an unusual isolated galaxy which nevertheless appears to have undergone an interaction. Furthermore, the gas – and hence star formation – is in

the outer parts rather than the nucleus (see ESO Press Release 43/06 and The Messenger 129). One of the star clusters in the north of the galaxy is actively forming stars, and contains in excess of 20 very massive young Wolf-Rayet stars (Crowther and Hadfield 2007). This cluster was observed in the *K*-band with NACO and LGS-AO, using a tip-tilt star $50''$ away. The data reveals numerous individual stars, but the PSF is rather large, $0.3''$ FWHM, and also appears slightly elongated in the direction of the tip-tilt star (Figure 4). If this is due to the effects of tip-tilt anisoplanatism, then the observations might actually have better been done without tip-tilt.

Figure 2: Simulated performance for LGS-AO with and without tip-tilt. **Left:** Predicted *K*-band Strehl as a function of the number of tip-tilt photons, tending towards 35 % for full LGS-AO and 11 % with no tip-tilt. **Right:** The ensquared energy as a function of aperture size shows that tip-tilt has no impact on the flux measured in a box of size $0.3''$ or more, and that this flux is still significantly higher than for the seeing-limited case.



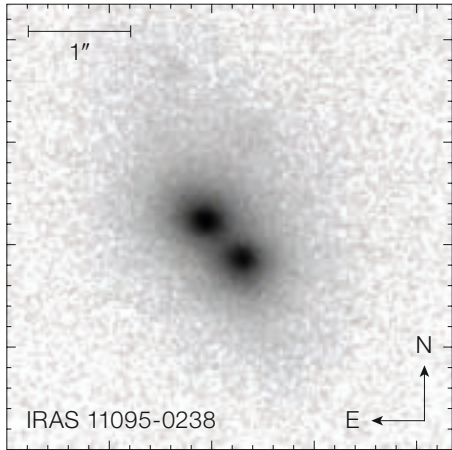


Figure 3: *K*-band image of the ULIRG IRAS 11095-0238 taken using LGS-AO without tip-tilt during LGSF commissioning. The two progenitor nuclei are clearly resolved to have a separation of 0.53".

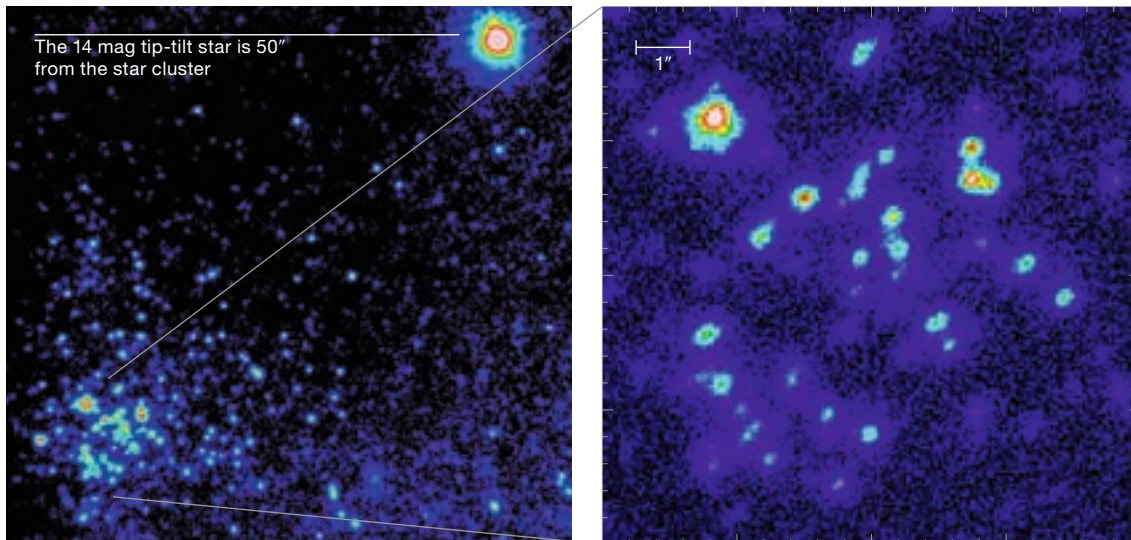
Arp 220 is a prototypical merger system in which the progenitor nuclei are separated by only 0.9" (400 pc), and hence are in the final stages of coalescing (see ESO Press Release 27/07). This is a very difficult target for adaptive optics because there are no compact sources from which the tip-tilt can be measured; even the optical light from the galaxy itself is extremely diffuse (in stark contrast to the infrared light). Thus the LGS-AO observations are in effect performed without tip-tilt. Nevertheless the resolution achieved is comparable to that from HST at the same wavelength (Figure 5), about 0.15–0.20". However, the SINFONI data are much richer due to the spectroscopic informa-

tion, and are able to measure the very different kinematics and morphologies of the stars and gas (Davies et al. in prep.).

Although one might expect it to be easy to find tip-tilt stars for Galactic targets, there are on the contrary many such sources where this is not possible. One very clear example is the Butterfly star system, which consists of an edge-on circumstellar disc around a young low-mass T-Tauri star. Scattered light images from the Hubble Space Telescope have shown that the width of the dust lane (i.e. the apparent vertical extension of the disc) decreases dramatically at longer wavelengths (Wolf et al. 2003). This wavelength dependence allows one to investigate the vertical structure of the disc as well as the dust grain properties. At longer wavelengths, the reduction in dust opacity makes it possible to probe deeper layers of the disc. As a result, combining *J*-band to *M*-band data enables one to constrain the grain growth processes and the settling of dust grains towards the mid-plane of the circumstellar disc, which are key processes in the early stages of planet formation. The optically brightest star within 60" of the Butterfly Star has $R \sim 19.3$; and the nearest star bright enough for tip-tilt with $R \sim 14.8$ is 90" away. Hence one has to use LGS-AO without tip-tilt. However, for *L*- and *M*-band observations, individual integrations are rather short and so one can recover at least some of the lost resolution by performing a shift-and-add combination afterwards (Roccatagliata et al. in prep.).

The final example we give here for LGS-AO without tip-tilt is that for high-redshift galaxies, detailed observations of which are a key to understanding galaxy formation and evolution. For such applications, diffraction-limited observations are impracticable because of the faintness of distant galaxies. However, the gain of enhanced resolution that can be provided by LGS-AO without tip-tilt is very substantial given the typical angular sizes of high-redshift galaxies of $\sim 1''$ or smaller. The two $z \sim 2$ star-forming galaxies shown in Figure 6 were observed as part of the 'SINS' survey (Förster Schreiber et al. 2006a, 2006b, and in prep.), and were selected from the wide-area imaging survey of the 'Deep3a' field (Kong et al. 2006). BzK-15504 was observed with both SINFONI using NGS-AO to map the $H\alpha$ line emission (Genzel et al. 2006, ESO Press Release 31/06) and also with NACO using full LGS-AO to measure the stellar continuum. The emission is extremely faint: BzK-15504 has a *K*-band magnitude of 19.2 integrated over about 1". Thus, in terms of sensitivity requirements at the diffraction limit, detecting it is comparable to detecting a point source with $K > 25$. As a result, despite two hours integration with NACO using the largest (54 mas) pixel scale, the data still

Figure 4: NACO *K*-band image of a star cluster in NGC 1313 taken with full LGS-AO during LGSF commissioning. **Left:** The full image shows the star cluster (lower left) 50" from the bright tip-tilt star (top right). **Right:** A close-up of the star cluster reveals that the PSFs have a FWHM of about 0.3" and are elongated towards the tip-tilt star.



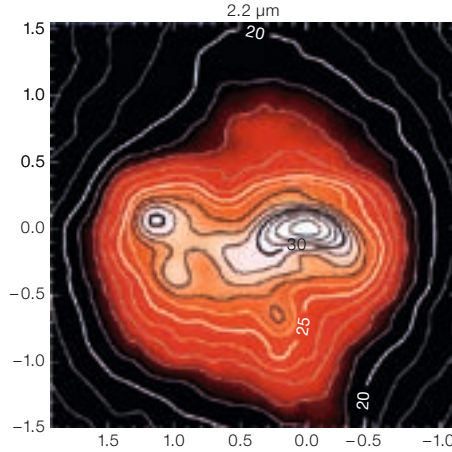
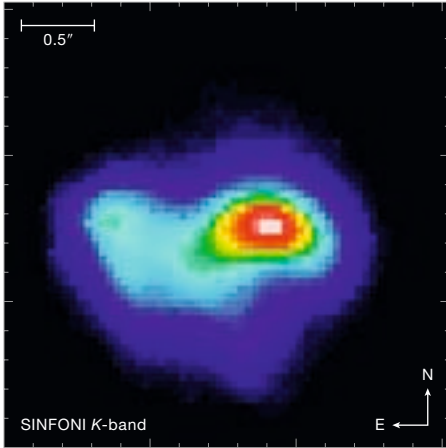


Figure 5: $3'' \times 3''$ K -band images of the prototypical merger galaxy Arp 220. **Left:** SINFONI with LGS-AO but effectively no tip-tilt (Davies et al. in prep). **Right:** HST NICMOS (from Scoville et al. 2000). Both images show the same level of detail (resolution 0.15–0.2''), but the SINFONI data set is much richer due to the spectroscopic information.

had to be smoothed to 0.2'' in order to reach sufficient signal-to-noise – as was done for similar reasons to the data from the six-hour integration on SINFONI using the intermediate (100-mas) pixel scale. The effective resolution of 0.2'', which can be achieved without tip-tilt, is nevertheless of extreme scientific value, corresponding to a physical scale as small as 1.6 kpc at the redshift of BzK-15504. For the SINFONI observations of the $H\alpha$ -line emission of BzK-6004 (Shapiro et al. 2008, Genzel et al. in prep.), the largest pixel scale was used to maximise the observing efficiency and signal-to-noise. This gives an 8'' field of view within which it is possible to dither, and so no additional sky frames are needed. In this case, the spatial resolution is then limited by the pixel scale rather than by the lack of a suitable tip-tilt star. Hence LGS-AO is used simply to enhance the resolution to 0.4'' rather than reach the diffraction limit. Thus, the lack of a tip-tilt star had no direct impact on the observations.

Prospects for future observations

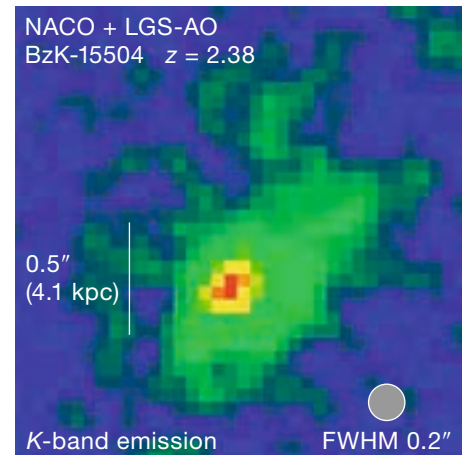
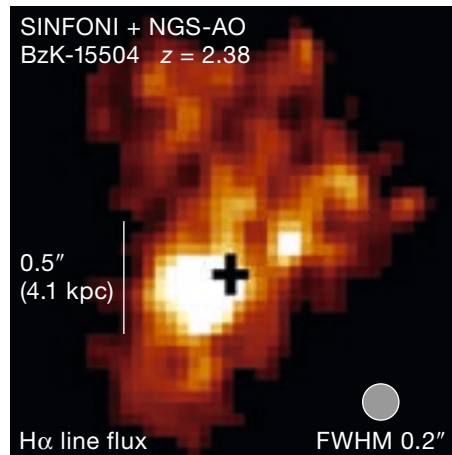
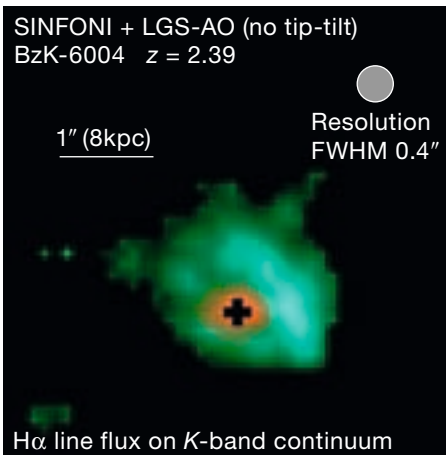
There are many astronomical instances where there are no suitable tip-tilt stars for laser guide star adaptive optics, but for which improved spatial resolution can bring immense benefits to the scientific analysis. Simulations and observations have shown that LGS-AO without tip-tilt stars does work on the VLT, and that the typical K -band resolution that can be achieved in good conditions appears to be around 0.2'' with 100% sky coverage. At the time of writing, ESO's adaptive optics team is hoping to obtain additional technical data to evaluate this seeing enhancement mode further. In closing, we are glad to report that this mode, although not yet fully commissioned, has been implemented on SINFONI; and that there are plans to implement it also on NACO. Although the LGS can only be used in good seeing conditions – which inevitably limits the time it can be available – it is likely that LGS-AO without tip-

tilt may soon become available to the community.

References

Bushouse H. et al. 2002, ApJS 138, 1
 Crowther P. and Hadfield L. 2007, The Messenger 129, 53
 Förster Schreiber N. M. et al. 2006a, ApJ 645, 1062
 Förster Schreiber N. M. et al. 2006b, The Messenger 125, 11
 Genzel R. et al. 2006, Nature 442, 786
 Kasper M. et al. 2007, NACO LGS commissioning report, VLT-TRE-ESO-11650-4255
 Kong X. et al. 2006, ApJ 638, 72
 Mannucci F. 2007, "Astronomy with Laser Guide Star Adaptive Optics", http://www.mpia-hd.mpg.de/PARSEC/Ring2007/TalksPostersPDF/Tuesday/Highz_FilippoMannucci.pdf
 Scoville N. et al. 2000, AJ 119, 991
 Shapiro K. et al. 2008, ApJ, accepted
 Wolf S. et al. 2003, ApJ 588, 373

Figure 6: High-redshift ($z = 2.4$) galaxies observed with SINFONI and NACO. **Left panel:** BzK-6004 (Shapiro et al. 2008; Genzel et al. in prep) has no tip-tilt star; LGS-AO was used with the large pixel scale to enhance the resolution while still allowing dithering within the field to maintain observing efficiency. **Centre and right panels:** BzK-15504 (Genzel et al. 2006; ESO Press Release 31/06) was observed using NGS-AO for SINFONI and full LGS-AO for NACO. But because the targets are so faint, both data sets had to be smoothed to 0.2'' resolution in order to reach sufficient signal-to-noise.



DAZLE on the VLT

Richard McMahon¹
 Ian Parry¹
 Bram Venemans¹
 Dave King¹
 Emma Ryan-Weber¹
 Joss Bland-Hawthorn²
 Anthony Horton²

¹ Institute of Astronomy, University of Cambridge, United Kingdom

² Anglo-Australian Observatory, Sydney, Australia

We report on the commissioning and first observing run of the VLT visitor instrument DAZLE. DAZLE (Dark Ages 'Z' Lyman Explorer), is an innovative near-infrared narrowband imager optimised to detect faint emission lines between the intense hydroxyl (OH) airglow emission lines that dominate the terrestrial night sky in the wavelength range 0.8–1.8 microns. The scientific goal is to detect redshifted Lyman- α line emission from hydrogen gas ionised by the young stars in galaxies at redshifts greater than 7.5.

How and when the first galaxies formed are questions at the forefront of work in both observational and theoretical cosmology. In recent years the observational horizon has expanded rapidly and radically for those observing distant galaxies. Large-format red-sensitive detectors on wide-field imaging instruments, the new generation of 8-m-class telescopes such as the VLT and the refurbished 2.5-m Hubble Space Telescope (HST), have pushed the limits to which we can routinely detect star-forming distant galaxies progressively from redshifts of one to beyond six.

At redshift greater than seven, we probe the first 5% of the history of the Universe, 700 million years after the Big Bang. Recently the search for young forming galaxies at redshifts greater than seven has taken on a new urgency with the remarkable recent WMAP satellite detection of polarisation in the cosmic microwave background, which indicates that there must be a significant source of ionising radiation in the redshift range $z = 7$ –14. There is also supporting evidence for

high rates of star formation in some galaxies up to $z \sim 10$ from the detection of old stars in $z = 6$ galaxies using the Spitzer satellite.

At the highest redshifts currently accessible, narrow-band emission lines searches using the Lyman- α emission line, from ionised hydrogen, with a rest frame wavelength of 121.6 nm, have pushed from redshifts of four (Hu and McMahon, 1996) progressively to higher redshifts and now routinely reach the boundary of Silicon-based optical detector technology at $z = 6.5$ –7.0 (e.g. Iye et al. 2006). However tempered with the above successes, we have rapidly reached a watershed in the study of the high-redshift galaxies. On the ground, this is due to the inherent difficulty of detecting faint continuum emission due to the steadily increasing brightness of the night sky as one goes to redder and redder wavelengths.

The success in detecting galaxies at higher and higher redshifts using redshifted Lyman- α emission from ionised hydrogen makes it worthwhile to consider whether it is feasible to extend such searches beyond the limits of conventional Silicon-based CCD detectors used in optical astronomy and move into the near-infrared regime of HgCdTe detectors. However, in the range 1.0 to 1.8 microns, the terrestrial night sky is 10–100 times brighter than in the optical, due to intense hydroxyl (OH) airglow emission lines. In a seminal paper, Maihara et al. (1993) showed that these OH lines are extremely narrow with widths of less than 20 km/sec and, moreover, between the OH airglow line emission the background sky was 1/50th the average flux due to these lines.

To capitalise on this dark background, one needs to observe the sky at a spectral resolution of 1000 with special narrowband filters that are ten times narrower than filters normally used in the optical regime. The VLT visitor instrument, DAZLE (Dark Ages 'Z' Lyman- α Explorer, Horton et al. 2004) is designed to image between these night sky emission lines and to detect faint extraterrestrial emission lines between the intense hydroxyl airglow emission lines that dominate the terrestrial night sky in the wavelength range 0.8–1.8 microns. Prior to the DAZLE

project it was considered impossible to manufacture large high-throughput interference filters with this resolution and good out-of-band blocking.

The DAZLE instrument

The original proposal was to mount DAZLE at the Cassegrain focus of the Gemini South telescope, and initial work was directed towards this goal. However, following the announcement in July 2001, that the UK would be joining ESO, the design effort was redirected to mounting DAZLE on the Nasmyth visitor focus of the VLT on UT3 (Melipal). The design of DAZLE was a collaboration between the Institute of Astronomy, Cambridge, and the Anglo-Australian Observatory.

The DAZLE instrument was designed to be mounted on the Nasmyth platform of Melipal (UT3). It does not directly contact the Nasmyth rotator and the instrument has its own motorised derotator. The instrument is shown in Figure 1 mounted on UT3. The instrument consists of an f/15 collimator that delivers light from the VLT Nasmyth field to a fold mirror. To turn the beam through 90 degrees, a filter/mask wheel assembly contains the narrowband filters and mask, a cold stop, a motorised derotator and a downward-looking cryogenic camera. The cryogenic camera operates at liquid nitrogen temperatures. The complete instrument is enclosed in a cold room, maintained at -40°C .

The technical specification of DAZLE is summarised in Table 1.

Integration of DAZLE onto the Nasmyth platform of UT3 was completed successfully prior to the start of the scheduled commissioning nights on 30 and 31 October 2006. We ensured that the integration of DAZLE on Paranal had minimal impact on ESO staff effort by shipping by boat to Antofagasta the major components of DAZLE already assembled within a standard 40 ft (12.2 m) ISO shipping container. Figure 2 shows the DAZLE commissioning team including ESO staff in the Melipal (UT3) control room.



Figure 2: DAZLE Commissioning team including ESO staff in the VLT UT3 (Melipal) control room.

Detector array	Rockwell Hawaii-2; 2048 × 2048 pixels
Spatial scale	0.2 arcsec per pixel
Field of view	6.8 arcmin × 6.8 arcmin
Central wavelength	1.056, 1.063 microns
Peak transmission	72 %
Spectral resolution	1200
Bandwidth (FWHM)	9 ångströms
Redshift of Lyman- α	7.70

Table 1: The technical specification of DAZLE.

Figure 1: DAZLE being mounted on the VLT UT3 (Melipal) visitor focus.

First results

Data from a science verification observation is shown in Figure 3. Science verification for the DAZLE programme involved the determination of the filter throughputs and sky background via observations of spectrophotometric standards with IR coverage from the FORS2 calibration plan. In addition we selected a quasar with a redshift that placed the narrow forbidden [O III] 5007 Å line within the bandpass of one of the filters. Figure 3 shows images of the $z = 1.110$ quasar. The [O III] 5007 Å line has a predicted observed wavelength of 1056.5 nm. The left-hand image is through the NB 1056 nm filter and the right-hand image is through the NB 1063 nm filter. The quasar is clearly detected in the 1056 nm filter centred on the predicted wavelength of redshifted [O III] whereas the quasar is undetected in the 1063 nm image.

The science programme was carried out primarily on the nine nights from 2 to 10 November. Around 0.5 nights were lost over two nights due to high wind when

UT3 was closed. Apart from this, no observing time was lost due to DAZLE or the VLT systems. During the remaining time we accumulated a total on-sky integration time of 69 hrs excluding time spent on calibration such as spectrophotometric standards and twilight flats. Twilight flat observations were started soon after sunset each night and science observations would commence before the end of astronomical twilight.

The measured seeing in our images during the run ranged from 0.4 arcsec to 1.3 arcsecs. As proposed, we executed the shallow survey when the seeing was poor. The two deep survey pointings in the GOODS-South field have exposures of 10 hours per filter. The on-sky measured sensitivity of DAZLE, which includes detector (Rockwell HgCdTe HAWAII-2) dark current, read-out noise, instrument and sky background, gives a 5σ sensitivity of $3\text{--}5 \times 10^{-18} \text{ erg s}^{-1} \text{ cm}^{-2}$ in 10 hours in a 1 arcsecond aperture.

A dark-corrected, flat-fielded image in the 1056 nm filter of the GOODS-South field

can be seen in Figure 4. We are reasonably confident that we were seeing the ‘true’ sky background because we could see rings of very marginally higher background due to expected faint OH lines encroaching on the wings of the filter transmission profile. Figure 5 shows a ‘colour-magnitude’ diagram for objects detected in the 1056 nm filter image of the GOODS-South field. Objects with an emission line in the 1056 nm filter will have a positive flux excess. One such object is shown in Figure 6. The object is detected in the 1063 nm filter, but absent in the 1056 nm image. Based on the colours in the COMBO-17 survey, the galaxy has a photometric redshift of 0.606. Therefore this object is most likely a galaxy with a redshifted H- α line emission in the 1063 nm filter at redshift of 0.62.

Acknowledgements

We are grateful for the level of support provided by ESO staff in both Garching and Chile over the last few years, and particularly during the observing runs from Pascal Robert and Keiran O’Brien.

References

- Horton A. et al. 2004, SPIE 5492, 1022
- Hu E. and McMahon R. 1996, Nature 382, 231
- Iye M. et al. 2006, Nature 443, 186
- Maihara T. et al. 1993, PASP 105, 940

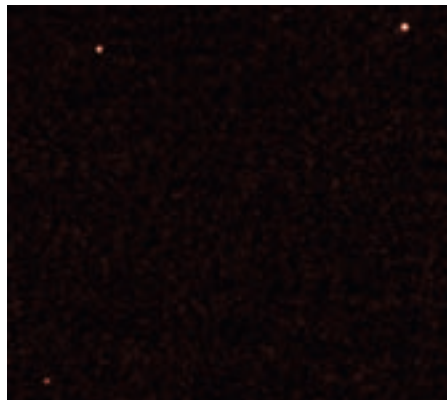
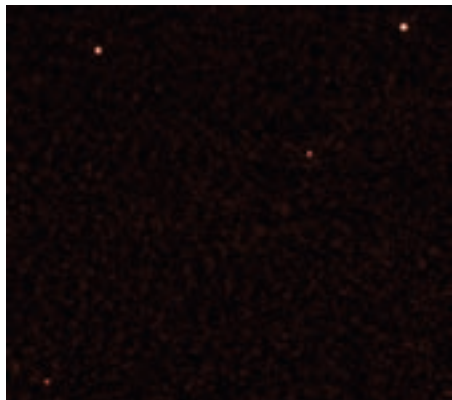


Figure 3: DAZLE images of the quasar ($z = 1.11$) taken in the narrow 1056 nm filter (left) and in the 1063 nm filter (right), showing the prominent [O III] emission line in the 1056 nm filter.

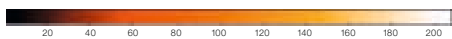


Figure 5: A DAZLE 'colour magnitude' diagram of the objects in the GOODS-South field positively detected in the 1056 nm filter.

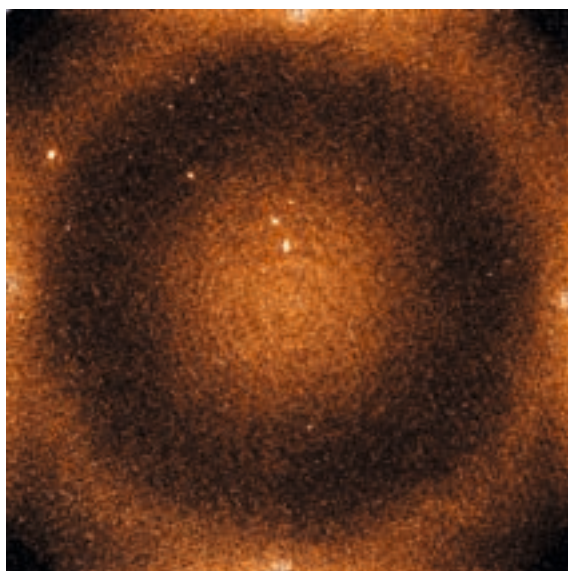


Figure 4 (left): 10-hour DAZLE image of the GOODS-South field in the 1056 nm filter.

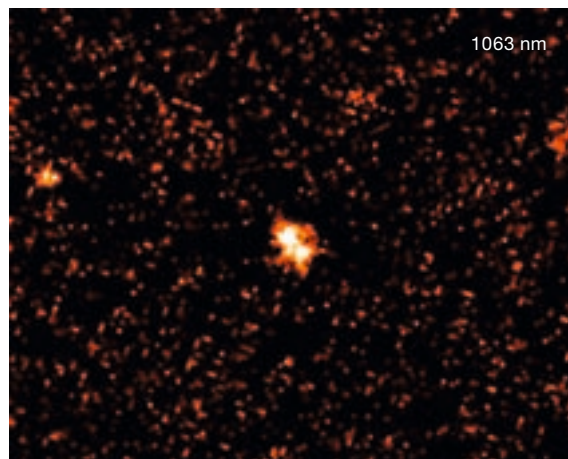
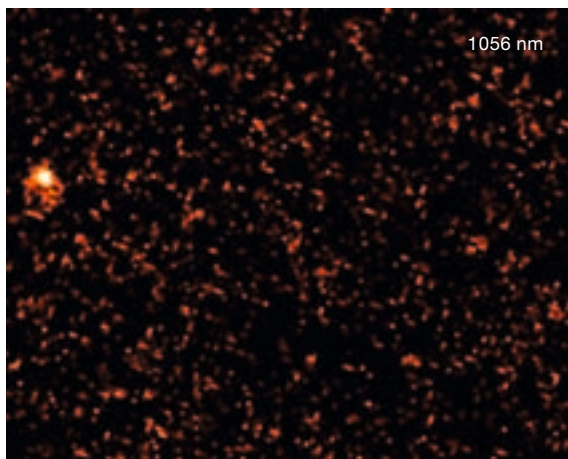
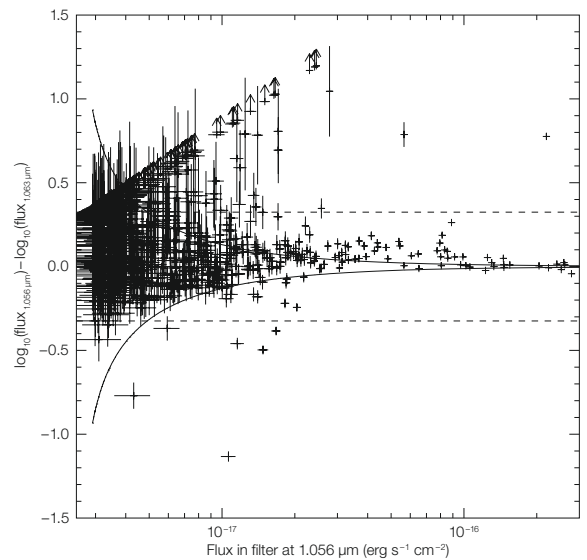


Figure 6: DAZLE images in the 1056 nm and 1063 nm filter showing an emission-line galaxy in the 1063 nm filter with an assumed redshift of 0.62 for H- α .



Phase Correction for ALMA: Adaptive Optics in the Submillimetre

Bojan Nikolic¹
John Richer¹
Richard Hills²
Alison Stirling³

¹ University of Cambridge,
United Kingdom

² Joint ALMA Office, Chile

³ Met Office, United Kingdom

Inhomogeneities in the Earth's atmosphere corrupt the wavefront of incoming submillimetre radiation and, similarly to the seeing at optical wavelengths, this limits the resolution and sensitivity of submillimetre aperture synthesis arrays. ALMA will correct for these wavefront errors by a combination of frequent observations of known nearby point sources (predominately quasars) and by measuring the properties of the atmosphere along the line of sight of each telescope using dedicated 183 GHz radiometers. These techniques are critical for enabling ALMA's goal of resolution as fine as 0.005 arcseconds.

Seeing in the submillimetre

The Atacama Large Millimetre Array (ALMA) is now under construction at its high and extremely dry site in Northern Chile, close to the existing APEX telescope and the CBI experiment. The progress in the construction of individual telescopes making up the array was reported by Stefano Stanghellini in the last issue of *The Messenger*. By the end of 2007, some seven 12-m antennas have been delivered to Chile, and these are currently undergoing final assembly and testing.

Operating together, the 66 telescopes that comprise this interferometric array will provide a view through the millimetre and sub-millimetre atmospheric windows that is orders of magnitude better in terms of resolution and sensitivity than what can be achieved with existing instruments. Transformational science with ALMA is eagerly anticipated.

But to achieve its ambitious goals, ALMA must solve a key problem: it must be able to correct the effects of the earth's turbu-

lent atmosphere. These effects place a direct limitation on the sensitivity and resolution of the array. In effect, an adaptive optics system for the array must be developed.

Astronomers used to infrared and optical facilities will be familiar with this problem. At these wavelengths, the turbulent motions of the earth's atmosphere result in relatively fast and small-scale temperature fluctuations. These cells of hotter and cooler air have different refractive indices, which distort the incoming plane waves, causing the well-known seeing problem. At radio wavelengths, the turbulent atmosphere causes similar problems, but it is only at the highest radio frequencies where the effect becomes hard to correct. Unlike in the optical, at these wavelengths, the refractive index variations are dominated by the tropospheric water vapour content ('wet fluctuations'), rather than fluctuations of the dry air.

Beyond the state of the art

The best images yet made at millimetre and sub-millimetre wavelengths have a resolution of around 0.3–0.4 arcseconds (e.g. Krips et al. 2007 at the Smithsonian SubMillimeter Array – the SMA; Cabrit et al. 2007 at the Plateau de Bure in France). These images are made using the longest available baselines at these arrays, and are diffraction-limited. However, these are also close to the practical limits imposed by atmospheric turbulence. Even if these arrays had much longer baselines, only in the most phase-stable weather would it be possible to make diffraction-limited images without using an adaptive optics system. The longest baselines for these arrays are around 500–1000 m. It is intriguing that the limiting angular resolution of around 0.4 arcsec is somewhat similar to the best seeing obtainable on infrared and optical telescopes, even though the cause of the seeing is different.

The goal for ALMA is to produce images with diffraction-limited resolution at the highest frequencies and most extended configuration. With baselines up to 18 km in length, this corresponds to about 5 mas resolution at the highest frequency of about 950 GHz. This is a massive step forward in resolution, and requires

the ability to correct for the atmospheric errors very precisely. Although this is an extreme example of ALMA's capabilities, which will be used only in the best weather conditions, even routine ALMA science observations will require resolution in the range 50–200 mas, so that adaptive optics correction of the atmosphere must be a routine part of ALMA's capabilities.

To put this in context, the required improvement in resolution is comparable to that required for the next generation of planned optical and infrared telescopes such as the ELT. For a 50-m optical telescope operating at 1 micron wavelength, the diffraction limit is about 5 mas. To achieve this, the adaptive optics system must beat the natural seeing, which is typically 500 mas, by a factor of 100. ALMA must achieve a similar increase in resolution beyond the seeing-imposed limit to achieve its goals.

Atmospheric effects on submillimetre data

We typically characterise atmospheric effects at optical wavelengths by specifying the seeing – the angular size of an unresolved star – or by the Fried parameter r_0 . In radio interferometry, it is more natural to specify the fluctuations in the phase between two points on the incoming wavefront, because this is a quantity which can be directly measured. For a point source, it is equal to the root-mean-square fluctuations of the phase of the complex visibility, measured on a given baseline. (This is the square root of the *structure function*.) Even without the atmosphere, phase errors arise from changes in the path length of the signals from each antenna to the correlator, due to electrical and opto-mechanical effects. But the design of ALMA is such that the atmosphere-induced phase errors always dominate, so that it is the atmosphere which provides the fundamental limit to ALMA's performance.

Water vapour is the component of the atmosphere with typically the greatest impact on observations at millimetre and submillimetre wavelengths. The water molecule's high dipole moment gives water vapour a high index of refraction: at

frequencies far away from the strong water emission lines (where dispersion becomes important), one millimetre of precipitable water vapour in the atmosphere corresponds to about 6.8 mm of extra optical path.

The effect of opacity is of course irreversible: it attenuates the signal from the science target and increases the background noise against which this signal must be detected. Therefore, sites with the minimum of water vapour in the atmosphere are essential for submillimetre astronomy and this was one of the main criteria for the choice of the ALMA site. However, although Chajnantor is a spectacularly dry site, the turbulent fluctuations of the water content are significant.

The magnitude of atmospheric path fluctuations at the site of ALMA has been continuously monitored at 11 GHz on a 300 m long baseline over the course of several years by the site-testing interferometer. The findings, which are summarised in ALMA memo 471, show that the median path fluctuations are 187 μm , and that in the best 10% of the weather, the fluctuations are less than 49 μm . Additionally, the magnitude of path fluctuations was found to be not perfectly correlated with total column density of water

vapour, and so best transparency conditions are not necessarily associated with the most stable phase conditions. In other words, there are periods of excellent dry weather when one wants to observe at the highest frequencies, but when the seeing is rather poor.

Where do the fluctuations arise? We know that in general most of the moist air is located close to the ground, typically within 1 km. During the night time, models suggest that an exponential distribution of water with a scale height of around 1 km is appropriate. During the day, strong solar-driven convection mixes the water up, and a more uniform distribution is expected from the ground up to a height of the order of 1 km, where a temperature inversion is often seen. Regardless of the overall water vapour distribution with height, the fluctuations in water vapour content which give rise to the phase errors are often thought to be dominated by thin layers where the fluctuations are strong. Using two site-test interferometers, it has been possible to infer the height of the dominant fluctuations on several occasions and these results, published in ALMA memo 345, show that the dominant fluctuations are typically within 400–800 m of the ground at the ALMA site.

As in the optical and infrared regimes, the magnitude of path fluctuations increases with increasing length of the baseline, placing a limit on the maximum usable baseline. This increase is not as steep as it is in the regime of most optical telescopes because the lengths of baselines of ALMA are comparable and exceed the thickness of the turbulent layer giving rise to water vapour fluctuations. This change of the properties of the effective phase screen with the change of relative thickness of the turbulence is illustrated by simulations shown in Figure 1. As an example from the lower radio frequency regime, the measured phase errors and their dependence on baseline length at the Very Large Array in New Mexico is shown in Figure 2. This shows the power-law behaviour expected of Kolmogorov turbulence. In this case, the exponent is close to 0.6, which is also typical for data from the ALMA site.

Correction of ALMA phase errors

ALMA will operate up to frequencies just below 1 THz, which corresponds to a wavelength of 300 microns. To achieve good image quality, we need to measure the phases of the complex visibilities to better than 30 degrees, or one twelfth of a turn of phase. This implies correcting the path to better than 25 microns. As we have seen, even on 300-m baselines, the fluctuations are known to be typically 200 microns of path. So it is clear that a very precise path correction system is needed by ALMA. Note that the scale of the path error increases typically as the baseline to the power 0.6, for baselines up to a few km, so this problem gets worse as we go to longer baselines. But also note that the problem is reduced for longer wavelengths: at 3 mm (100 GHz), we can tolerate an order of magnitude greater path error (i.e. 250 microns) and still measure the phase to 30 degree accuracy.

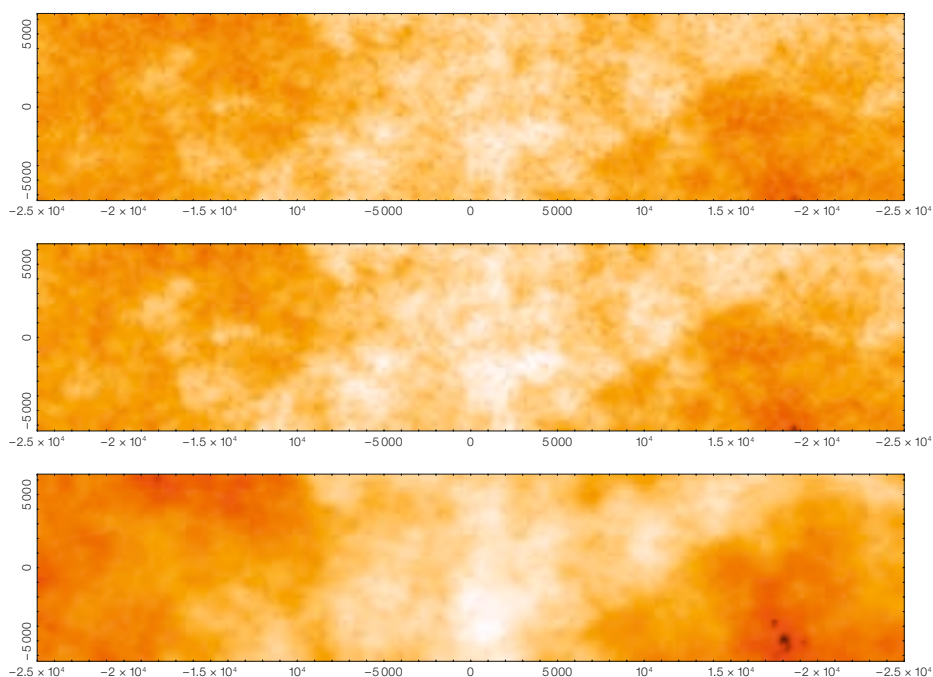


Figure 1: Maps of vertically integrated models of water vapour content generated assuming three-dimensional Kolmogorov statistics. The three maps (top to bottom) correspond to increasing vertical thicknesses of the turbulent volume showing the expected steepening (i.e., increasingly more power on the larger scales) of the fluctuation structure function. The horizontal dimensions of the maps are 50 km \times 14 km and the resolution is 24 m.

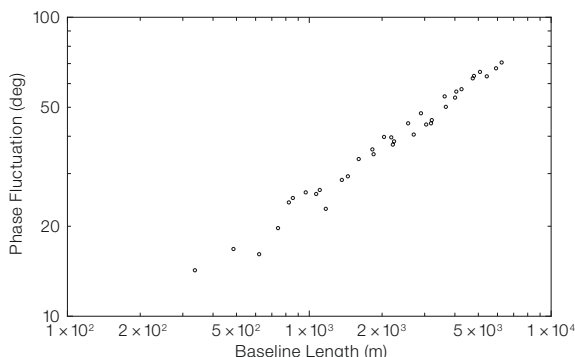


Figure 2: Measured phase fluctuations at the VLA at 22 GHz as a function of baseline length. The baselines shown in this plot are all between the antennas of one of the arms of the VLA and so are co-linear.

In order to meet the specifications and deliver on its promise of outstanding imaging resolution, ALMA will employ a combination of two techniques for correction of phase errors introduced by the atmosphere: fast switching, and water vapour radiometry (WVR). The established technique of fast-switching involves regularly observing known nearby point sources, and will be used for correcting phase fluctuations on the longer time scales. In addition, measurements from the 183 GHz water vapour radiometers (WVRs) installed at each telescope will be used to make corrections on time scales as short as 1 s.

The fast-switching technique is in some ways analogous to adaptive optics, in that point-like astronomical sources are used to infer the variation of atmospheric properties across the telescope (or array of telescopes in ALMA's case) and correct for these. Instead of using stars, ALMA will observe the brightest quasars. However, the field of view of the ALMA antennas (about one arcminute at an observing wavelength of 3 mm) means that typically there is no usable calibration source within it, so the telescopes have to periodically point ('switch') to a nearby calibrator and back to the science target. This fast switching requires extremely agile telescopes, which can accelerate and decelerate rapidly: calibrators of sufficient strength are expected to be typically one to two degrees away from the science target and the ALMA antennas are required to be able to do calibrator-target-calibrator cycles as short as 10 seconds. This ability to switch quickly was one of the key design drivers for the ALMA 12-m antennas, resulting in very stiff designs with powerful drive motors.

But fast switching will not alone correct all the phase errors. First, although the 10-second cycle is relatively short compared to existing aperture synthesis telescopes, we know there are significant atmospheric fluctuations on timescales as short as 1 second: this timescale is given roughly by ratio of the diameter of the antenna (12 m) to the wind speed (typically 10 m/s). The second reason is that observations of a calibrator some one or two degrees away gives a measurement of the atmospheric properties in a slightly different direction to the science target that we actually wish to correct. Therefore applying this correction will leave some residual phase error. This problem is similar to the limited size of the isoplanatic patch in adaptive optics.

For these reasons, ALMA will also employ the second phase correction technique: water vapour radiometry. This technique exploits the fact that the same water molecules which delay the incoming wavefronts also emit thermal radiation in the form of rotational transitions. In particular, there is a convenient and strong rotational emission line of water at 183 GHz, shown in Figure 3. Each antenna is equipped with a well-calibrated and sen-

sitive 183-GHz radiometer looking along the line of sight to the astronomical source. It is then possible to infer to high accuracy the quantity of water along each line of sight. With the assistance of an atmospheric model, we can infer the absolute delay due to the water vapour at each antenna. Finally, for a given baseline, we subtract the delays to each antenna to predict the phase error due to atmospheric water. This phase error can then be removed from the given baseline either off-line in the final data processing, or in real time in the correlator.

This WVR technique bears some similarities to laser guide star adaptive optics at optical and near-infrared wavelengths. In that technique, artificial stars are stimulated by lasers shone out along the line of sight, and their resulting stellar images are used to infer and correct the atmospheric effects. In the submillimetre, life is somewhat easier because the water molecules emit passively in the submillimetre bands, so no laser excitation is required.

WVRs for ALMA

For ALMA, the atmospheric water emission will be measured by dedicated absolute microwave radiometers situated next to the main astronomical receivers at the Cassegrain focus of the antennas. One radiometer is needed for each antenna, and the lines of sight of the radiometer beams are very closely aligned with those of the astronomical beams. This ensures that the radiometer beam samples as closely as possible the volume of air causing the extra optical path, so allowing the greatest possible accuracy in the phase correction. As part of the ALMA design and development project,

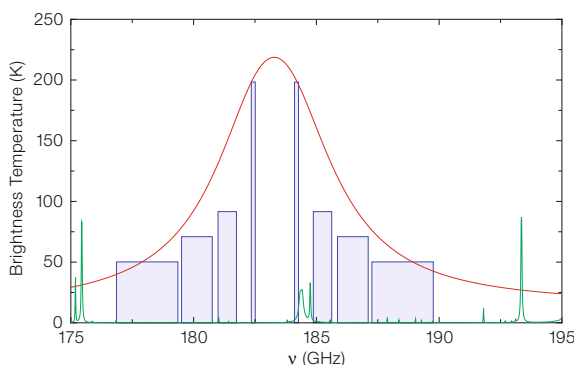


Figure 3: The brightness temperature of the 183 GHz water vapour line for a precipitable water vapour column density of 1 mm (red line) and the four double sideband channels of the prototype system (rectangles) with heights scaled in inverse proportion to bandwidth to illustrate their relative sensitivity. Also shown is exaggerated ozone emission (green lines).

two prototype radiometers of different designs were built by a collaboration between Onsala Space Observatory and Cambridge University. Both met the ALMA specifications by a comfortable margin.

After laboratory testing, the two prototypes were taken to the SubMillimetre Array (SMA) on Mauna Kea for further testing (Figure 4). Each was installed on an SMA 6-m antenna using purpose-built relay optics. The magnitude of the atmospheric phase fluctuations at this site are similar to those on Chajnantor, although the absolute water content is significantly higher. The aim was to test both the engineering performance of the radiometers and also how well they could be used to correct the astronomical phase fluctuations.

The most relevant tests consisted of observing a strong point source – a quasar typically – and recording both the phase of the interferometric visibility on the relevant baseline as well as the outputs of the two radiometers. We then computed the linear combination of radiometer outputs which optimally matches the observed phase (this consists of fitting for four parameters). This results in the best possible phase correction for given radiometer outputs, which would only be achievable in real life if we had very good models for the atmosphere. A sample result from one such test is shown in Figure 5. In this example, one can see that the predicted phase error tracks the observed quasar phase extremely well. In fact, by subtracting the predicted phase error, the rms phase fluctuations on the quasar are reduced from around 200 to 62 microns of path.

These tests showed that the radiometers mounted at the SMA can meet the top level specifications most of the time. The primary limiting factors of performance of radiometers in this system appeared to be related to interfacing issues rather than fundamental sensitivity, which bodes very well for their performance on ALMA.

Integrating WVR into ALMA

For ALMA, each of the 54 12-m antennas will be instrumented with an identical 183-GHz radiometer. After an open ten-

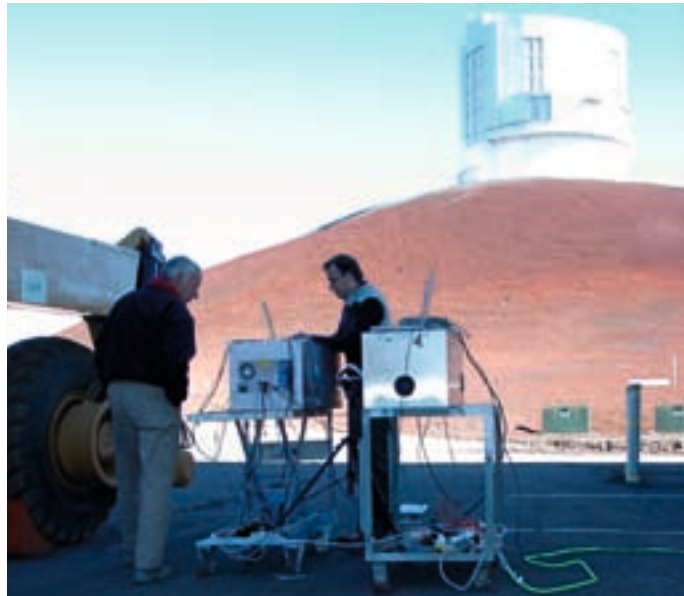


Figure 4: The two prototype water vapour radiometers on Mauna Kea, in initial tests before installation on the SMA.

der process, the contract to build the production radiometers was let by ESO to Omnisys Instruments AB, Sweden. Their preparations for production have been progressing well and the Project expects to receive the first production radiometers in September of this year.

The majority of the computing effort to integrate the radiometers into ALMA and make best use of them is being coordinated by ESO: the low level interface layer is being written at ESO; the on-line telescope calibration system (TelCal) will have the basic algorithms for phase correction using the WVRs and is being developed primarily at IRAM, Grenoble; and at Cambridge we are funded under the European Union Framework Programme 6 to develop advanced phase correction algorithms.

Modelling the atmosphere

There has been a significant effort to model atmospheric properties and phase fluctuations recently, both under previous agreements with ESO, and as a part of our current work. The primary motivation in the first stages was to relate the top level specification to the engineering specifications for the radiometers; presently, the main motivation is to create the tools needed to develop the algorithms which will correct the phase fluctuations as well as possible, and to understand the impact of any residual phase fluctuations that remain after the correction.

We have been using two different approaches to model the atmospheric properties at Chajnantor. Large Eddy Simulations (LES) are meteorological hy-

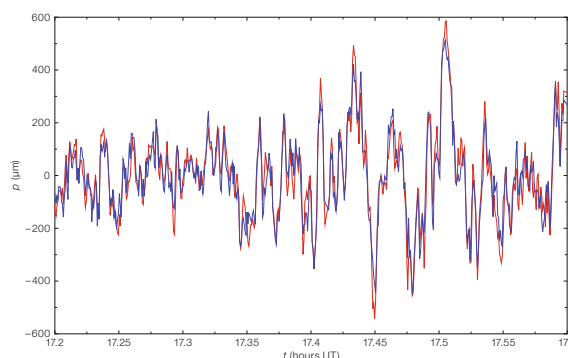
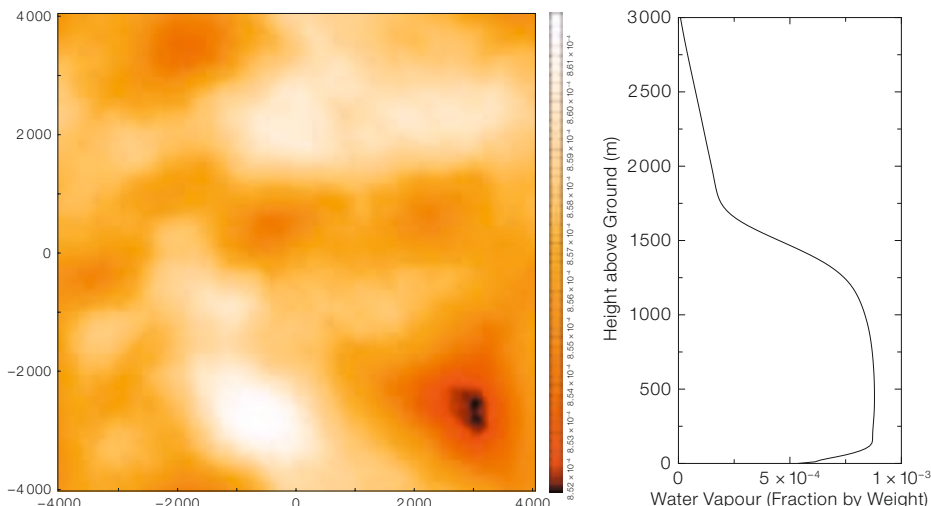
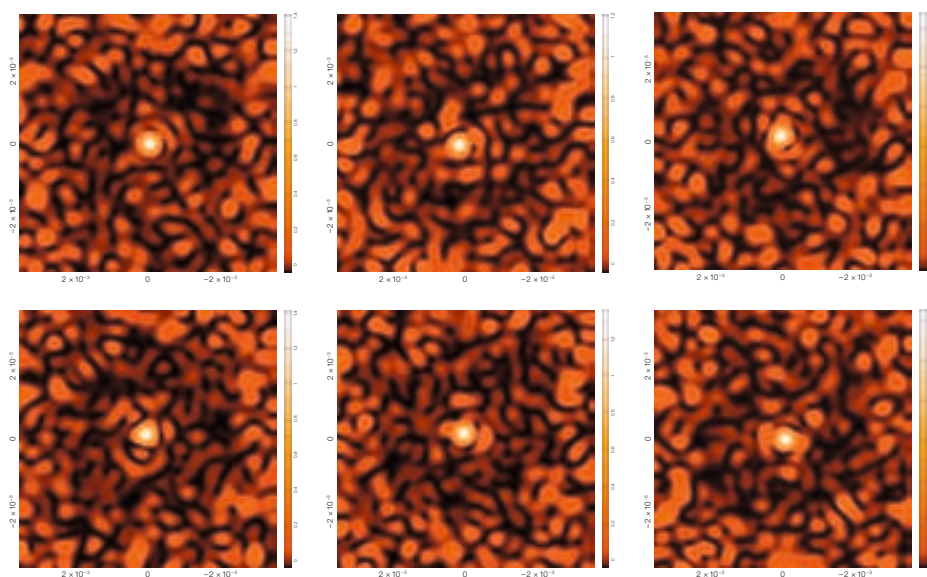


Figure 5: A sample of results from the Water Vapour Radiometer prototypes at the SMA. The red line is the fluctuating atmospheric path difference measured by the interferometer; the blue line is the best possible estimate from the radiometers.

drodynamic codes that solve the Navier-Stokes equation for a given set of boundary conditions, and accurately follow the air and water properties. An example of the results of such a simulation is shown in Figure 6, showing both the inhomogeneity of the horizontal distribution of water vapour and its vertical profile. These simulations have been used to predict the structure function of phase fluctuations as well as the relative importance of 'wet' (due to water vapour content) and 'dry' (due to temperature differences) fluctuations (these results are published in ALMA memo 517). Although the LES models represent the physics that gives rise to water vapour density fluctuations very well, they are extremely computationally expensive and so are both of limited spatial extent and of limited resolution.

For detailed modelling of the performance of the radiometers and of the final imaging performance of ALMA, we therefore use models based on statistical realisations of idealised Kolmogorov turbulence. Rather than simulating two-dimensional phase screens, we generally simulate complete three-dimensional volumes. The reason for this is that the ALMA baselines are of the order of the vertical extent of the turbulent layer and

Figure 7: Time sequence of simulated 'dirty' snapshot images of a point source with ALMA with the presence of uncorrected phase fluctuations due to turbulence. Intrinsic source strength was 2 Jy.



also because we wish to simulate the divergence of the astronomical and WVR beams as they travel through the atmosphere. When the three-dimensional turbulence is flattened by integrating in the line-of-sight direction, the expected steepening of the structure function is naturally reproduced (Figure 1).

The resulting phase screens can be used to simulate in detail both the phase fluctuations in ALMA data and the outputs of the radiometers. For example, Figure 7 shows a sequence of simulated images of a point source in the presence of turbulence. Both the decrease in sensitivity and the random shift in apparent source position can be seen in the sequence. This simulation also illustrates the similar-

Figure 6: Results of Large Eddy Simulation of night time atmospheric conditions at Chajnantor. Left: Horizontal cross section of water vapour density at a height of 850 m (colour bar indicates density of water vapour by weight; overall horizontal dimensions are 8 km by 8 km). Right: The mean vertical profile of water vapour.

ity of the effect of seeing on submillimetre and optical/infrared imaging.

Future plans

Now that the SMA tests are complete, we are focusing our attention on simulating the phase correction problem for ALMA, and developing algorithms that can be used to correct optimally the phase errors, incorporating both fast switching and water vapour radiometer techniques. Within 12 months or so, there should be a working interferometer in Chile, plus the first production WVR systems from Omnisys. As part of the ALMA commissioning process, it will then be possible to further test and refine the ALMA phase correction technique using test data from the ALMA hardware. The ultimate goal is a sophisticated hardware and software system which can correct the majority of atmospheric phase errors in a wide range of conditions, and so allow astronomers to exploit ALMA to the full.

References

Cabrit S. et al. 2007, A&A 468, L29
 Krips M. et al. 2007, ApJ 671, L5



FORS1 and 2 colour composite image of the grand design spiral galaxy Messier 83 (Hubble type SABc) from *B*, *R*, *I* and H-alpha filters (see ESO Press Photo 24b/05 for details).

A Multi-Wavelength Study of the 2003–2006 Outburst of V1647 Orionis

Mario van den Ancker¹
 Davide Fedele^{1,2,3}
 Monika Petr-Gotzens¹
 Piero Rafanelli³

¹ ESO

² Max-Planck Institut für Astronomie,
 Heidelberg, Germany

³ Dipartimento di Astronomia, Università
 degli studi di Padova, Italy

The birth of a star is accompanied by the formation of a circumstellar disc which interacts with the star, but most young stars accrete matter at rates that do not influence the mass of the disc on short timescales. However, in so-called FU Orionis stars, a significant fraction of the total disc mass is accreted onto the central star within a short time. During these FU Orionis events, the light generated by accretion outshines the star by up to 6 magnitudes for a period of several years to decades. The star, V1647 Orionis, underwent such an event. We have used FORS2 and NACO on the VLT and TIMMI2 at the ESO 3.6-m telescope to monitor V1647 Orionis from four months after outburst until the system returned to its pre-outburst brightness level, nearly three years later. Our optical photometry and spectroscopy confirm that V1647 Orionis has indeed undergone an outburst whose characteristics resemble those of the FU Orionis stars.

Violent phenomena in young stars

One of the clearest pieces of evidence for disc accretion during early stages of stellar evolution are FU Orionis and EX Lupi outbursts. These outbursts are thought to be the consequence of a sudden and steep increase of the mass accretion rate onto the central star, which changes from those commonly found around T Tauri stars ($\sim 10^{-7} M_{\odot} \text{ yr}^{-1}$) into values of 10^{-3} – $10^{-4} M_{\odot} \text{ yr}^{-1}$. Statistical studies suggest that young low-mass stars experience several FU Orionis-like outbursts during the early phase of stellar evolution. During these rare occurrences, the protoplanetary disc reaches high temperatures ($> 1500 \text{ K}$). Interestingly enough, studies of chondritic material – little droplets

of rock that have melted and then re-condensed – found in comets have shown that our own Solar System must also have gone through one or more such FU Orionis events early in its lifetime. The mechanism responsible for the disc instability which leads to a FU Orionis event is still unclear.

Observationally, studies of FU Orionis outbursts have been hampered by the low frequency with which they have been detected (the last such event reported in our Galaxy dates from 1984). The emergence of a new pre-main-sequence outburst object is thus a unique opportunity to address the physical processes that occur in the disc's interior.

The appearance of a new nebula in Orion

In late 2003, amateur astronomer J. W. McNeil reported the mysterious appearance of a bright new nebula within the Orion B molecular cloud complex (McNeil et al. 2004). Rapid follow-up observations from several observatories confirmed the existence of extensive bright nebulosity, associated with the previously anonymous young star V1647 Orionis, and never previously detected (see Figure 1). In the months following the discovery, this star showed an increase of its optical/IR brightness of up to 6 magnitudes. The outburst has been observed from the X-ray regime (Grosso et al. 2005) to infrared wavelengths (Muzerolle et al. 2005). In February 2004, four months after the onset of the outburst, the brightness rise stopped and the magnitude remained (relatively) constant. In November 2005, V1647 Ori began to fade fast, returning to

its pre-outburst optical brightness level in April 2006.

Using optical imaging and spectroscopy with FORS2 at ESO's Very Large Telescope (VLT), and photometry and spectroscopy in the mid-infrared with TIMMI2 at the ESO 3.6-m telescope, we have monitored the evolution of McNeil's nebula and V1647 Ori from February 2004 until January 2006. In addition, we have performed a more in-depth study of V1647 Ori and McNeil's nebula in the near-infrared using AO-assisted imaging and polarimetry with NACO in April 2005.

Figure 2 shows the light curve of V1647 Ori in the *R*-band based on our new FORS2 data and on previous measurements by other authors. The optical light curve of V1647 Ori can be divided into three parts: i) from October 2003 to February 2004 – the rising period; ii) from February 2004 to August 2005 – the plateau phase; and iii) from August 2005 to January 2006 – the fading period. The rising part is very steep: from October 2003 to January 2004 the optical magnitude increased by more than 3 magnitudes in *R*. From the pre-outburst magnitude level, $R \sim 23.5$, the total rise in brightness of V1647 Ori is larger than 6 magnitudes in *R*. From Figure 1 we find a rate of increase of *R* of ~ 1.5 magnitudes per month. Assuming that this rate

Figure 1: Comparison of the vicinity of V1647 Ori and McNeil's nebula, pre- and post-outburst. **Left:** Pre-outburst Digital Sky Survey image. **Right:** Post-outburst *BRz* colour-composite image obtained with FORS2 on 30 December 2004. Blue, green and red colours correspond to the *B*, *R* and Gunn *z* photometric bands. The dimension of both images is $2.0' \times 1.9'$. North is up, East to the left.



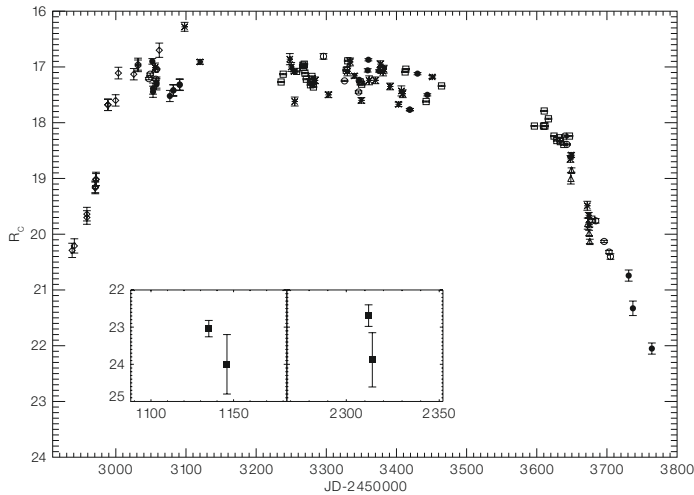


Figure 2: 2003–2006 *R*-band light curve of V1647 Ori. Filled circles show data taken with FOR2, whereas the open plot symbols indicate data taken at other observatories. The insets show the pre-outburst magnitude level of V1647 Ori.

remained constant during all the rising phase, we estimate that the outburst began around the middle of August 2003.

During the plateau phase the optical brightness shows a slow decline with time ($\Delta R = 0.02$ mag/month), on top of which *R* displays a non-periodic, flickered, oscillation on a short timescale. From our data we measure a variation of ~ 0.5 mag between 17 and 18 February 2004. Thus, V1647 Ori at its maximum light shows an optical brightness variation on a time-scale of 24 hours. For five nights we have two consecutive acquisition images (separated by a few minutes) from which we searched for variations on very short time-scales. However, no significant changes in optical brightness are detectable from these measurements. The total duration of the plateau phase is less than two years.

From August 2005 to January 2006, *R* dropped by four magnitudes, indicating the start of the fading period. On 29 January 2006 the last *R*-band measurement taken of V1647 Ori, we estimate $R = 22.05$. From the light curve we estimate a fading rate of ~ 0.8 magnitudes per month during this phase. Assuming a constant fading rate, V1647 Ori thus returned to its pre-outburst brightness at the beginning of April 2006.

The nature of McNeil's nebula

The morphology of McNeil's nebula (Figure 3) resembles that of FU Orionis ob-

jects, which often show an arc-like morphology. The nebular emission of such objects mimics the lobes of a bipolar structure, produced by the powerful outflows from the central star. The secondary lobe may be obscured by the circumstellar disc and/or envelope, so that in many cases the nebula appears to have a cometary shape, such as is also seen in V1647 Ori. The emission within McNeil's nebula is not uniform in intensity or in colour. There are two main 'blobs' of higher emission (labelled B and C in Figure 3): the first is close to the star extending to

North-West. It is very bright in all bands. The second blob is farther away from the star in direction North-East at a distance of $\sim 35''$. This structure emits mainly in *B* and *R* bandpasses and is spatially coincident with knot A of the Herbig-Haro object HH 22.

In Figure 3 we show a temporal sequence of images of V1647 Ori and McNeil's nebula in *B*, *R*, *I* and Gunn *z*, taken on 17 February and 20 December 2004 and 2 January 2006. During the first two epochs V1647 Ori was at the maximum light of the outburst (plateau phase). On January 2006 the star was quickly fading returning to its quiescent brightness level. The overall morphology of the nebula (including the substructures B and C) does not show major changes during such a period. Given the FWHM of the FOR2 images ($< 0.85''$ in *R*) and the nearly two-year time interval, we conclude that no evidence of spatial motion was identified within McNeil's nebula down to a resolution of $0.43'' \text{ yr}^{-1}$, corresponding to an upper limit to the projected expansion velocity of 800 km s^{-1} at the adopted distance toward V1647 Ori of 400 pc.

The temporal evolution of the brightness of McNeil's nebula closely follows that of the outbursting star: the nebular emis-

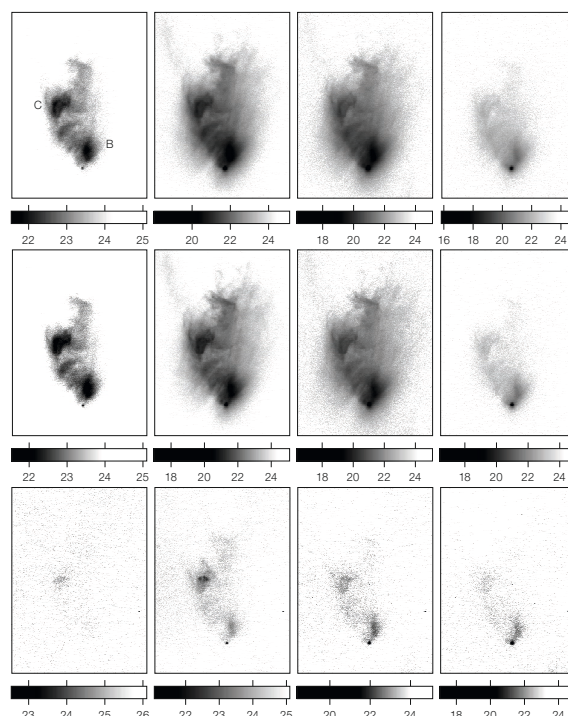


Figure 3: FOR2 images of V1647 Ori and McNeil's nebula taken on 17 February 2004 (top row), 20 December 2004 (central row) and 2 January 2006 (bottom row). The four columns correspond to images in *B*, *R*, *I* and Gunn *z* filters. The intensity scale (bottom of each image) is in mag/arcsec^2 .

sion remains unchanged during the plateau phase, as is clear from the top and middle rows of Figure 3. By early 2006 the nebula has mostly disappeared. It is no longer visible in the blue, where also V1647 Ori was not detected up to a limiting magnitude of $B > 24.9$. A faint emission from blob B and C is still visible in the R , I and Gunn z filters. Given the spatial coincidence with HH 22A, such emission is likely produced by $H\alpha$ and forbidden lines (all falling in the R bandpass) within the Herbig Haro knot.

The close resemblance of the light curve of V1647 Ori and the brightness variations shown by its associated nebulosity strongly suggest that McNeil's nebula is illuminated by light from V1647 Ori that is reflected and scattered by small dust grains within the nebula. In this scenario, the different colours of the nebula would be due to the presence of different amounts of scattering material. Using the method by Magnier et al. (1999) we use the colour dependence of the scattered light to probe the distribution of material inside the nebula. Figure 4 shows the resulting map of the differential extinction in the V -band, ΔA_V , for McNeil's nebula. It is clear that the extinction is not uniform in the nebula. Close to V1647 Ori and at the base of the nebula ΔA_V is lower. Moving from the star to the North-East, a region of higher extinction shows up. The total optical extinction in the direction of V1647 Ori caused by material within McNeil's nebula is ~ 6.5 mag. As this estimate does not include foreground extinction, it is a lower limit to the total optical extinction towards V1647 Ori.

The NACO K -band polarisation map of V1647 Ori (Figure 5) reveals a compact region of aligned vectors with high degree of polarisation. At larger scales the polarisation pattern is centro-symmetric. Such structures are often seen in near-infrared polarimetric maps of young stars with circumstellar nebulae. These systems show a region of aligned vectors, known as a 'polarisation disc', at the location of the central source, and a gradual transition to a centro-symmetric pattern of vectors in the surrounding nebula. The polarisation disc is attributed to multiple scattering in cases where the optical depth toward the central source is too high for direct observation. The aligned vectors of the polari-

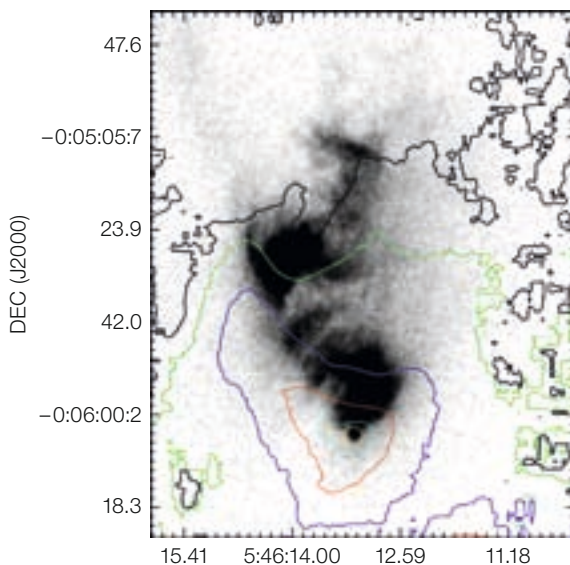


Figure 4: Differential extinction map of McNeil's nebula. The grayscale shows the V -band image of the nebula. Overplotted are the ΔA_V contour levels 1.5 (yellow), 2.5 (cyan), 3.5 (red), 4.5 (blue), 5.5 (green) and 6.0 (black). The extinction can be seen to increase gradually as the line of sight from the star to the nebula tilts towards the East.

sation disc are usually parallel to the disc plane. Interestingly, the position angle of the observed polarisation in the vicinity of V1647 Ori (90 ± 9 degrees, Figure 5) is perpendicular to the major axis of the reflection nebula seen in the optical. If the large-scale reflection nebula can be interpreted as being shaped by a wind or outflow from the central star, the polarisation vectors would indeed be aligned with the disc plane.

Optical and mid-infrared spectroscopy

The positive slope of the optical spectrum of V1647 Ori (Figure 6) reveals a red energy distribution of the source. Clearly visible are the $H\alpha$ and $H\beta$ lines, both characterised by a P-Cygni profile. The He I 5875 Å line and the Na I D1 and D2 doublet are present in absorption and Fe I and Fe II lines in emission are detected

in all spectra taken during the plateau phase. The P-Cygni profile of $H\alpha$ and $H\beta$ is in both cases asymmetric with the emission components lacking the high velocity part. This profile, commonly observed in FU Ori objects and T Tauri stars, can be explained by the presence of an opaque disc which occults part of the red-shifted emission. The profiles of the two lines differ significantly: $H\beta$ has a strong and wide absorption and a weak narrow emission while $H\alpha$ has strong emission and a weak absorption. In both cases, the blue-shifted absorption shows at least two components: one at -450 km s^{-1} , and the other at -150 km s^{-1} . While the low-velocity component remains almost constant over all the plateau phase, the high-velocity one is variable. In particular, in both lines, the latter shows a progressive decrease in extinction from February 2004 to March 2005 until the whole absorption disappears

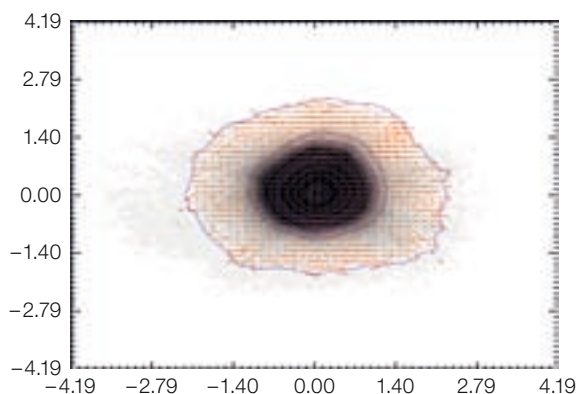


Figure 5: K -band polarimetric map of V1647 Ori and McNeil's nebula taken with NACO on 1 March 2006. North is up, East is to the left. Polarisation vectors are superimposed upon total intensity map and contours. Alignment and subtraction residuals are present in the inner region as well as along the diffraction pattern of the telescope. Polarisation values range from 10 to 20%. The highest values are detected North of V1647 Ori.

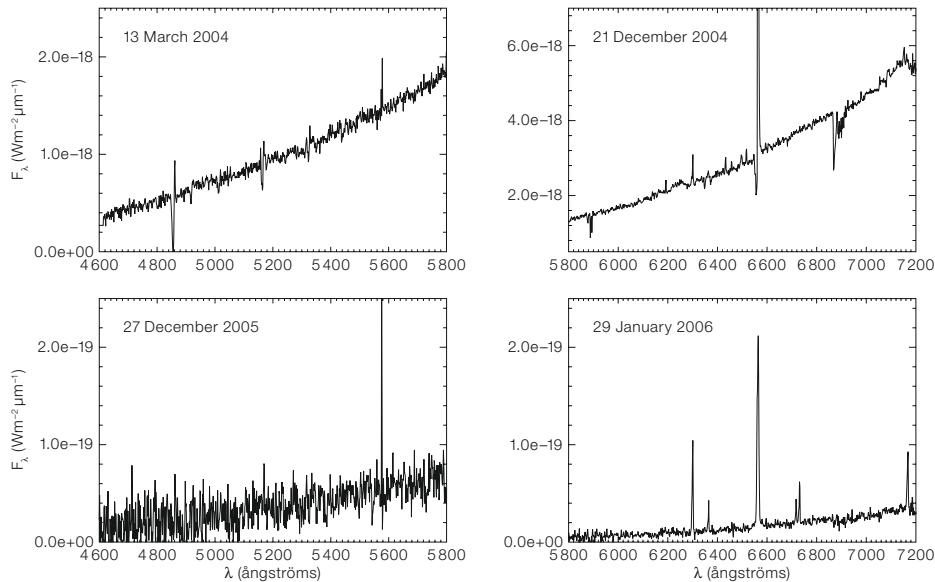


Figure 6: Examples of FORS2 optical spectra of V1647 Ori obtained during the plateau phase (top two panels) and during the fading phase (bottom two panels). *Plateau spectrum:* Clearly visible are H α and H β with P-Cygni profiles, Fe I (5328, 6191, 6494 Å), and Fe II (5169, 6432, 6516 Å) in emission, and absorption from the Na I doublet at 5889 and 5895 Å and the He I line at 5875 Å. *Fading phase spectrum:* No lines are detected in the blue part of the optical spectrum, while the red spectrum is characterised by strong emission lines from H α , [O I] 6300, 6363 Å, [Si II] 6717, 6731 Å and [Fe II] 7172 Å.

in the fading phase spectrum. Furthermore, on three nights (5 January, 18 February and 15 March 2005) the bluest absorption component of H α is seen in emission. The emission component also varies from night to night, displaying a change in equivalent width and line flux. P-Cygni signatures are also displayed by Fe lines. However, due to the low S/N of the spectra, the absorption component is clearly detected only for the Fe II 5169.08 Å transition.

In contrast to what is observed in the plateau phase, the spectra of V1647 Ori taken during the fading phase also show strong forbidden line emission (see Figure 6), providing evidence for hot (a few thousand K) gas close to V1647 Ori. The emission lines are used as tracers of Herbig-Haro objects, where a collimated jet from the central star collides with the ambient medium. Similar and perhaps newly formed ejecta could be responsible for the forbidden emission lines seen here. None of these forbidden lines were previously detected in the plateau spectrum.

Surprisingly, the outburst of V1647 Ori is also seen at longer wavelengths. Our TIMMI2 data confirm the increased mid-infrared flux: from the pre-outburst level of 0.53 Jy up to 7.6 Jy in the *N*-band on 8 March 2004. The 8–14 μ m spectrum is essentially featureless and flat all along the spectral range. Ten months later, in

December 2004, the mid-infrared flux of V1647 Ori had dropped by a few Jy. The spectrum is again flat and featureless. Within the accuracy of these measurements ($\sim 10\%$), the flux level remains constant between December 2004 and March 2005. Thus, also in the mid-IR the system experienced a plateau phase. The rapid fading seen in the optical is also experienced by the system in the mid-infrared: on 11 January 2006, the flux level at 12 μ m had dropped to 0.9 Jy, still considerably higher than the pre-outburst level. Also in this case the spectrum is flat and featureless.

A consistent model for the 2003–2006 outburst of V1647 Ori

Pre-main-sequence stars are known to be intrinsically variable objects. Commonly observed variability mechanisms include solar-like coronal activity, spots on the stellar surface, stellar pulsation, partial obscuration and subsequent clearing of the line of sight. These processes are however unable to generate the $44 L_{\odot}$ luminosity increment produced by V1647 Ori and to produce a six-magnitude burst in the optical lasting for more than two years. To release such an amount of energy, the existence of a secondary luminosity source is necessary. Similar brightening events from FU Orionis stars are explained by a sudden increase of the mass accretion rate from

a circumstellar disc onto the central star. The increased accretion rate produces an accretion luminosity which may overwhelm the stellar brightness. Such a process can explain both the dramatic brightening (from X-ray to the infrared) as well as the strong H α emission observed in the recent outburst of V1647 Ori.

As a consequence of the enhanced accretion rate, a strong wind develops from the disc's surface. The blue-shifted absorption components of H α and H β in the spectrum of V1647 Ori are signatures of this wind. The disappearance of the absorption component in H α during the fading phase is a confirmation that the strong wind ceased and that the system has been going back to a phase of slow accretion. The accretion disc alone is not able to produce the long wavelength ($\lambda \geq 10 \mu$ m) emission observed, unless it flares strongly over a large range of distance scales. The submillimetre continuum flux during the outburst remained at its pre-outburst level and there are no signatures of flux changes in these wavelength regimes (Andrews et al. 2004). These findings are consistent with the presence of a dusty circumstellar envelope, probably a remnant of the natal cloud which formed V1647 Ori.

Muzerolle et al. (2005) attempt to reproduce the spectral energy distribution (SED) of V1647 Ori by means of a standard viscous accretion disc and of an

optically thin envelope. Their model predicts a 10 μm emission feature that is produced by silicate dust grains. However, our multi-epoch mid-infrared spectroscopy reveals a flat and featureless spectrum during the whole outburst duration, which is highly unusual. In FU Orionis objects the silicate feature is seen sometimes in emission and sometimes in absorption. These differences are probably caused by differences in the optical thickness of the system at 10 μm . Our suggestion is that even in the mid-infrared the bulk of the emission is produced by the gas in a dust-free region of the disc, naturally producing a nearly featureless spectrum in the mid-infrared. The emission at longer wavelengths would still be dominated by the dust in the envelope, and therefore not experience the brightness variations associated with the outburst.

Outbursts in pre-main-sequence stars historically have been classified into two main groups, based upon their similarity to the prototypes FU Orionis and EX Lupi (Herbig 1977), depending on outburst duration, maximum magnitude variation and spectral features at maximum light. Since the onset of the outburst of V1647 Ori, it has been debated whether this system is either an FUOR (after FU Orionis) or an EXOR object (after EX Lupi). Table 1 shows that V1647 Ori resembles some aspects of an EXOR (outburst duration, recurrence of the outburst), and some aspects of an FUOR (magnitude rise, SED). However the recurrence timescale of the outburst has an intermediate value between the two classes. The emission line spectrum is clearly distinct from either the absorption line spectrum of an FUOR or the T Tauri-like spectrum of an EXOR (where the H lines show an inverse P-Cygni profile). V1647 Ori may thus be considered an intermediate case between these two classes of objects.

Implications for disc instability mechanisms

A common denominator in all young eruptive stars detected so far seems to be the presence of circumstellar material as well as that of a reflection nebula. These structures are likely remnants of the infalling envelope. The infalling envelope is a potential reservoir of mass for the disc which experiences recursive outbursts. Assuming that the bolometric luminosity during the outburst is dominated by the accretion luminosity, Muzerolle et al. (2005) estimate a mass accretion rate of $\sim 10^{-5} M_{\odot} \text{ yr}^{-1}$ for V1647 Ori. Considering the 2–3-year duration of the outburst and the 37-year recurrence timescale, a constant envelope infall rate of $\sim 7 \times 10^{-7} M_{\odot} \text{ yr}^{-1}$ is necessary to replenish the disc after each outburst. The disc accretion rate during the quiescent phase is estimated to be $\sim 6 \times 10^{-7} M_{\odot} \text{ yr}^{-1}$.

Submillimetre maps reveal that FU Orionis stars have accretion discs that are larger and more massive than those of T Tauri stars and are comparable in mass to those seen around Class I sources (i.e. young stellar objects with flat or rising infrared spectral energy distribution and which are believed to be in an earlier evolutionary stage than T Tauri stars). The circumstellar material around V1647 Ori accounts for 0.04 M_{\odot} which is slightly larger than the disc mass of a T Tauri star ($\sim 0.01 M_{\odot}$). All these findings suggest that outbursts *only* occur in Class I sources, when the star is still embedded in the infalling envelope. The outburst duration and mass accretion rate during outburst seem to correlate with the infall rate (see Table 1): objects with higher infall rates have longer outbursts and reach higher accretion rates, while objects with smaller infall rates experience short-lived outbursts. The occurrence of short outbursts might suggest that the

envelope is becoming thinner, i.e. that the system is in a transition phase from an embedded Class I source to an optically visible star surrounded by a protoplanetary disc (Class II).

The cause of the 2003–2006 outburst of V1647 Ori, seems clear: a disc instability event occurred in mid-2003, which led to a temporary increase of the mass accretion rate onto the central star. In due time, the disc will be replenished again by infall of matter from the circumstellar envelope and we may expect another outburst of this system around 2040. Our infrared data shows that the disc around V1647 Ori does not appear to be sufficiently massive for its outburst to have been caused by a gravitational collapse of the disc. Instead, our data are consistent with the occurrence of a thermal instability in the inner disc. The presence of a circumstellar envelope around the star/disc system and the outburst statistics of all FUOR and EXOR events suggest that these instability events must be recursive and occur only in a specific stage of the evolution of a young star. At present, the parameter(s) that lead to differences in outburst properties are still unclear, although the mass of the central star and the infall rate from the envelope seem to be good candidates.

References

- Andrews S. M., Rothberg B. and Simon T. 2004, ApJ 610, L45
 Grosso N. et al. 2005, A&A 438, 159
 Herbig G. H. 1977, ApJ 217, 693
 Magnier E. A. et al. 1999, A&A 346, 441
 McNeil J. W., Reipurth B. and Meech K. 2004, IAU Circular 8284, 1
 Muzerolle J. et al. 2005, ApJ 620, L107

	FUORs	V1647 Ori	EXORs
Outburst duration	> 10 yr	2.6 yr	~ 1 yr
Outburst recurrence	> 200 yr	37 yr	5–10 yr
Mass accreted during outburst	> $10^{-3} M_{\odot}$	$2.5 \times 10^{-5} M_{\odot}$	10^{-6} – $10^{-5} M_{\odot}$
Magnitude variation	$\Delta V = 4$ –6 mag	$\Delta V = 6$ mag	$\Delta V = 2$ –5 mag
Outburst accretion rate	$10^{-4} M_{\odot} \text{ yr}^{-1}$	$10^{-5} M_{\odot} \text{ yr}^{-1}$	10^{-6} – $10^{-5} M_{\odot} \text{ yr}^{-1}$
Envelope infall rate	$5 \times 10^{-6} M_{\odot} \text{ yr}^{-1}$	$7 \times 10^{-7} M_{\odot} \text{ yr}^{-1}$	10^{-7} – $10^{-6} M_{\odot} \text{ yr}^{-1}$
Spectral features	F/G supergiant absorption-line spectrum	Emission-like spectrum, P-Cygni lines	T Tauri-like emission-line spectrum

Table 1: Comparison of outburst properties of V1647 Ori with those of FU Orionis objects (FUORs) and EX Lupi type outbursts (EXORs).

The VLT-FLAMES Survey of Massive Stars

Chris Evans¹
 Ian Hunter²
 Stephen Smartt²
 Danny Lennon^{3,8}
 Alex de Koter⁴
 Rohied Mokiem⁵
 Carrie Trundle²
 Philip Dufton²
 Robert Ryans²
 Joachim Puls⁶
 Jorick Vink⁷
 Artemio Herrero⁸
 Sergio Simón-Díaz⁹
 Norbert Langer¹⁰
 Ines Brott¹⁰

- 1 UK Astronomy Technology Centre, Edinburgh, United Kingdom
- 2 Queen's University Belfast, Northern Ireland, United Kingdom
- 3 Space Telescope Science Institute, Baltimore, USA
- 4 University of Amsterdam, the Netherlands
- 5 OC&C Strategy Consultants, Rotterdam, the Netherlands
- 6 Universitäts-Sternwarte, Munich, Germany
- 7 Armagh Observatory, Northern Ireland, United Kingdom
- 8 Instituto de Astrofísica de Canarias, Tenerife, Spain
- 9 Geneva Observatory, Switzerland
- 10 University of Utrecht, the Netherlands

The VLT-FLAMES Survey of Massive Stars was an ESO Large Programme to understand rotational mixing and stellar mass loss in different metallicity environments, in order to better constrain massive star evolution. We gathered high-quality spectra of over 800 stars in the Galaxy and in the Magellanic Clouds. A sample of this size is unprecedented, enabled by the first high-resolution, wide-field, multi-object spectrograph on an 8-m telescope. We developed spectral analysis techniques that, in combination with non-LTE, line-blanketed model atmospheres, were used to quantitatively characterise every star. The large sample, combined with the theoretical developments, has produced exciting new insights into the evolution of the most massive stars.

Massive stars dominate their local environment via their intense radiation fields, their strong winds and, ultimately, in their death as core-collapse supernovae. Larger telescopes and new instrumentation have provided the means to observe individual massive stars beyond the Milky Way – in the Large and Small Magellanic Clouds (LMC and SMC), in M31, and beyond. In parallel to this, the theoretical models needed to interpret the observations have become increasingly sophisticated, incorporating the effects of stellar winds (a far from trivial problem!) and opacities for the millions of metallic transitions occurring in their atmospheres. While our understanding of massive stars has improved significantly over the past 30 years, key questions remain concerning the role of metallicity (i.e. environment) on their stellar winds and rotational velocities, and the efficiency of rotational mixing in their interiors and atmospheres.

The delivery of FLAMES to the VLT was the catalyst for our Large Programme, targeting O- and early B-type stars in fields centred on stellar clusters in the Galaxy and in the Magellanic Clouds (e.g. NGC 346 in the SMC, Figure 1). The LMC and SMC are metal poor when compared to the Solar Neighbourhood, with metallicities of ~ 50 % and 25 % solar, respectively. With the multiplex advantage of

FLAMES, we were able to obtain a large observational sample of massive stars, in three distinctly different environments. Six of the standard, high-resolution ($R \sim 20\,000$) settings of the Giraffe spectrograph were used, giving continuous coverage from 385–475 nm in the blue, combined with red spectra covering 638–662 nm (which includes the H α Balmer line). An overview of the observations was reported in this publication by Evans et al. (2005a), with more detailed descriptions given by Evans et al. (2005b; 2006). This unique data set has enabled us to test theoretical predictions of the physical properties of massive stars, and to provide valuable empirical information to groups working on evolutionary models. Here we summarise the key results from the ten refereed papers now published from the survey.

Metallicity-dependent stellar winds

The out-flowing winds observed in massive stars are thought to be driven by momentum transferred from the radiation field to metallic ions in their extended atmospheres. A logical consequence of this mechanism is that the intensity of the outflows should vary with metallicity (Z), with the prediction from Monte-Carlo models that the mass-loss rates should



Figure 1: VLT-FORS H α -image of NGC 346, the largest H II region in the Small Magellanic Cloud and one of our target fields observed with FLAMES (E. Tolstoy/ESO Archive).

scale as $Z^{0.69}$ (Vink et al. 2001). Such predictions are far from just an interesting quirk of stellar astrophysics; reduced mass-loss rates at low metallicity mean that an O-type star will lose less of its initial mass and angular momentum over its lifetime – this not only has a direct effect on the late stages of stellar evolution, but also on the nature of the final explosion as a supernova or a gamma-ray burst (GRB).

Analysis of O-type spectra with model atmospheres can be a complex, time-consuming process. In addition to the usual parameters used to characterise a star (temperature, luminosity, gravity, chemical abundances), we also need to describe the velocity structure and mass-loss rate of the wind. For the FLAMES project we adopted an innovative, semi-automated approach to the analysis, employing genetic algorithms to fit the observations with synthetic spectra from FASTWIND model atmospheres (Mokiem et al. 2005). Comparisons with published results for Galactic stars demonstrated the validity of the method, which was then used to analyse the O-type spectra from the FLAMES observations in the SMC and LMC (Mokiem et al. 2006, 2007a).

To investigate the effects of metallicity we have considered the modified wind-momentum–luminosity relation (WLR). This is a function of the mass-loss rate, terminal velocity and stellar radius, which is well correlated with stellar luminosity. In Figure 2 we show the observed WLRs for the LMC and SMC samples, compared to Galactic results obtained using the same models; the 1-sigma confidence intervals are shown as grey areas. The three empirical fits are clearly separated, providing quantitative evidence for reduced wind intensities at decreased metallicities, and showing for the first time that the wind intensities of stars in the LMC are intermediate to those in the Galaxy and SMC. Figure 2 also shows the theoretical predictions using the prescription from Vink et al. (2001). There is a systematic offset between the observed and predicted relations (perhaps arising from clumping of material in the winds), but the relative separations are in good agreement. From the FLAMES results we find a Z -dependence with exponents in the range 0.72 to 0.83 (depending on

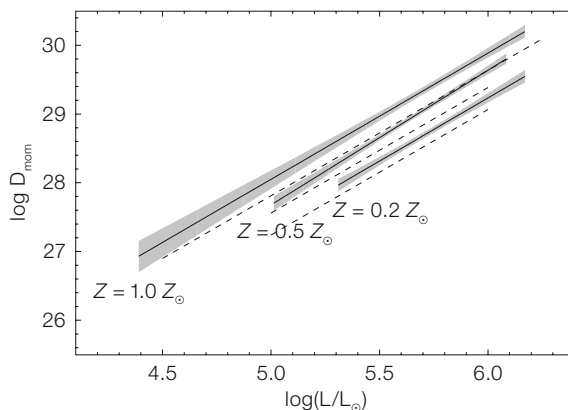


Figure 2: Comparison of the observed wind-momentum–luminosity relations (solid lines) with theoretical predictions (dashed lines). For each set, the upper, middle and lower relations correspond to Galactic, LMC and SMC results respectively.

assumptions regarding the clumping), as compared to $Z^{0.69 \pm 0.10}$ from theory (Vink et al. 2001).

This observational test is important for a number of areas in contemporary astrophysics. The reduced mass-loss rates at lower metallicity mean that less angular momentum will be lost over the star's lifetime, i.e. an evolved star in a low metallicity environment would be expected to retain a larger fraction of its initial rotational velocity compared to a similar star in the Milky Way. Indeed, the rotational velocity distribution for our unevolved (i.e. luminosity class IV or V) SMC stars, appears to have preferentially faster velocities when compared to Galactic results – unfortunately the statistical significance of this result is limited by the relatively small number of unevolved O-type stars in our sample, but we will return to this later using the much larger sample of B-type stars. These effects mean that at low metallicity a larger fraction of stars would be expected to undergo chemically-homogeneous evolution, suggested as a channel for the progenitors of long-duration GRBs (e.g. Yoon et al. 2006).

This empirical test of the mass-loss scaling also reinforces the need to consider metallicity when interpreting observations of distant, unresolved star-forming galaxies, e.g. via the inclusion of low-metallicity spectral libraries in population synthesis codes to interpret the rest-frame ultraviolet observations of Lyman-break galaxies.

Chemical composition of the Magellanic Clouds

Studies of stellar abundances in rapidly-rotating stars are complicated by their broadened lines, which is why most observational effort in the past has been directed at narrow-lined (i.e. slowly-rotating) stars. Thus, before investigating the global trends in the whole sample, we first used the narrow-lined B-type stars ($v \sin i < 100$ km/s) to determine precise, present-day abundances for the LMC and SMC.

The TLUSTY model atmosphere code was used to analyse this sample of over 100 B-type stars (Hunter et al. 2007, Trundle et al. 2007). The present-day composition of the LMC and SMC, as traced by these slowly-rotating B-type stars, is listed in Table 1. Note that the relative fraction of our SMC and LMC abundances, as compared to Solar values, changes from element to element. Specifically, it has been known for some time that the initial abundances of carbon and nitrogen are significantly underabundant when compared to the heavier elements in the Clouds, i.e. simply scaling solar abundances does not best reproduce the observed patterns.

Stellar temperatures as a function of metallicity

The narrow-lined B-type stars were also used to investigate effective temperatures as a function of spectral type (Trundle et al. 2007); the resulting temperature calibrations are presented in Table 2. The well-known dependence of temperatures

Element	Solar	LMC	SMC
C	8.39	7.73 (0.22)	7.37 (0.10)
N	7.78	6.88 (0.13)	6.50 (0.05)
O	8.66	8.35 (0.49)	7.98 (0.21)
Mg	7.53	7.06 (0.34)	6.72 (0.15)
Si	7.51	7.19 (0.48)	6.79 (0.19)
Fe	7.45	7.23 (0.51)	6.93 (0.27)

Table 1: Present-day composition of the LMC and SMC, taken from Hunter et al. (2007) and Trundle et al. (2007). Abundances are given on the scale $12 + \log[X/H]$, with the relative fraction compared to the Solar results (Asplund et al. 2005) given in parentheses. Due to uncertainties of the absolute values, the fractions quoted for iron are relative to our Galactic results.

Spectral Type	Milky Way V	LMC			SMC		
		I	III	V	I	III	V
B0	30,650	28,550	29,100	31,400	27,200		32,000
B0.2	(29,050)	(26,950)	(27,850)	30,250	(25,750)		30,800
B0.5	27,500	25,350	(26,650)	29,100	(24,300)		29,650
B0.7	(25,900)	23,750	(25,400)	(27,950)	(22,850)	25,300	28,450
B1	24,300	22,150	24,150	26,800	22,350	23,950	27,300
B1.5	22,700	20,550	22,950	25,700	20,650	(22,550)	(26,100)
B2	22,100	18,950	21,700	24,550	18,950	21,200	24,950
B2.5	19,550	17,350	20,450	23,400	17,200	19,850	
B3	17,950	15,750	19,250		15,500	18,450	
B5		14,150			13,800		

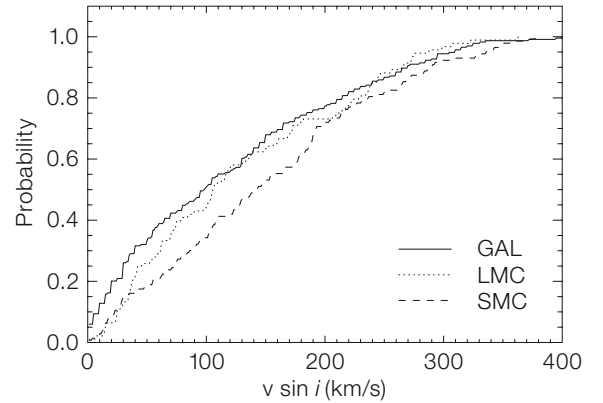


Table 2: Effective temperatures of B-type stars as a function of spectral type, metallicity, and luminosity class, taken from Trundle et al. (2007). The values in parentheses are interpolated.

Figure 3: Cumulative distribution functions for the rotational velocities of Galactic field stars, compared with the LMC and SMC results from FLAMES – faster velocities are seen at lower metallicity.

on luminosity class is evident, i.e. supergiant stars with their lower gravities, and more extended atmospheres, are found to be cooler than dwarfs of the same spectral type. We also find evidence of a metallicity dependence of the temperatures at a given spectral type. This is thought to arise from the effects of line blanketing, whereby the cumulative opacity of the huge number of spectral lines introduces additional back scattering, leading to changes in the ionisation balance and effective temperature in the atmosphere (see Mokiem et al. 2006, and references therein). This effect is well documented in O-type stars (e.g. Mokiem et al. 2007a), but the FLAMES survey has provided the first evidence for it in B-type stars – there is a relatively small difference between the results for the LMC and SMC, but there is a clear offset seen for the Galactic stars.

Calibrations such as these are widely used to provide temperature estimates in instances where high-quality spectroscopy of a star is not available, but its spectral type is known; the FLAMES results highlight the need, and provide the necessary information, to consider

metallicity effects when adopting such temperature estimates.

Low-metallicity stars spin faster

The prevailing viewpoint for the past decade has been that rotation strongly influences the evolutionary path of O- and B-type stars. Furthermore, it has long been assumed that stars should rotate more quickly at low metallicities. While there have been some reason to believe this (e.g. higher fractions of Be-type stars in the Clouds) it has never been verified quantitatively. As rotating stellar models predict that excess nitrogen and helium, produced during core hydrogen burning, can be mixed to the surface, abundances of these elements from the FLAMES survey can be used to test the theories.

We developed new spectral-analysis tools based on TLUSTY model atmospheres to rapidly analyse large numbers of quickly-rotating stars. We were able to determine physical parameters, rotational velocities and nitrogen abundances for all of the B-type stars observed in the LMC and SMC with velocities up to

300 km/s (~ 400 stars, Hunter et al. 2008a). The size of the sample is the most extensive to date, and the first in the Clouds that is large enough to model the underlying distribution of rotational velocities by assuming random angles of inclination of the rotation axes. As mentioned earlier, the O-type stars will be expected to slow down over their main-sequence lifetimes as they will loose angular momentum as a consequence of mass loss by their winds; we therefore only considered stars with masses less than $25 M_{\odot}$. In Figure 3 we show the cumulative probability functions for $v \sin i$ of the core-hydrogen-burning (i.e. giant and dwarf) B-type stars in the SMC and LMC – there is a clear difference between the two curves, with the SMC stars characterised by faster rotational velocities.

To extend this comparison to higher metallicity, we first needed to define an appropriate Galactic sample. Most of the Galactic stars observed in the survey were members of the central clusters, whereas our LMC and SMC stars are predominantly field stars. This distinction is important given that rotational veloci-

ties for our Galactic stars were found to be larger than for the field star population (Dufton et al. 2006). The Galactic curve shown in Figure 3 was therefore constructed using $v \sin i$ results from published surveys of field stars (see further discussion by Hunter et al. 2008a). Assuming random angles of inclination, the median intrinsic rotational velocities for the Galactic, LMC and SMC stars ($M < 25 M_{\odot}$) are 125, 135, and 183 km/s respectively. We have clear evidence (which is significant at the 3-sigma level) that the massive stars in the SMC rotate more quickly than in the Milky Way, and for the first time have a reliable intrinsic rotational velocity distribution in the SMC and LMC. The results for the O-type SMC stars have already been used by Yoon et al. (2006) to predict the rate of GRBs in the Universe from homogeneously-mixed massive stars. However, it is clear from recent work that stars in bound clusters appear to rotate significantly more quickly than stars in the field. It remains to be seen if the place of birth is as important as initial metallicity in determining the intrinsic rotation rate of a star. This is an important open question for future surveys of massive stars.

Rotational mixing is not as dominant as we thought

To investigate the impact of rotation on surface nitrogen abundances, new evolutionary models were calculated at LMC metallicity (Brott et al. in prep.). Aside from the effects of mass loss, other factors lead to changes in $v \sin i$ with time, primarily the contraction/expansion of the star, meridional circulation, internal magnetic fields and diffusion effects. Rather than simply scaling solar abundances, the new models adopt the chemical composition from Table 1. The mixing efficiency in the models was then calibrated to reproduce the observed surface nitrogen abundance at the end of core hydrogen burning for a $13 M_{\odot}$ model (the mean mass of the LMC stars in our sample).

Figure 4 shows the nitrogen abundances, as a function of $v \sin i$, for the LMC B-type stars (Hunter et al. 2008b). Typical uncertainties are of order 0.2–0.3 dex, so the scatter in the results indicates genuine differences in the surface nitro-

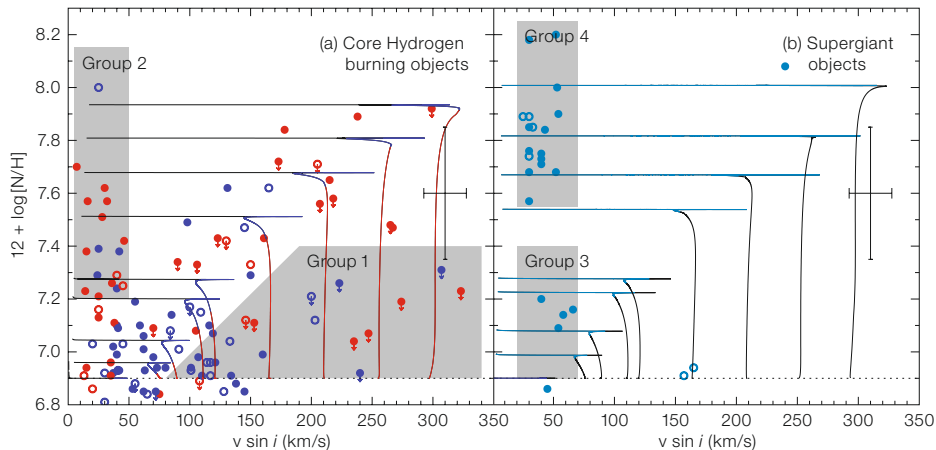


Figure 4: Nitrogen abundances ($12 + \log[\text{N}/\text{H}]$) compared to projected rotational velocities for core-hydrogen-burning (left panel) and supergiant B-type stars (right panel) in the LMC. The solid lines are new evolutionary

tracks (Brott et al., in prep.), open circles are radial velocity variables, downward arrows are upper limits, and the dotted horizontal line is the LMC baseline nitrogen abundance.

gen enrichment in both the core-hydrogen-burning stars (dwarfs and giants, left panel) and the supergiants (right panel).

There are two groups (labelled as Groups 1 and 2 in the shaded regions of the left-hand panel) that appear inconsistent with rotating models. The blue points in Group 1 comprise rapidly-rotating stars that appear to have undergone little chemical mixing, and yet they have surface gravities that indicate they are near the end of core hydrogen burning. According to the single-star models that include the effects of rotational mixing, the observed nitrogen overabundances in these stars are expected to be larger by ~ 0.5 dex (at least for the more massive objects, in which the mixing is expected to be most efficient). We see no evidence of binarity in the spectra of many of these stars (although we note that the observations were not optimised for binary detection), presenting a conflicting picture when compared with the single-star predictions of rotationally-induced mixing.

The 14 (apparently single) core-hydrogen-burning stars in Group 2 are equally puzzling in that they are rotating very slowly (less than 50 km/s) and yet show significant nitrogen enrichment. For a random orientation, we would expect about two of these to be rapidly-rotating stars viewed pole-on, but this is highly unlikely

for all 14, and we conclude that the majority are intrinsically slow rotators. Recent studies of Galactic β -Cepheid stars have found a correlation between nitrogen enrichment and magnetic fields (Morel et al. 2006); perhaps the enrichments found in the slowly-rotating B-type stars in Figure 4 are somehow linked to magnetic fields.

The results for the supergiants can be considered as two groups: Group 3, with relatively normal levels of enrichment, and Group 4, with much larger abundances ($12 + \log[\text{N}/\text{H}] > 7.6$). Simplistically one might think of these as pre-red-supergiant stars (Group 3) and post-red-supergiant stars (Group 4). However, while the abundances in Group 4 are consistent with predictions, the models cannot reproduce their effective temperature on the Hertzsprung-Russell diagram; some of the enriched objects show evidence of binarity, so mass transfer may also be important. These results are also supported by analysis of the SMC and Galactic stars (Hunter et al. in prep.); reconciling these observations with the evolutionary models demands further study.

A serendipitous benefit of multi-epoch service observations

Owing to the time-sampling of the service observations, the survey has discovered

a wealth of new binary systems, some of which will be the subject of forthcoming papers. Moreover, cross-correlation of the radial velocities of the Calcium *K* line in repeat exposures of the same stars show a typical scatter of ± 2 km/s, demonstrating the excellent stability of the Giraffe spectrograph. The global picture in terms of binarity is also of interest – the lower limit to the binary fractions in our three fields with the best time coverage (N 11, NGC 346, and NGC 2004) are in the range 25–35%. Curiously, we find a much lower binary fraction for stars in the NGC 330 FLAMES field (4%) – whether this is simply a consequence of less thorough time-sampling, or if the binary fraction is genuinely different to that found in the other fields, remains unclear. Optimised follow-up of each of the fields will provide more rigorous binary fractions, a vital constraint to models of star formation that is lacking in the current literature.

Unanswered questions and problems

The FLAMES survey has provided a valuable and unique source of empirical information, enabling a huge step forward in our understanding of massive star evolution. However, it has unexpectedly raised new and critical problems that still challenge our understanding of these enigmatic stars:

– While rotational mixing appears to play a role in the enrichment of surface nitro-

gen in massive stars, our results from B-type stars demonstrate that it is not the only process, particularly at low rotational velocities. This result presents a significant new challenge to theorists working on evolutionary models.

– We have found tentative evidence that O-type stars in the SMC lose less angular momentum via their stellar winds than Galactic stars, i.e. the unevolved SMC stars are rotating more quickly. This principle underpins one of the potential channels for long-duration GRBs, but the significance of our result is limited by the number of O-type stars in the FLAMES sample. A more expansive programme examining the rotational velocities of O-type stars in the SMC is required to confirm this result.

– The intrinsic rotational velocity distribution of O- and B-type stars appears indistinguishable, but the B-type stars tend to rotate at a greater fraction of critical (Keplerian) velocity, potentially leading to a greater number of GRBs at low metallicity than predicted by current models – new theoretical calculations of GRBs from stars with initial masses ranging from 10 to 25 M_{\odot} are required to investigate this.

– Evolutionary models of single stars do not reproduce the observed temperatures of the nitrogen-rich B-type supergiants (Group 4 in Figure 4), i.e. they do not predict ‘blue loops’ at sufficiently high temperatures, nor high enough

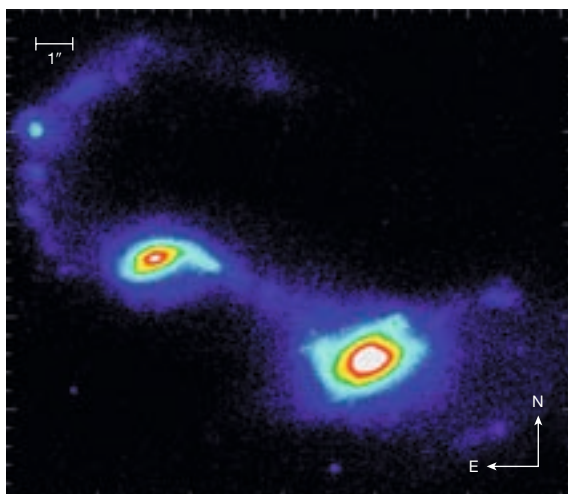
masses. Continued spectroscopic monitoring of the nitrogen-enhanced supergiants for long-period binaries would provide an essential constraint on further work in this area.

– There is compelling evidence that stellar winds in O-type stars are clumped. If the clump properties do not depend on metal content, nor the rate of mass loss, the wind scalings presented here will not be affected. However, to quantify the effects of wind clumping properly requires further observational and theoretical investigation.

Finally, we note that all of the spectra from the survey are now publicly available at <http://star.pst.qub.ac.uk/~sjs/flames/>.

References

- Asplund M. et al. 2005, ASPC 336, 25
- Dufton P. L. et al. 2006, A&A 457, 265
- Evans C. J. et al. 2005a, The Messenger 122, 36
- Evans C. J. et al. 2005b, A&A 437, 467
- Evans C. J. et al. 2006, A&A 456, 623
- Hunter I. et al. 2007, A&A 466, 277
- Hunter I. et al. 2008a, A&A 479, 541
- Hunter I. et al. 2008b, ApJ, arXiv:0711.2267
- Mokiem M. R. et al. 2005, A&A 441, 711
- Mokiem M. R. et al. 2006, A&A 456, 1131
- Mokiem M. R. et al. 2007a, A&A 465, 1003
- Mokiem M. R. et al. 2007b, A&A 473, 603
- Morel T. et al. 2006, A&A 457, 651
- Trundle C. et al. 2007, A&A 471, 625
- Vink J. S. et al. 2001, A&A 369, 574
- Yoon S.-C., Langer N. and Norman C. 2006, A&A 460, 199



The image shows the infrared source IRAS 06035-7102 which is here resolved into two spiral galaxies in the process of interacting. The image was taken by NACO on the VLT and the high spatial resolution was enabled by adaptive optics and an artificial guide star produced by the Laser Guide Star Facility. More details can be found in ESO Press Release 27/07.

Seeking for the Progenitors of Type Ia Supernovae

Ferdinando Patat¹
 Poonam Chandra^{2,3}
 Roger Chevalier²
 Stephen Justham⁴
 Philipp Podsiadlowski⁴
 Christian Wolf⁴
 Avishay Gal-Yam⁵
 Luca Pasquini¹
 Ian Crawford⁶
 Paolo Mazzali^{7,8}
 Adalbert Pauldrach⁹
 Ken'ichi Nomoto¹⁰
 Stefano Benetti¹¹
 Enrico Cappellaro¹¹
 Nancy Elias-Rosa^{7,12}
 Wolfgang Hillebrandt⁷
 Douglas Leonard¹³
 Andrea Pastorello¹⁴
 Alvio Renzini¹¹
 Franco Sabbadin¹¹
 Josh Simon⁵
 Massimo Turatto¹¹

¹ ES0

² Department of Astronomy, University of Virginia, Charlottesville, USA

³ Jansky Fellow, National Radio Astronomy Observatory

⁴ Department of Astrophysics, University of Oxford, United Kingdom

⁵ Astronomy Department, California Institute of Technology, Pasadena, USA

⁶ School of Earth Sciences, Birkbeck College London, United Kingdom

⁷ Max-Planck-Institut für Astrophysik, Garching, Germany

⁸ INAF – Osservatorio Astronomico, Trieste, Italy

⁹ Institut für Astronomie und Astrophysik der Ludwig-Maximilians-Universität, Munich, Germany

¹⁰ Department of Astronomy, University of Tokyo, Japan

¹¹ INAF – Osservatorio Astronomico, Padova, Italy

¹² Universidad de La Laguna, Tenerife, Spain

¹³ Department of Astronomy, San Diego State University, USA

¹⁴ Astrophysics Research Centre, Queen's University Belfast, United Kingdom

Type Ia supernovae are thought to be thermonuclear explosions of accreting white dwarfs that reach a critical mass limit. Despite their importance as cosmological distance indicators, the nature of their progenitors has remained controversial. Observations carried out by our team with VLT-UVES led us to the detection of circumstellar material in a normal Type Ia supernova. The expansion velocities, densities and dimensions of the circumstellar envelope indicate that this material was ejected from the system prior to the explosion. The relatively low expansion velocities appear to favour a progenitor system where a white dwarf accretes material from a companion star which is in the red-giant phase at the time of the explosion.

The quest

Due to their enormous luminosities and their homogeneity, Type Ia Supernovae (hereafter SN Ia) have been used in cosmology as reference beacons, with the ambitious aim of tracing the evolution of the Universe (Riess et al. 1998; Perlmutter et al. 1999). Despite the progress made in this field, the nature of the progenitor stars and the physics which governs these powerful explosions are still uncertain. In general, they are thought to originate from a close binary system (Whelan and Iben 1973), where a white dwarf accretes material from a companion until it approaches the Chandrasekhar limit and finally undergoes a thermonuclear explosion. This scenario is widely accepted, but the nature of both the accreting and the donor star is not yet known, even though favourite configurations do exist (see Parthasarathy et al. 2007 for a recent review). But why is it so important to investigate the nature of the progenitor system? Besides the fundamental implications on the cosmological usage of SNe Ia, there are actually several other reasons to bother (Livio 2000). First of all, galaxy evolution depends on the radiation, kinetic energy and nucleosynthesis yields of these powerful events. Secondly, the knowledge of the initial conditions of the exploding system is crucial for understanding the physics of the explosion itself. Finally, identifying the progenitors and determining the SN rates

will allow us to put constraints on the theory of binary-star evolution.

Having in mind *why* we want to do this, the next question is, as usual, *how*. A discriminant between some of the proposed scenarios would be the detection of circumstellar material (CSM). However, notwithstanding the importance of the quest, all attempts at detecting direct signatures of the material being transferred to the accreting white dwarf in normal SNe Ia were so far frustrated, and only upper limits to the mass-loss rate could be placed from optical, radio and UV/X-ray emission. Claims of possible ejecta-CSM interaction have been made for a few normal objects, in which the presence of CSM is inferred by the detection of high-velocity components in the SN spectra. However, it must be noted that these features can be explained by a 3D structure of the explosion and, therefore, circumstellar interaction is not necessarily a unique interpretation. Furthermore, no velocity or density estimate is possible for the CSM material, even in the case that the high-velocity components in the SN spectra are indeed the effects of ejecta-CSM interaction.

Two remarkable exceptions are represented by the peculiar SNe 2002ic and SN 2005gj, which have shown extremely pronounced hydrogen emission lines, that have been interpreted as a sign of strong ejecta-CSM interaction. However, the classification of these supernovae as SNe Ia has been questioned, and even if they were SN Ia, they must be rare and hence unlikely to account for normal Type Ia explosions. As a matter of fact, the only genuine detection may be represented by the underluminous SN 2005ke, which has shown an unprecedented X-ray emission, at a 3.6 σ -level, accompanied by a large UV excess (Immler et al. 2006). These facts have been interpreted as the signature of a possible weak interaction between the SN ejecta and material lost by a companion star.

All the channels explored so far to detect CSM around Type Ia SN progenitors are based on the fact that sooner or later the fast SN ejecta will crash into the slow-moving material lost by the system in the pre-explosion phases in the form of stellar wind. This implicitly requires two

conditions to be fulfilled: a) there has to be interaction; and b) the amount of CSM and its density must reach some threshold values in order to produce a detectable interaction. Therefore, methods based on ejecta-CSM interaction will not be able to reveal this material if its amount is small and/or if it is placed rather far from the explosion site. But there is another possibility of revealing CSM, basically because of the transient nature of the SN event and its high luminosity.

In fact, if the SN is surrounded by a dusty environment, the scattered light will add with some delay to the SN signal (this is why this phenomenon is also known as a *light echo*), leaving certain signatures in the observed light curves and spectra (see Patat 2005 for a review on this subject). These effects are expected to be dependent on the distance of the scattering material from the SN itself. More precisely, if the dust is contained in a distant cloud (like for example in an intervening spiral arm of the host galaxy), the late time epochs of the observed SN evolution will be completely dominated by the light echo, as in the well-known cases of SNe 1991T and 1998bu. On the contrary, if the scattering material is confined within a small region surrounding the SN, the effects although present at all epochs, are subtle and can be confused with intrinsic SN properties (Patat et al. 2006).

Of course, if the dust is close enough to the SN, this is expected to feel the strong

radiation field produced during the explosion. Therefore, it is reasonable to expect variations in the physical conditions of the CSM, like dust evaporation and/or gas photoionisation.

It was while investigating these effects that we saw a possible way of revealing low amounts of CSM material without the need of having matter interaction. In fact, since in SNe Ia the UV flux bluewards of 350 nm undergoes severe line blocking by heavy elements like Fe, Co, Ti and Cr, they are capable of ionising possible CSM only within a rather small radius. Once the UV flux has significantly decreased past the post-maximum phase, then, if the material has a sufficiently high density, it can recombine, producing time-variable absorption features. Of course, if the material where these features arise is reached by the fast-moving ejecta, it will be shocked and ionised, causing the disappearance of such absorptions.

Among all possible inter/circumstellar absorption lines, the ubiquitous sodium D lines (589.0 and 589.6 nm) are the best candidates for this kind of study. In fact, besides falling in an almost telluric absorption-free spectral region, they are produced by a very strong transition, and hence detectable for rather small gas column densities. In addition, the ionisation potential of NaI is low (5.1 eV), and this ensures that even a weak UV field is able to have a measurable effect on its

ionisation, without the need for direct interaction.

With this idea in mind, the experimental path was rather clearly traced: obtain multi-epoch, high-resolution spectroscopy of the next bright SN Ia and look for absorption-line variability.

SN 2006X in M100

The first chance to test our idea came when SN 2006X was discovered in the Virgo Cluster spiral galaxy M100 on 4 February 2006 (Figure 1). A few days later, the object was classified as a normal Type Ia event occurring 1–2 weeks before maximum light and suffering substantial extinction. Prompt Very Large Array (VLA) observations have shown no radio source at the SN position, establishing one of the deepest and earliest limits for radio emission from a Type Ia, and implying a mass-loss rate of less than a few 10^{-8} solar masses per year (for a low wind velocity of 10 km s^{-1}). The SN was not visible in the 0.2–10 keV X-rays band down to the SWIFT satellite detection limit. All of this made of SN 2006X a perfect candidate to verify our idea.

An ESO Director General Discretionary Time proposal was submitted on 15 February and approved immediately afterwards. The observations started on 18 February and were carried out with the Ultraviolet and Visual Echelle Spec-

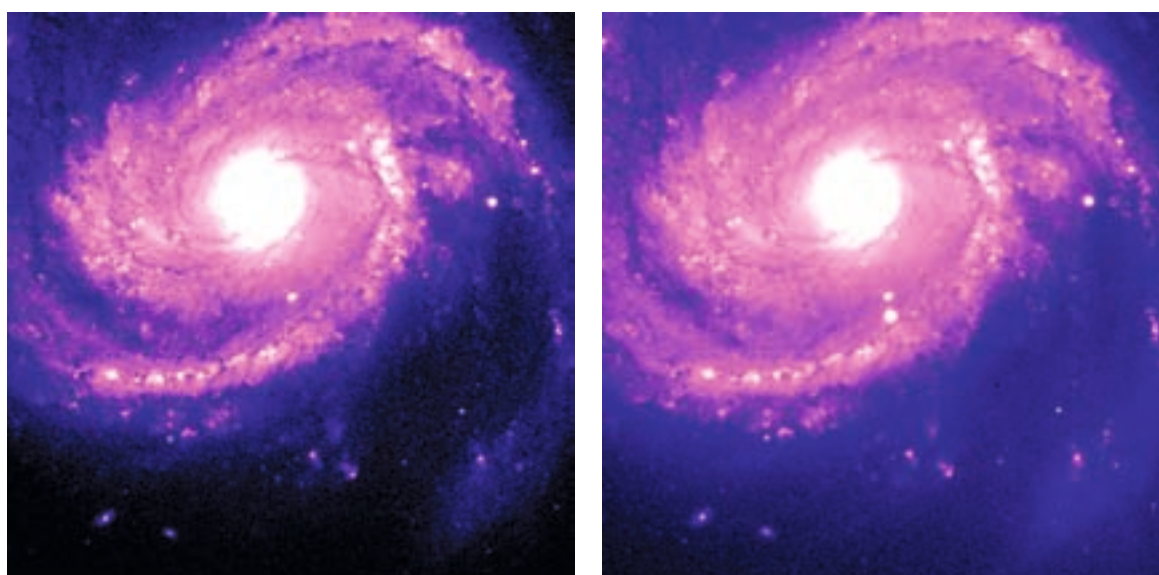


Figure 1: The host galaxy M100 before (left) and after (right) the explosion of SN 2006X. The images were taken with VLT-FORS1 in the R passband.

trograph (UVES) mounted at the Very Large Telescope on four different epochs, which correspond to days -2 , $+14$, $+61$ and $+121$ with respect to the B -band maximum light. Additionally, a fifth epoch (day $+105$) was covered with the High Resolution Echelle Spectrometer mounted at the 10-m Keck telescope. The data show a wealth of interstellar features, but the most remarkable finding is the clear evolution seen in the profile of the Na I D lines (Patat et al. 2007a). In fact, besides a strongly saturated and constant component, arising in the host galaxy disc, a number of features spanning a velocity range of about 100 km s^{-1} appear to vary significantly with time (Figures 2 and 3). SN 2006X is situated on the receding side of the galaxy, and the component of the rotation velocity along the line of sight at the apparent SN location is about $+75 \text{ km s}^{-1}$, which coincides with the strongly saturated Na I D component, the saturated Ca II H and K lines, and a weakly saturated CN vibrational band (see Figure 2). This feature, and its lack of time evolution, proves that the deep absorption arises within the disc of M100 in an interstellar molecular cloud (or system of clouds) that is responsible for the bulk of the reddening suffered by SN 2006X.

In contrast, the relatively blue-shifted structures of the Na I D lines show a rather complex evolution. For the sake of discussion, four main components, which we will indicate as A, B, C and D, can be tentatively identified in the first two epochs (Figure 3). Components B, C and D strengthen between day -2 and day $+14$ while component A remains constant during this time interval. The situation becomes more complicated on day $+61$: components C and D clearly start to decrease in strength; component B remains almost constant; component A becomes definitely deeper and is accompanied by a wide absorption that extends down to a rest-frame heliocentric velocity of about -50 km s^{-1} (Figure 3). After this epoch there is no evidence of evolution, and component A remains the most intense feature up to the last phase covered by our observations, more than four months after the explosion.

Variable interstellar absorption on comparably short timescales has been claimed for some Gamma Ray Bursts (GRB), and

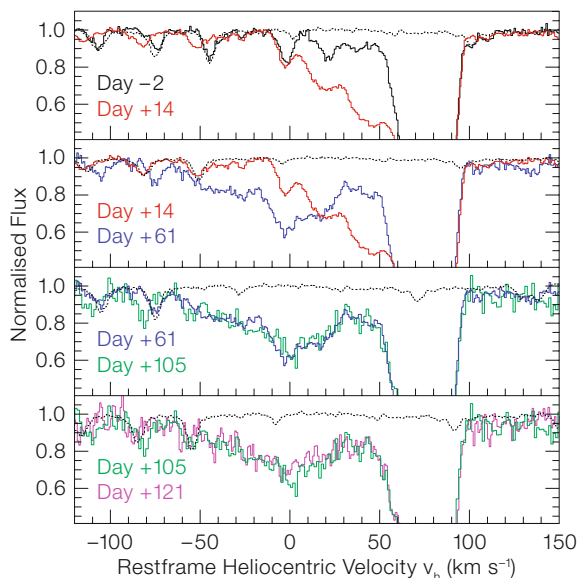


Figure 2: Time evolution of the sodium D_2 component region as a function of elapsed time since B -band maximum light. The heliocentric velocities have been corrected to the rest-frame using the host galaxy recession velocity. All spectra have been normalised to their continuum. In each panel, the dotted curve traces the atmospheric absorption spectrum.

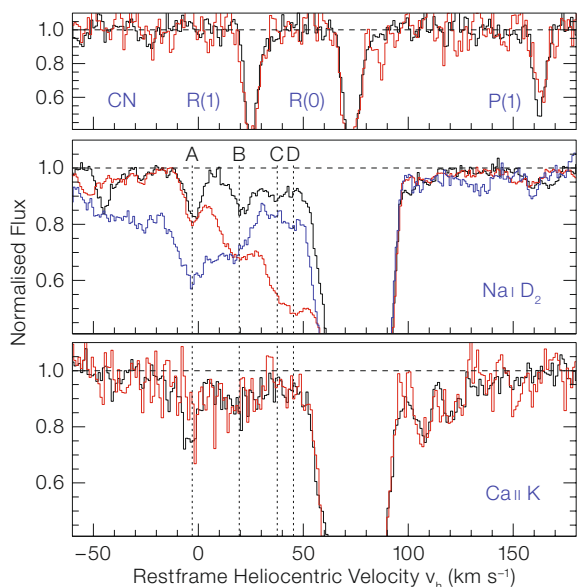


Figure 3: Evolution of the Na I D_2 and Ca II K line profiles between day -2 (black), day $+14$ (red) and day $+61$ (blue, Na I D_2 only). The vertical dotted lines mark the four main variable components at -3 (A), $+20$ (B), $+38$ (C) and $+45$ (D) km s^{-1} . For comparison, the upper panel shows $\text{R}(0)$, $\text{R}(1)$ and $\text{P}(1)$ line profiles of the CN (0-0) vibrational band. Colour coding is as for the other two panels.

it has been attributed by some authors to line-of-sight geometrical effects, due to the fast GRB expansion coupled to the patchy nature of the intervening absorbing clouds. Our data clearly show that despite the marked evolution in the Na I D lines, Ca II H and K components do not change with time (see Figure 2). Therefore, in the case of SN 2006X, transverse motions in the absorbing material and line-of-sight effects due to the fast SN photosphere expansion (typically 10^4 km s^{-1}) can be definitely excluded, since they would cause variations in all absorption features.

For this reason we conclude that the Na I features seen in SN 2006X, arising in a number of expanding shells (or clumps), evolve because of changes in the CSM ionisation conditions induced by the variable SN radiation field. In this context, the different behaviour seen in the Na I and Ca II lines is explained in terms of the lower ionisation potential of Na I (5.1 eV) with respect to Ca II (11.9 eV), their different recombination coefficients and photoionisation cross sections, coupled to a UV-deficient radiation field. Regrettably, not much is known about the UV emission of SNe Ia shortwards of 110 nm . As

we have already anticipated, from a theoretical point of view, one expects a severe UV line blocking, which reduces dramatically the flux of ionising radiation. Nevertheless, in the case of a SN Ia, the models show that this flux is sufficient to fully ionise Na I up to a distance of one light year ($\sim 10^{18}$ cm). However, since the recombination timescale must be of the order of 10 days to account for the observed variations, this requires a large electron density (10^5 cm $^{-3}$). Given the low abundance of any other element, such a high electron density can be produced only by partial hydrogen ionisation. On account of the severe line blocking, the flux of photons capable of ionising H is expected to be very small and this implies that the gas where the Na I time-dependent absorptions arise must be confined within a few 10^{16} cm from the SN.

In a SN Ia, the UV flux decreases by a factor of ten in the first two weeks after maximum light. Since at a distance of 10^{16} cm from the SN, the ionisation timescale for Na I is much shorter than the recombination timescale, the ionisation fraction grows with time following the increase of the UV flux during the pre-maximum phase, while after maximum it decreases following the recombination timescale. This would explain the overall growth of the blue component's depth, as shown by our data, in terms of an increasing fraction of neutral Na, while the different evolution of individual components would be dictated by differences in the densities and distances from the SN. Moreover, once all the sodium has recombined (which should happen within a month), there should be no further evolution, in qualitative agreement with the observations. Additionally, since the flux of photons that can ionise Ca II is more than four orders of magnitude less than in the case of Na I, the corresponding ionisation fraction is expected to be of a few per cent only. Therefore, the recombination does not produce measurable effects on the depth of Ca II H and K lines, as is indeed observed.

An upper limit to the H mass contained in the clumps generating the observed absorptions can be estimated from our observations, after making some conservative assumptions and using the Na I column densities deduced from the data.

The H mass turns out to be a few 10^{-4} solar masses (this value is reduced by a factor 100 for material at about 10^{16} cm, the most likely distance for components C and D; see below). Even in the case of complete ionisation, such an H mass would produce an H α luminosity which is two orders of magnitude below the upper limits set by our observations at all epochs and by any other SN Ia observed so far. Therefore, the absence of narrow emission lines above the detection limit is not in contradiction with the presence of partially ionised H up to masses of the order of 0.01 solar masses.

However, photo-ionisation alone cannot account for the fact that not all features increase in depth with time (Figure 2). In fact, on day +61, components C and D turn back to the same low intensity they had on day -2. One possible explanation is that the gas is re-ionised by some other mechanism, like the ejecta-CSM interaction. In this case, the absorbing material generating components C and D must be close enough to the SN so that the ejecta can reach it in about one month after the explosion (10^{16} cm for maximum ejecta velocities of 4×10^4 km s $^{-1}$). Similarly, in order not to be reached by the ejecta more than four months after, components A, B and the broad high-velocity components must arise at larger distances ($> 5 \times 10^{16}$ cm). This scenario is

not ruled out by the lack of radio emission from SN 2006X. In fact, in the light of our current understanding of the ejecta-CSM interaction mechanism, the presence of similar shells with masses smaller than a few 10^{-4} solar masses, cannot be excluded by radio non-detections of SNe Ia in general. Our findings are also consistent with upper limits on the radio flux set by our VLA observations, obtained about ten months after the explosion, which also confirm that SN 2006X is not more radio luminous than any other normal SNe Ia.

A new beginning?

If we adopt the velocity of the CN lines as indicative of the host galaxy rotation component along the line of sight at the SN location, then our observations provide solid evidence of CSM expanding at velocities that span a range of about 100 km s $^{-1}$ (Figure 2).

The most important implication of these observations is that they show that this circumstellar material was ejected from the progenitor system in the recent past. This almost certainly rules out a double-degenerate scenario for SN 2006X, where the supernova would have been triggered by the merger of two CO white dwarfs. In this case, no significant mass loss would

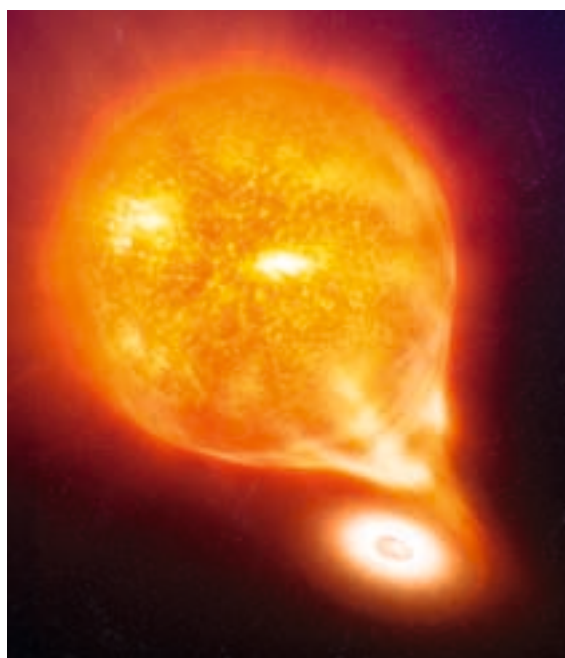


Figure 4: Artist's impression of the favoured configuration for the progenitor system of SN 2006X before the explosion. The White Dwarf (on the right) accretes material from the Red Giant star, which is losing gas in the form of stellar wind (the diffuse material surrounding the giant). Only part of the gas is accreted by the White Dwarf, through an accretion disc which surrounds the compact star. The remaining gas escapes the system and eventually dissipates into the interstellar medium (see ESO Press Release 31/07).

be expected in the phase immediately preceding the supernova. Thus, a single-degenerate model is the favoured model for SN 2006X, where the progenitor accreted from a non-degenerate companion star.

Mean velocities for the circumstellar material of 50 km s^{-1} are comparable to those reported for the winds of early red giant (RG) stars; velocities matching our observations are also expected for late subgiants. The observed material is moving more slowly than would be expected for winds from main-sequence donor stars or from compact helium stars. Of the two major formation channels proposed for SN Ia with a non-degenerate donor star, these wind velocities seem more consistent with the shorter-period end of the 'symbiotic' formation channel. Symbiotic systems are interacting binaries consisting of a late-type mass-losing giant in orbit with a hot companion, which accretes material from wind or Roche lobe overflow; they have been proposed as a viable channel for Type Ia SN explosions (Munari and Renzini 1992). The observed structure of the circumstellar material could be due to variability in the wind from the companion RG; considerable variability of RG mass loss is generally expected.

A potentially more interesting interpretation of these distinct features is that they arise in the remnant shells (or shell fragments) of successive nova outbursts, which can create dense shells in the slow-moving material released by the companion, also evacuating significant volumes around the progenitor star. Our cal-

culations have difficulty in matching the velocities in our observations if the nova shells are decelerated in a spherically symmetric wind. However, if the wind is concentrated towards the orbital plane this discrepancy could be removed, since the nova shell would be more strongly decelerated in the equatorial plane; in that case we would be observing the supernova close to the orbital plane. Not only might this be expected a priori, but observations of the 2006 outburst of RS Ophiuchi show that the nova ejecta are bipolar and that there is an equatorial density enhancement which strongly restrains the expansion of the nova shell, thus providing some support for such a scenario.

One crucial issue is whether what we have seen in SN 2006X represents the rule or is rather an exceptional case. Other cases of SNe Ia showing negative velocity components are known, like SNe 1991T and 1998es. Unfortunately, multi-epoch high-resolution spectroscopy is not available for these objects (to our knowledge, the SN 2006X data set is unique in this respect), and therefore time variability cannot be demonstrated. Nevertheless, the data clearly show components approaching the observer at velocities which reach at least 50 km s^{-1} with respect to the deep absorption that we infer to be produced within the discs of the respective host galaxies. This, and the fact that SN 2006X has shown no optical, UV and radio peculiarity, supports the conclusion that what we have witnessed for this object might be common at least for some normal SN Ia, even though variations due to different inclina-

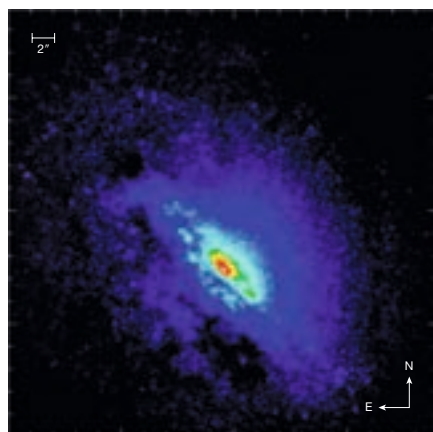
tions of the line of sight with respect to the orbital plane may exist.

What we have seen in 2006X is far from being completely understood and we are certainly left with more questions than answers. Even though the results obtained with multi-epoch, high-resolution observations of this event have already triggered a couple of similar studies (Patat et al. 2007b, Simon et al. 2007), the sample is simply too small to allow for any conclusion. Most likely, there is more than one channel leading to the same explosive theme, on top of which nature adds some variations, as the non perfect homogeneity of SNe Ia seems to tell us.

Rather than the end of an old story, we consider these findings as the beginning of a new one. We hope that the telescope time that has been allocated to our project will bring more insights into this field, answering at least a few of the questions that SN 2006X has posed us.

References

- Immler S. I. et al. 2006, ApJ 648, L119
 Livio M. 2000, in "Type Ia Supernovae: Theory and Cosmology", eds. J. C. Niemeyer and J. W. Truran, (Cambridge: CUP), 33
 Munari U. and Renzini A. 1992, ApJ 397, L87
 Parthasarathy M. et al. 2007, New Astronomy Reviews 51, 524
 Patat F. 2005, MNRAS 357, 1161
 Patat F. et al. 2006, MNRAS 369, 1949
 Patat F. et al. 2007a, Science 317, 924
 Patat F. et al. 2007b, A&A 474, 931
 Perlmutter S. et al. 1999, ApJ 517, 565
 Riess A. G. et al. 1998, AJ 116, 1009
 Simon J. D. et al. 2007, ApJ 671, L25
 Whelan J. and Iben I. 1973, ApJ 186, 1007



Colour coded K-band adaptive optics image obtained with VLT NACO and the Laser Guide Star Facility of the galaxy NGC 4945 which contains an obscured active nucleus. Close to the nucleus several luminous star clusters can be resolved. See ESO Press Photo 27e/07 for more details.



Fifteen ESO Fellows and the Head of the Office for Science in Chile in front of the APEX telescope.



Participants at the 2007 ESO Fellowship Symposium in Santiago.

Photos: (Upper) C. De Breuck, ESO;
(Lower) M. E. Gomez, ESO

The 2007 Users Feedback Campaign

Francesca Primas, Stéphane Marteau, Olivier Hainaut, Gautier Mathys, Martino Romaniello, Michael Sterzik (all ESO)

In a service organisation like ESO, user feedback is a vital component of its success, but receiving feedback on a regular basis is a rather challenging task. This article focuses on the main findings of the Feedback Campaign launched in early 2007, which targeted all Principal Investigators of Service Mode programmes approved over the last five years. Feedback collected from visiting astronomers about operational issues is also presented.

Very robust and efficient data flow operations, on one side, and a high degree of satisfaction among users, on the other, constitute two of the main ingredients for the success of ESO facilities. There are two major ways in which ESO operates its telescopes: Service Mode and Visitor Mode. The underlying operational model is roughly the same, i.e. both modes rely on established operational procedures and policies, sharing the same tools. These rules and their implementation are under constant evaluation and scrutiny by ESO staff, with the aim of improving the quality of the services offered. Feedback from those who make direct use of the ESO facilities and services, the user community, remains a key ingredient in this optimisation process. This feedback is triggered via the Users Committee and via questionnaires that include different sets of questions, on different topics and phases of the operational cycle. Service Mode users are asked to fill out the Service Mode Questionnaire (always available on the ESO Web), and visiting astronomers are always reminded to fill out the End of Mission report at the end of their observing run. This article aims at presenting and discussing the feedback ESO receives from its users. The main outcome of the 2007 Feedback Campaign, as well as of the End of Mission reports, is that users of ESO facilities are largely satisfied with our services.

How to trigger and receive feedback

ESO operates and maintains observing facilities and instruments on behalf of and for its user community and is always keen to receive feedback. However, implementing a constant feedback flow is a very challenging task, especially in an era where everybody's life is full and busy, and we are all bombarded with User Feedback requests, both from professional and private service providers. Answering a User Survey is probably one of the most likely requests that a person is tempted and willing to drop in order to save time and accomplish other goals. However, for ESO, feedback is vital because one of the main reasons for ESO's existence is to serve the astronomical community, and to serve it as well as possible.

For the users, there are different channels to provide feedback: i) the Users Committee, the members of which are selected by the ESO Director General based on recommendations received from the ESO Member States, meets with ESO representatives of various operational groups and departments once per year; ii) individual questionnaires that are available for both Visitor Mode (VM) and Service Mode (SM) users¹; iii) interaction with ESO staff during programme preparation and execution, both in Service and Visitor Mode. The latter is a constant, unsolicited source of feedback, which can take place via direct (personal) interactions (e.g. during a VM run) or via established communication channels like the User Support helpdesk usd-help@eso.org and the observatory entry points (paranal@eso.org and lasilla@eso.org).

Feedback from observers in Visitor Mode should in principle be easier to receive since the observatory staff interacts personally with the visiting astronomers, reminding them about the importance to fill out the End of Mission (EoM) report, at the end of their observing run. The questions are formulated in order to evaluate the level of support received at the telescope, the availability of computer facilities

and communication channels, the informative material necessary to prepare for the run and the trip to the site, but also probe the observer's satisfaction about logistics, like transportation to the telescope site, food and lodging.

Service Mode users, instead, are reminded to fill out the Service Mode Questionnaire when they receive their SM data package (unless a targeted feedback campaign is launched), and they are asked to provide feedback on a broader range of topics, from the submission of a Phase 1 proposal to the quality of the data. The longer the time since the submission of the Phase 1 proposal and the receipt of the Phase 2 package, the fuzzier are the memories about a given run with respect to these particular phases of the operational cycle.

The questionnaire asks for feedback on different areas related to SM observing, but with specific reference to a given observing run, i.e. it aims at collecting as many details as possible on the experience of any given PI with respect to a specific run. In order to facilitate this flow of information, questions are grouped under the following different areas:

- a) a general section (at the very beginning and at the very end of the questionnaire), where the PIs first identify themselves, as well as the run(s) for which they are going to provide feedback and then assess the completion of the run and usefulness of the data set they have received with respect to the scientific goals of their proposal;
- b) a section on Phase 1, including the Call for Proposals and its related supporting tools and documentation;
- c) a section on Phase 2, probing all aspects related to the preparation and execution of SM observations, i.e. informative material, procedures and software tools available for the preparation and submission of the Phase 2 package, and its verification and acknowledgement, as well as follow-up support during the semester of observations;
- d) a section on data quality, processing and delivery, which covers all operational aspects after an observation has been executed, i.e. the assessment of the data quality, its processing and final delivery to the PI.

¹ Feedback questionnaires for Visitor and Service Mode users are available respectively from <http://www.eso.org/paranal/sciops/EoM/> and http://www.eso.org/org/dmd/usg/survey/sm_questionnaire.php.

Both types of questionnaires (VM and SM) include questions with multi-choice answers and free-format text boxes where further comments may be provided.

The 2007 Service Mode Feedback Campaign

Following up an official request made by the Users Committee enquiring about user feedback, in early 2007 it was decided to revamp and launch a new Feedback Campaign. Considering the sporadic feedback we had received since the last such targeted action (Comerón et al. 2003), it was recognised that this campaign was indeed timely.

We decided to target all SM Principal Investigators of the last five years (only four years for PIs of Large Programmes, because, running over multiple semesters, they usually need more time to assess and evaluate the data quality), thus covering ESO observing semesters corresponding to Periods 69–77 (69–75 for Large Programmes). In total, 941 PIs were contacted and asked to fill out the SM questionnaire. One should note that the number of runs that we asked for feedback is much larger than this, as many PIs had several SM programmes scheduled during the targeted periods. The response has been positive, though not overwhelming: 334 questionnaire reports were received by the deadline (that was set to the end of March 2007), from 170 individual PIs. Since then, only 17 new questionnaire forms have been submitted (for a total of 187 individual PIs), showing once again how difficult it is to reach a steady flow of feedback. The responses cover all VLT/I instruments, plus FEROS and the Wide Field Imager at La Silla. In percentage and per instrument, the responses we have received represent on average 10–15 % of all SM runs that were approved during the P69–P77 period on a specific instrument, except for the Wide Field Imager for which the response rate is around 7 %.

Table 1 summarises the number statistics of the 2007 campaign (including the extra 17 reports received after the deadline), listing the number of responses received per period (one response per run). In order to better evaluate the significance of the response rate we have obtained, the number of received responses should be compared to the total number of SM runs approved per semester. For completeness, also the number of individual PIs corresponding to the number of received questionnaires is provided.

The comparison between ‘Received Responses’ and ‘Targeted Runs’ indicates a success rate in the range 11–14 % for the most recent periods (P76 and P77) and slightly below 10 % (7–8 %) for older semesters (e.g. P74 and P75). Clearly, one may question the importance of this feedback and the significance of any conclusion ESO may draw about its user’s satisfaction. On the other hand, feedback (a lot or a little) is vital to a service organisation such as ESO, and we think that these results, though based on rather small number statistics, are important enough to be publicly presented as such. The distribution of responses per period shows that the results reported in this article better reflect the most recent observing periods, for which the response has been stronger (as expected).

Overall, the feedback we have received is very positive. Figure 1 gathers the user’s responses about their general satisfaction with the various phases of the operational cycle. Users appear to be satisfied about the support they receive and the quality of the data they obtain. With respect to the last (2002–2003) Feedback Campaign (Comerón et al. 2003), it is rewarding to see a higher degree of overall satisfaction (also shown in the figure). As far as the overall rating of the SM process is concerned (topmost entry on the y-axis in Figure 1), there is a remarkable inversion between the ‘Good’ and ‘Excellent’ votes: 63 % ‘Excellent’ and 32 % ‘Good’ in 2007, 33 % ‘Excellent’ and 60 % ‘Good’ in 2002–2003. The overall

rating on the Phase 2 SM process, i.e. the support provided by the User Support Department during the preparation of the Phase 2 SM package, has recorded a 20 % increase in the ‘Excellent’ choices, counterbalanced by a decrease in the ‘Good’ votes (by 12–15 %) and in the ‘Fair’ and ‘Poor’ choices. The responses of users about the quality of the data have also slightly changed: the percentage of ‘Fair’ and ‘Poor’ grades has decreased (from 20 % in 2002–2003 to 15 % in 2007), and these votes have now turned into ‘Good’. With respect to the SM Data Package, the percentage of ‘Excellent’ choices has doubled, going from 11 % in 2002–2003 to 22 % in 2007.

Furthermore, 60 % of the users said that their programme was 100 % completed, and another 21 % reached a 75 % completion rate. Those with only 50 % and 25 % of their programme executed, represent respectively 6 % each. These numbers reproduce rather closely what is derived from our constant monitoring of the completion rate of all SM runs. Over the same period covered by the 2007 Feedback Campaign, our monitoring shows average percentages of 60 % and 35 % for completed and incomplete runs respectively (the remaining 5 % corresponds to runs that were not started).

As far as the scientific goals are concerned, 57 % and 14 % respectively said they were fully or mostly reached, whereas those whose scientific goals were achieved only partially or not at all amount respectively to 10 % and 8 % (see Figure 2).

In the following, we will present and comment on the results obtained with respect to different aspects of ESO operations and services to the community, covering different phases of the Service Mode operation cycle, namely, Phase 1, Phase 2, programme execution, data processing and delivery.

Number of	P69	P70	P71	P72	P73	P74	P75	P76	P77	P78	P79
Received Responses	17	26	36	20	28	34	46	55	79	7	3
Individual PIs	16	16	27	14	21	25	29	36	54	7	3
Targeted Runs	389	394	490	403	416	423	510	504	568	0 ²	0 ²

Table 1: Number statistics of the 2007 Feedback Campaign. See text for more details.

² The number is set to zero since this feedback was not solicited via the Feedback Campaign.

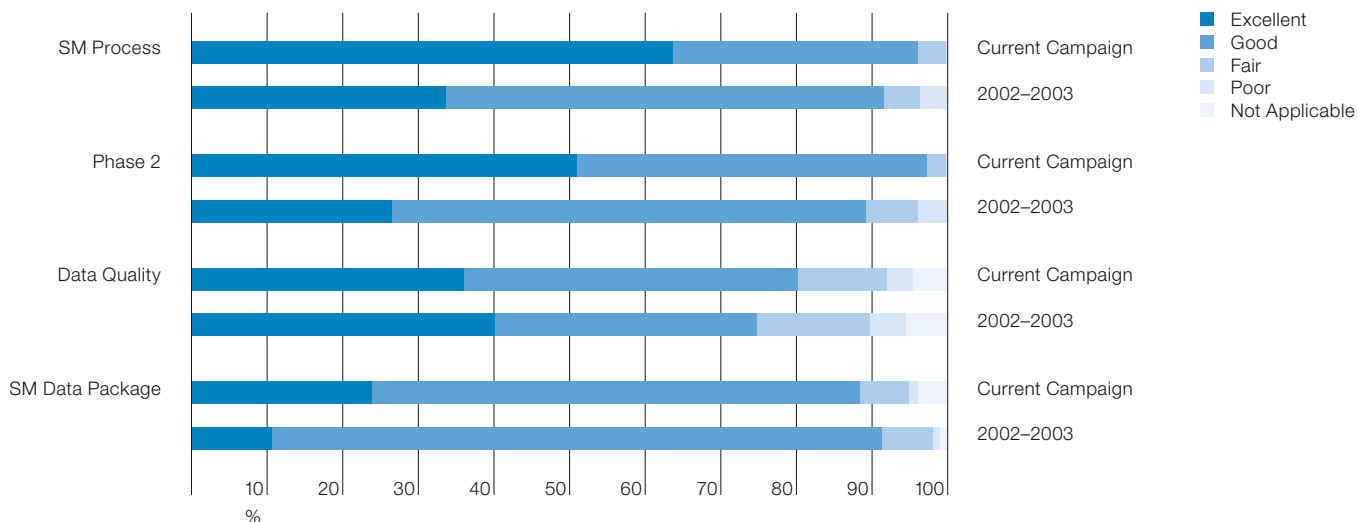


Figure 1 (above): Overall user feedback, i.e. how users have globally rated (from top to bottom on the y-axis): their interaction with ESO in relation to service observing; SM Phase 2 process; the quality of the data obtained; and the quality of the SM data package received. For comparison purposes, each topic has two entries, the current distribution of user's choices (upper) and the one from the last (2002-2003) campaign (lower).

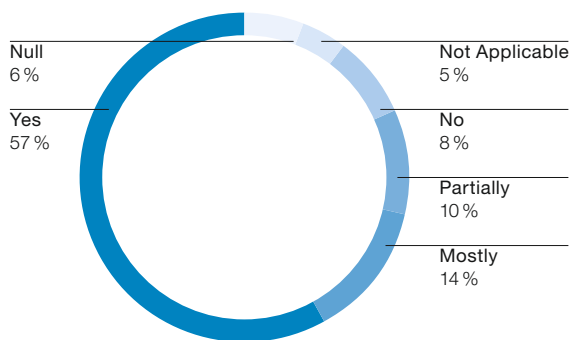


Figure 2 (right): User feedback to the question: "Did the data obtained allow the fulfilment of the scientific goals of your programme?"

Phase 1

Phase 1 is the process that runs between the announcement of availability of observing time (released in the form of the Call for Proposals³) and the deadline for submission of an observing proposal. On average, this process takes place over one month, twice per year (March and September).

The Call for Proposals is the main reference document for this phase, as it includes all information relevant to the preparation of a proposal: available instruments, observing modes, a brief description of the main characteristics and observing modes of the instruments on offer, a detailed summary of policies and procedures. In order to complete the preparation of an observing proposal, ancillary tools and documentation are made available to the user community.

In this section of the Service Mode Questionnaire, the users are asked to provide feedback on all these features, from the Call for Proposals and its web-based documentation, to the available support tools (e.g. Exposure Time Calculators, Object Observability and Airmass, Site Sky Ephemerides, Astro Climatology and Meteo Data) and the ESOFORM package. The latter includes the templates for writing the proposal and the user manuals to properly fill out the template. Instrument-specific User Manuals are also part of the Phase 1 material, as they contain all the details about characteristics, performance, observing modes and operational efficiency.

The responses show a clear majority of 'Good' and 'Excellent' choices for basically all Phase 1 related items. A higher number of 'Null' and 'Not Applicable' choices for the support tools is found, which is however rather difficult to interpret, as it could mean that people use other tools to check the same type of information, or that these tools are proba-

bly used more intensively at Phase 2, when for instance the air-mass constraint has to be specified in the constraint set of each Observation Block.

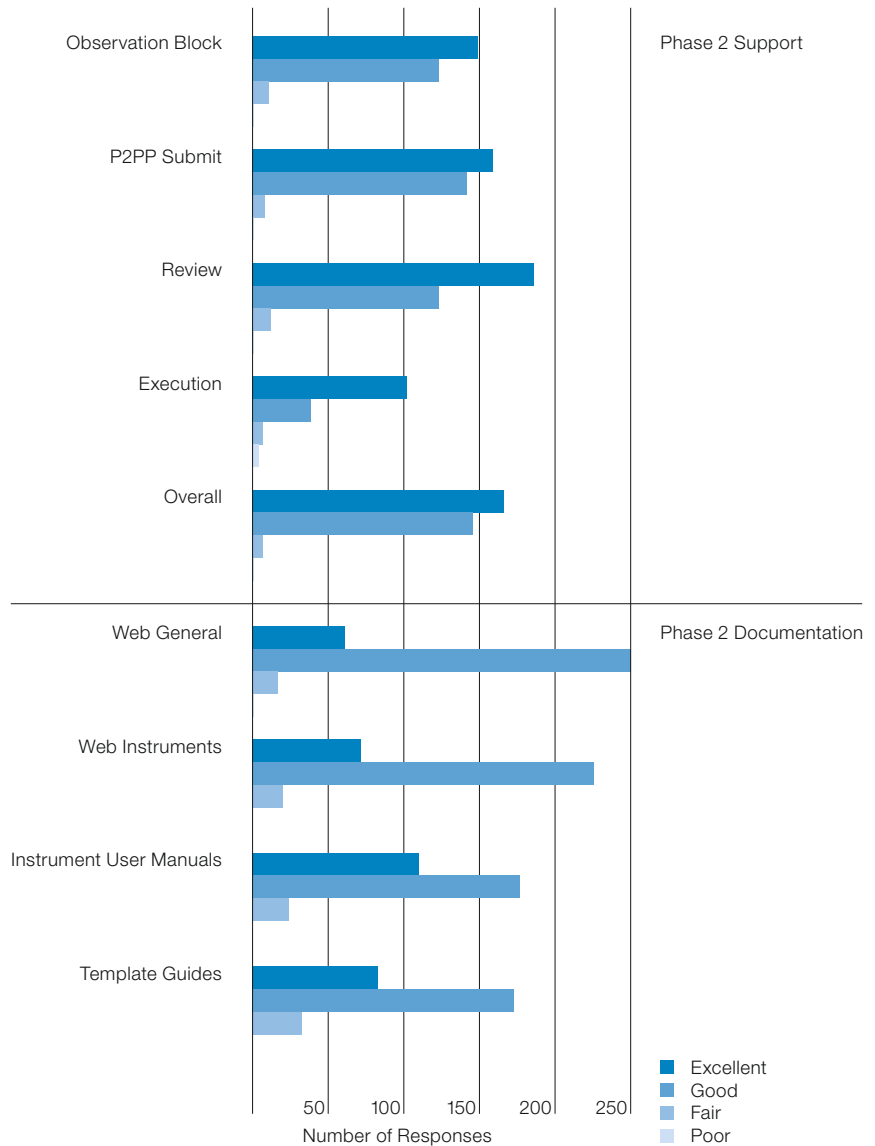
Another topic that is tackled in this section of the questionnaire is the computation of the overheads. This is a very critical point for both SM and VM observations, because the total requested time must correspond to the sum of 'time on target plus telescope and instrument overheads'. As such, it is very important that the method to compute overheads is properly described and understood by the users. Out of 345 replies we have received, 295 were 'Yes, it is clear how to account for overheads', i.e. approximately 85% of the users who replied found that the computation of the overheads is clearly explained. Unfortunately, not many extra comments were received that could help us to better understand the remaining 15% of the users who did not find easy/clear the computation of the overheads. On the other hand, it is important to note that in practice the wrong com-

³ The Call for Proposals is released twice per year via the following link: <http://www.eso.org/sci/observing/proposals/index.html>.

putation of the overheads affects a very small percentage of all OPC approved programmes. The technical feasibility performed by the observatory staff shows that over the last four semesters covered by the 2007 Feedback Campaign (P74–P77), the number of proposals with overheads that were wrongly accounted for amounts to merely 2–3%. Furthermore, this number seems to have become even lower (less than 1%) in the most recent semesters (P78 and P79).

Phase 2

The release of the telescope time allocations to the community marks the official start of the Phase 2 process, i.e. the preparation and submission of a complete (Phase 2) package to ESO. This basically includes the Observation Blocks (the single executable units) and a README file, summarising the main goal and requirements of that given programme (Finding Charts and Ephemerides files are now part of the Observation Block). One of the main functional tasks of the User Support Department is to support SM users in the preparation of their Phase 2 package, and review the material once it has been submitted. The support astronomers interact with the PI as needed in order to converge to a fully verified and optimised (in terms of scientific return and observing strategy) package to be sent to the observatory. For the Phase 2 preparation, dedicated tools have been developed (by ESO or by external consortia), as well as several documents, User Manuals, and informative web pages which are available and updated every semester. Therefore, the Phase 2 part of the SM questionnaire asks the users not only to express their degree of satisfaction about the level of support provided by USD at different phases of the process (preparation support, verification, acceptance and acknowledgement), but also to review the quality of the documentation and the four main characteristics of the available software tools: installation, manual, usability and functionality. Figure 3 describes the survey outcome for some of these items, whereas Table 2 reports the user feedback on specific Phase 2 tools (such as P2PP, SkyCat, observing support software tools).



Overall, the degree of satisfaction is quite high, with a clear majority of 'Good' and 'Excellent' choices on almost all of the items. We are clearly very satisfied about this, but the small percentages of 'Fair' and 'Poor' votes are particularly interesting as they usually highlight underlying problems that may affect only a minority of users. Some of the numbers reported in Table 2 hint at some dissatisfaction

Figure 3: Upper: Users impressions of different aspects of the Phase 2 Support provided by USD. Lower: User feedback on the quality of the information available from the USD public web pages (general and instrument-specific), as well as the quality of Instrument Manuals and Template Guides.

about some features of some support tools. Although these are very small number statistics, ESO will evaluate them carefully to see if there is room for im-

Tool	Installation	Manual	Usability	Functionality
P2PP	4/20/153/129	4/19/219/58	9/43/210/63	6/37/205/75
FIMS (FORS)	4/9/27/11	0/7/36/6	0/6/37/7	0/2/43/4
FPOSS (FLAMES)	0/1/5/7	0/1/7/3	0/4/4/5	0/2/7/4
VMMPS (VIMOS)	0/2/13/4	1/2/13/3	3/5/9/3	3/6/8/3
NAOS-PS (NACO)	4/3/9/9	0/4/14/7	1/2/15/7	2/2/13/8
SkyCat	8/21/89/68	5/21/100/26	1/22/115/51	5/34/18/38

Table 2: The user's feedback on specific functions of Phase 2 related tools. Numbers refer to responses received respectively for Poor/Fair/Good/Excellent choices.

provement; this evaluation takes into account a study of feasibility, the investment required to implement a given improvement and the final gain.

Programme execution, data quality, processing and delivery

This part of the questionnaire collects feedback about post-Phase 2 activities, i.e. the execution of a programme, its quality assessment and the final data processing, packaging and delivery. At the start of a new observing Period, all SM runs that have been verified and accepted will become available in the daily observing queues as soon as the targets are observable. In the majority of the cases, the execution is a smooth phase, because all the material has already been checked and verified by the User Support Department. However, there are instances, especially for the most demanding programmes and the most complex and sensitive instruments, in which the observatory staff asks for extra feedback and possibly further checks. Thus, some interactions between USD and the users also continue after Phase 2, when problems are detected or doubts arise at time of execution.

Principal Investigators can follow the progress of their observations from the Run Progress Report web-pages⁴ (one per run). These pages list the status of the run (Open/Completed/Terminated/Not Started), which OB has been executed and how good was the execution (i.e. Completed *versus* Executed, the latter implying that the OB will be repeated), and the atmospheric conditions during the night of observation. Figure 4 summarises what users think about the Run Progress Report pages of their runs.

Once the run is declared completed, the Quality Control (QC) group at the Data Flow Operations Department is informed that a final SM data package can be prepared for that run. This phase includes not only the processing of the entire data set, but also the collection and/or preparation of several pieces of ancillary in-

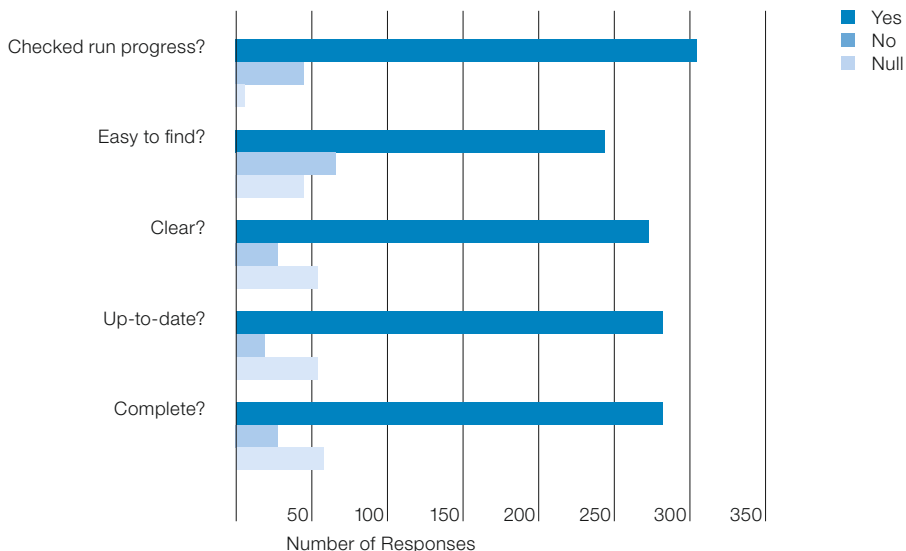


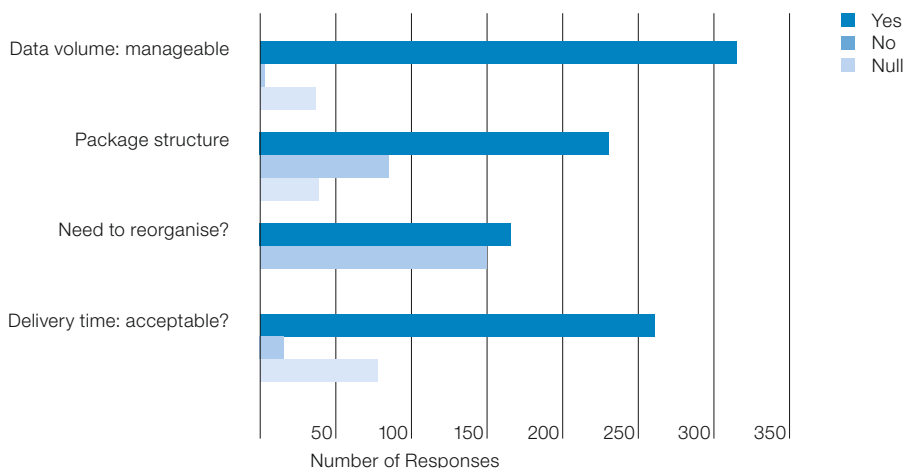
Figure 4: The main question of this section (first item on the y-axis) was: "Have you ever checked the progress of your programme during the Period?", and is followed by more specific questions about how good was the information provided. Only 5 (out of 355) replies (to the main question) were null, i.e. the user did not answer.

formation on various quality control checks and plots, master calibration files, README and help files to guide the PI through the data package. When the data package is ready, it is released to the Science Archive Operations group, in charge of cutting the package on DVDs and delivering it to the PI. SM PIs can now follow these phases of their data package from the same SM Run Progress Report pages mentioned above.

Figure 5 below shows the user feedback on issues specific to SM data packages, their content, organisation and delivery

times. Once again, it shows a high degree of user satisfaction. One interesting feature that does not emerge clearly from the graph in Figure 5 concerns the data volume and its manageability. All instruments, except the Wide Field Imager at the 2.2-m telescope, are characterised by a striking majority of positive replies. For WFI, instead, there is a perfect (50/50) balance in the answers. This, together with the low response received from PIs of WFI runs, may hint at problems in dealing with and analysing the large amount

Figure 5: Features of the SM Data Package: this section covered issues like data volume (How manageable is it?), structure of the data package (i.e. How raw, calibration and processed data are stored and organised) and if the delivery time was acceptable. The latter was related to a question about what the delivery time has been: less than four (42% of the replies), between four and six (33%), and longer than six weeks (25%).



⁴ Available from <http://www.eso.org/observing/usg/infopage.html>.

of data that a WFI run usually produces. Also, we note that the very well-balanced feedback on the need to reorganise the received SM data package is a good example of a very subjective problem that depends on how every single PI/Co-I is used to working with data. ESO has already once revised the structure of the data directories in the package, but clearly the community sampled by this feedback campaign is split into groups of similar weight. Some extra comments have been received about possible solutions; ESO is considering these and will reassess them in the near future.

Visiting Astronomers and the End of Mission Reports

The main difference between Service and Visitor Mode observers is the fact that the run is carried out on specific dates, with the presence of the PI (or Co-I) at the telescope, and that the main support is provided by the observatory staff (at La Silla and Paranal). The involvement of the User Support Department and Quality Control group is marginal (e.g. no data package is prepared by QC for VM runs).

As mentioned at the beginning of this article, the End of Mission (EoM) Report is tailored to immediate feedback on those features that are the most relevant to the observatory and its staff. Thus, the feedback that is collected is rather different compared to the SM Questionnaire. In order to be consistent with the main theme and purpose of this article, here we comment only on a very restricted number of features covered by the EoM Report, namely the user satisfaction about the support received by the observatory staff and the completion rate of the run. On average, approximately 50 reports per semester are received both at Paranal and La Silla.

Concerning user satisfaction, visiting astronomers give a rating to their Support Astronomers (including day support for the preparation of the observations and night support at the telescope), to the Telescope/Instrument Operators (TIOs), and to the general technical support they receive. Figure 6 shows a steady, very high satisfaction index for the VLT Support Astronomers on Paranal and La Silla,

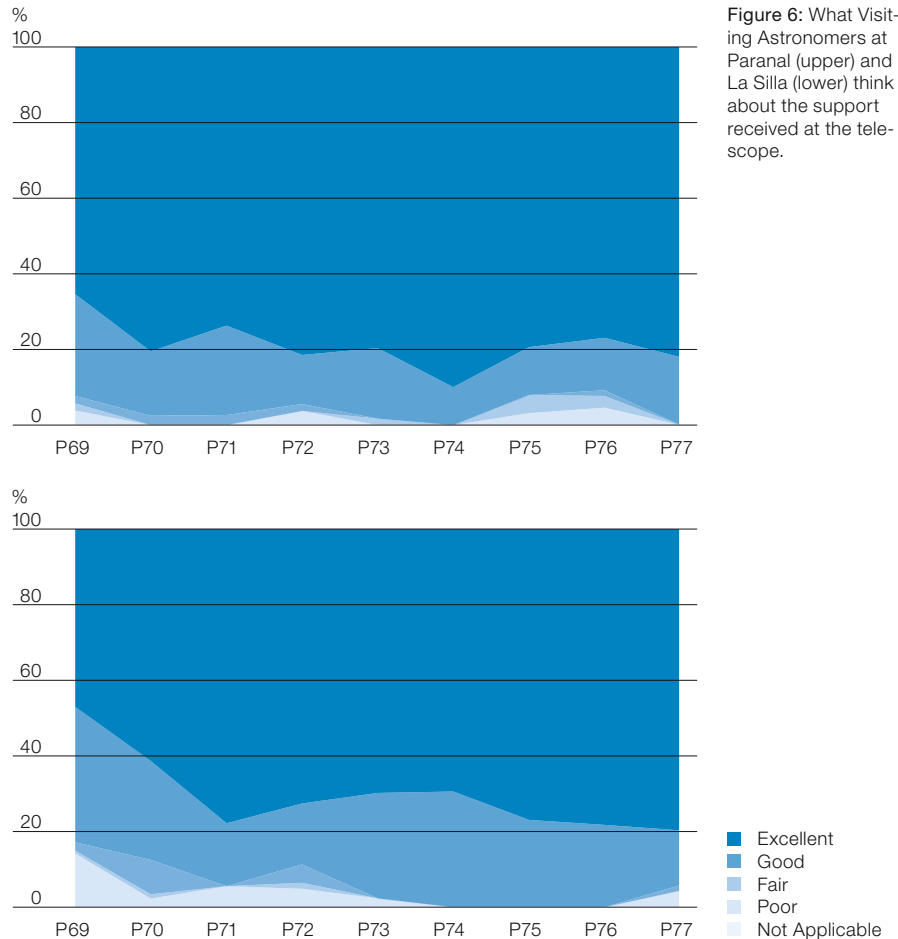


Figure 6: What Visiting Astronomers at Paranal (upper) and La Silla (lower) think about the support received at the telescope.

with a clear trend of improved satisfaction for the latter. A similar graph is also obtained for the TIOs (not shown).

The run completion information is the assessment by the observer at the end of his/her run, i.e. usually before s/he has had an in-depth look at the data. Here, the figures show a tight anti-correlation with weather downtime, but typically over 75% of the observers consider their programme at least 75% or more completed.

Concluding remarks

User feedback is very important but also very challenging to stimulate, as the 2007 Feedback Campaign has clearly shown. However, user surveys in general are very challenging and the experts in the field say that a 15–20% level of response is to be considered an important achievement. We are not quite at this

level yet (11% for P76 and 14% for P77), but with a better strategy, tailored to receive feedback closer in time to the existence of a given run (the best results are indeed obtained for the most recent period that was targeted), we believe things will improve.

Despite the caveat of the low number statistics, the main conclusion of this article is that the ESO user's community is highly satisfied with ESO services and support. This clearly emerges from all different sections of the SM Questionnaire, as well as from the operations-related sections of the VM EoM reports. Our users are satisfied with the efficiency at which ESO operates its facilities and the level of support the ESO operations groups provide to them. Their scientific projects get completed and their scientific goals are achieved, at least for the majority. When compared to the 2002–2003 Feedback Campaign, the overall user satisfaction has improved.

Clearly, ESO is pleased to see that their constant efforts and dedication are well received and appreciated, but would like to do more, and especially to hear from a larger audience. We are now in the process of evaluating all the extra comments we have received in the questionnaires and are investigating alternative

solutions with the aim of making our user surveys more attractive and hopefully increasing their feedback. In the future, we plan to extend our targeted audience to include APEX PIs, and all ESO PIs for those phases common to both SM and VM runs (e.g. Phase 1 and data quality).

Acknowledgements

We would like to warmly thank all the Principal Investigators who promptly responded to our SM Feedback Campaign in early 2007 and all visiting astronomers who submit the End of Mission report at the end of their observing runs. Your feedback is very important to us.

References

Comerón F. et al. 2003, *The Messenger* 113, 32

ESO Reflex: A Graphical Workflow Engine for Astronomical Data Reduction

Richard Hook^{1,5}
 Martino Romaniello¹
 Marko Ullgrén²
 Sami Maisala²
 Otto Solin³
 Tero Oittinen²
 Ville Savolainen⁴
 Pekka Järveläinen⁴
 Jani Tynnelä⁴
 Michèle Péron¹
 Carlo Izzo¹
 Pascal Ballester¹
 Armin Gabasch¹

¹ ESO

² Observatory, University of Helsinki, Finland

³ Space Systems Finland Ltd.

⁴ CSC, the Finnish IT Center for Science, Finland

⁵ ST-ECF

ESO Reflex is a software tool that provides a novel approach to astronomical data reduction. The reduction sequence is rendered and controlled as a graphical workflow. Users can follow and interact with the processing in an intuitive manner, without the need for complex scripting. The graphical interface also allows the modification of existing workflows and the creation of new ones. ESO Reflex can invoke standard ESO

data reduction recipes in a flexible way. Python scripts, IDL procedures and shell commands can also be easily brought into workflows and a variety of visualisation and display options, including custom product inspection and validation steps, are available. ESO Reflex was developed in the context of the Sampo project, a three-year effort led by ESO and conducted by a software development team from Finland as an in-kind contribution to joining ESO. It is planned that the software will be released to the community in late 2008.

The data reduction needs of ESO

ESO is currently operating a large suite of instruments covering the optical and the infrared, as well as the millimetre wavelength ranges. Although the responsibility for the quality of the scientific reduction of the data can only rest with the individual users, it is very difficult for users to be equally familiar with all the different observational techniques spanned by the ESO instruments at a level where general-purpose tools like IRAF and ESO-MIDAS can be effectively used. Instrument specific software, implementing carefully tuned algorithms, is therefore essential. Currently ESO aims to develop and export data reduction recipes for all VLT/VLTI instruments. These are based on

the ESO Common Pipeline Library (CPL) and may be run offline using either the Gasgano graphical tool or the EsoRex command line tool. Recipes have the primary tasks of running as automatic pipelines within the dataflow system and being used to create products suitable for quality control (Silva and Péron 2004, Ballester et al. 2006).

The challenge is to allow the user greater flexibility to interact with the data reduction process and to study data products, both intermediate and final, in order to optimise the quality of the results. In addition it is desirable to reuse existing software as much as possible, both current pipelines and legacy software tools. The aim was to embed the ESO recipes within a flexible environment without the need to recreate a complete and expensive new software system. We believe that this approach has the potential to deliver a significant improvement to users whilst making optimal use of available resources.

Introducing ESO Reflex

The Sampo project, a three-year effort led by ESO and conducted by a software development team from Finland as an in-kind contribution to joining ESO, has concentrated on developing a graphical user interface to run ESO data reduc-

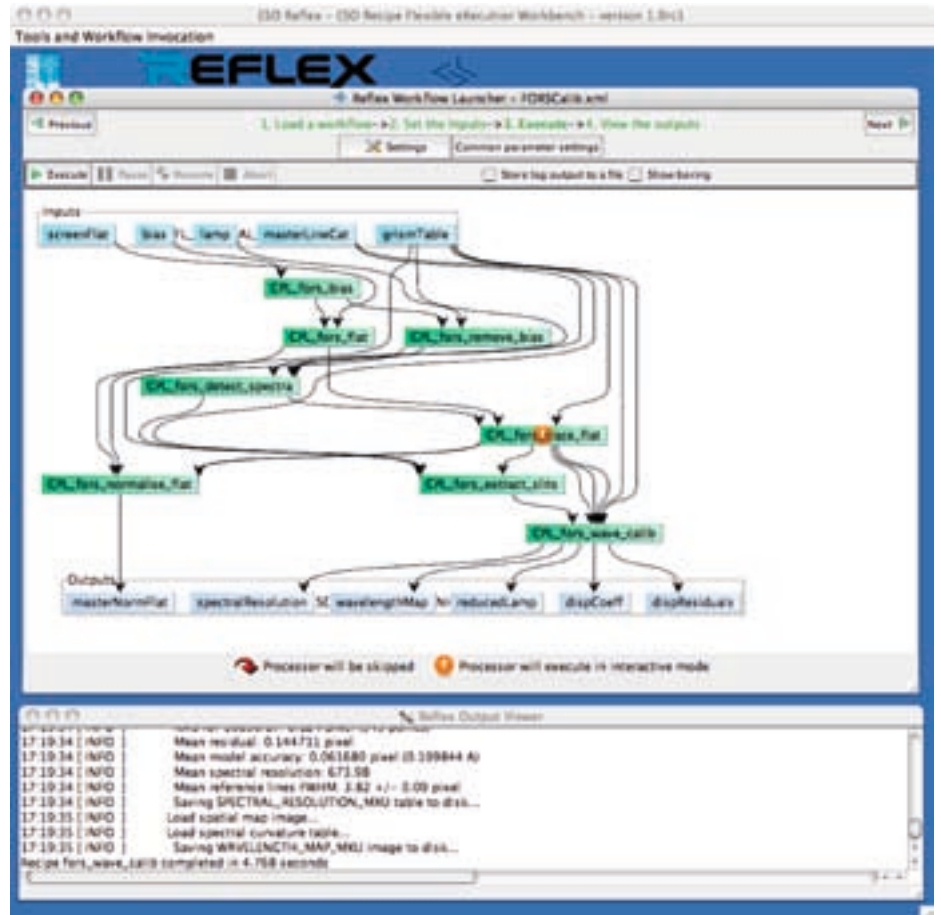
tion recipes. The high level goals of the project were described in an earlier article (Hook et al. 2005).

The primary outcome of the Sampo project is an application called ESO Reflex (ESO REcipe FLeXible EXecution workbench), in which the sequence of reduction steps is rendered and controlled as a graphical workflow. This approach allows users to follow and interact with the data reduction flow in an intuitive manner without the need for complex scripting. Figure 1 illustrates the look and feel of an ESO Reflex workflow. In this particular example, it is a reduction sequence to produce master calibrations for the FORS2 MXU mode. The input files are at the top of the workflow (light blue boxes) and the data percolate through the workflow to produce the final outputs at the bottom. The boxes in between the inputs and outputs represent the actual processors acting on the data, while the arrows mark the data flowing from one processor to the next.

ESO Reflex is based on a graphical workflow engine called Taverna that was originally developed for the e-Science community in the context of the myGrid initiative in the United Kingdom (the project page is available at <http://taverna.sourceforge.net>). Once adopted after a survey of other available scientific workflow engines, Taverna was customised by the Sampo team to tailor it to the requirements, of astronomical workflows. These additions include a new interface for launching workflows, support for FITS files and interfaces to CPL, Python and IDL.

Workflows in ESO Reflex are easily edited and customised by simply adding or removing processors, the boxes in the middle of Figure 1, and connecting the appropriate input and output ports with arrows. The underlying workflow engine takes care of all the additional complexities linked to making the data flow through the reduction workflow, as defined graphically by the user. The users of such a system are left to focus on their core task: making scientific sense of their data and exploiting them to the maximum.

The interface of ESO Reflex is not instrument specific and users are presented with the same look and feel independ-



ently of the actual instrument from which the data originated.

The key features of ESO Reflex

ESO Reflex aims to provide most of the key elements for a scientific data reduction:

- Convenient ways to select and organise data, based on code from the Gasgano application (<http://www.eso.org/gasgano>), to cope with the complexity of the headers of modern data.
- A CPL processor to include data reduction recipes for the vast majority of the data produced by ESO instruments into workflows. This dedicated processor is tailored to handling ESO data using CPL recipes and supports many extra features, including different processor modes (interactive, skipped, etc.), as well as control of recipe-specific parameter values.

Figure 1: Example of a workflow with ESO Reflex: this case is based on FORS2 MXU calibration recipes. The input data are represented by the light blue boxes at the top. The data percolate through the processors in the middle section to produce the outputs at the bottom of the figure. The orange circular symbol indicates that one recipe will execute in interactive mode – this allows the user to inspect the input and output files of this stage of the processing and modify parameters if desired.

- Processors through which Python scripts, IDL procedures and shell commands can be included within workflows.
- The possibility of basic flow control operators, such as conditional steps.
- Error handling: ESO Reflex catches errors returned by processors and offers options on how to proceed further, e.g. abort the workflow, reconfigure the offending processor and rerun it, proceed anyhow trying to execute the rest of the workflow.
- Skipping of processors and the possibility to allow optional steps.

- Automatic processing of lists of input files.
- Batch processing without the graphical user interface.
- The design of Taverna makes it very effective for building workflows that use web services such as those established within the Virtual Observatory. Experiments in this area have been successful and are described elsewhere (Järveläinen et al. 2008).
- A particularly important use of scripts is to analyse intermediate products within the reduction process. To illustrate this concept we have developed several interactive tools. A screenshot of such a tool, in this case to iteratively check and refine the wavelength solution of 2D spectra is shown in Figure 2.

It is perhaps inevitable that a graphical workflow system is, for some purposes, not as powerful as a well-crafted script. However, it is expected that the greater

ease of use of a graphical workflow system will compensate for the loss of power, when compared to traditional scripting.

Current status and future plans

At the time of writing, ESO Reflex is in a beta state and is expected to be released to the community at large in the fourth quarter of 2008 along with appropriate workflows and tools. People interested in early access to ESO Reflex in conjunction with the instrument modes for which workflows have been developed, namely FORS spectroscopy and AMBER, should contact reflex@eso.org.

Work is also in progress to enhance the data reduction recipes. The current algorithms are focused on processing calibrations and extracting the parameters required to monitor the health status of the

instruments. While in some cases the resultant products are of adequate quality for immediate scientific analysis, this is generally not yet the case. To this end, the data reduction recipes are being made available in modular form to allow interaction with the intermediate products at scientifically meaningful points and to work seamlessly with ESO Reflex. The data reduction algorithms themselves are also continuously being extended with the long-term aim of allowing the creation of high-quality science products on the user desktop.

References

- Ballester P. et al. 2006, Proceedings of the SPIE 6270
 Hook R. N. et al. 2005, The Messenger 120, 17
 Järveläinen P. et al. 2008, in ASP Conf. Ser., ADASS XVII, eds. J. Lewis, R. Argyle, P. Bunclark, D. Evans and E. Gonzalez-Solares, (San Francisco: ASP)
 Silva D. and Peron M. 2004, The Messenger 118, 2

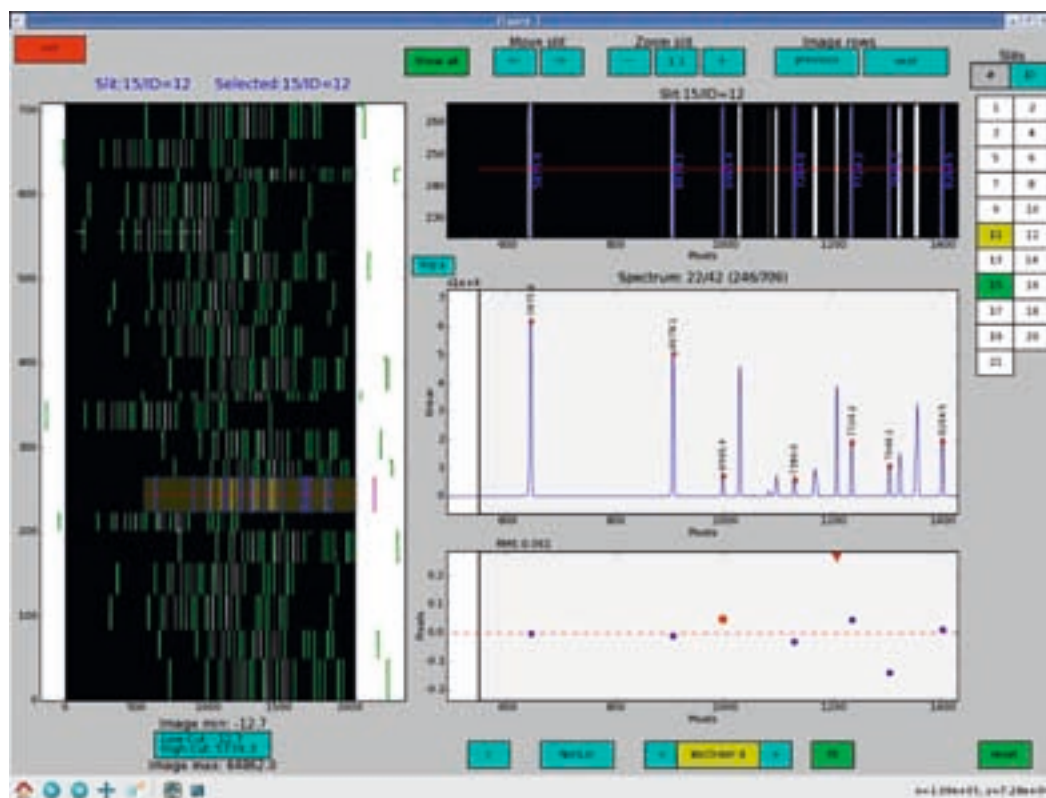


Figure 2: Screenshot of the Python tool to check and improve the wavelength solution of 2D spectra. Calibration spectral lines, either from an arc lamp or from the night sky, are displayed slit by slit and can be included or excluded when computing the wavelength solution with a polynomial fit, the order of which can also be set interactively. This example shows a FORS/MXU arc exposure.

News from the ESO Science Archive Facility

Nausicaa Delmotte (ESO) on behalf of the Data Management and Operations division

The latest developments of the ESO archive are presented. Information is provided to the astronomical community on new data releases, services and policies.

The end of 2007 brought several changes in the way to access the ESO archive. The Data Management and Operations division continues to look into improvements to enhance the scientific value and access to the large data volumes of the Archive, with the aim of increasing the legacy and scientific productivity of ESO data.

To better integrate the archive web with the main ESO web and to ease its maintenance, a content management system has been set up by the Virtual Observatory Systems (VOS) department so that any new archive web page now gets served with the look and feel of the ESO Web (see Warmels and Zech 2007). Already existing archive web pages are being progressively migrated to this new system. A significant fraction of this work was done as part of the in-kind contribution provided by Spain.

Apart from the traditional web interface, a subset of the ESO archival data can now be accessed through VirGO, the next-generation visual browser for the ESO archive, developed by the VOS department. Currently VirGO can be used to access all data products and an increasing fraction of raw data. We expect the ingestion of imaging data to be completed in 2008, followed by the spectroscopic data sets. VirGO is a plug-in for the popular open-source software Stellarium, adding capabilities for browsing professional astronomical data. Its main feature is to perform real-time access and graphical display of a large number of observations by showing instrumental footprints and image previews, and to allow their selection and filtering for subsequent download from the ESO Science Archive Facility (SAF) web interface. All data interfaces are based on VO standards which allow access to images and spectra from ex-

ternal data centres, as well as inter-application exchange and compatibility. For download and more information, see <http://archive.eso.org/cms/virgo>.

The ESO archive is now also integrated into a unique gateway, known as ESO's User Portal, a single sign-on infrastructure providing a central access point to the various scientific services offered, via the web, to the ESO user community (see Tacconi-Garman 2007). At the end of the proprietary period, ESO data become accessible worldwide. Although a user does not need to register with the ESO User Portal in order to browse the contents of the archive, it is required to be signed in to request data.

New data releases

Several major scientific data releases have also taken place through the ESO archive over the last months and are summarised here.

Processed data for the bulk of UVES echelle data acquired since the beginning of its operations in the year 2000 are now available online from the ESO archive. The one-dimensional extracted spectra, together with processing logs and ancillary files, can be accessed through a dedicated query form at <http://archive.eso.org/wdb/wdb/adp/ssa/form>. More than 50 000 raw frames of point-like sources were processed at ESO by the Data Flow Operations department with the latest version of the instrument pipeline (v3.2). Only quality-controlled master calibration frames were used for the processing and all science products have undergone a certification procedure. This approach results in a large data set processed in a homogeneous, controlled and well-understood way. Those UVES products were ingested into the ESO archive, in a VO-compliant manner by capturing all relevant meta-data, using a tool developed by the VOS department. The meta-data are available for searching and the data themselves can be accessed with VO-compliant applications through the Simple Spectral Access Protocol (SSAP). In addition, archive users can search the UVES processed data by target name, object class, redshift or radial velocity as provided by SIMBAD/NED.

The archive query form also gives access to several other Advanced Data Products (ADPs): HARPS, zCOSMOS, and GOODS/FORS2. Public HARPS reprocessed data have been produced and released by the ADP group within the VOS department, using the latest version (v3.0) of the automatic HARPS pipeline developed by the Observatoire Astronomique de l'Université de Genève. Currently these data cover the first four years of operation (2003–2006). Other data will follow as soon as possible. ADPs from the first release (DR1) of zCOSMOS (ESO Large Programme 175.A-0839, PI Lilly) were made public on 30 October 2007. They include 1264 one- and two-dimensional VIMOS spectra. This is the first data release of an external ESO large programme. Finally, the GOODS/FORS2 final data release v3.0 took place on 31 October 2007 and contains 1715 one-dimensional spectra of 1225 unique targets, providing in total 1165 redshift measurements. Associated spectral previews and colour image cut-outs (5" × 5") are also available for each target. This release was a collaborative effort of the ADP group in VOS with the GOODS team and the ST-ECF. Also the ADPs from the imaging project 'Monitor' (ESO Large Programme 175.C-0685, PI Aigrain) were released on 21 January 2008 (see Aigrain et al. 2007).

The ESO archive now provides on-line access to WFI data previews through the main-archive query form, as they are produced by the ADP group in the VOS department. Previews of data from 2002 to March 2006 are already available. Previews come in JPG and H-compress FITS format. They are obtained by processing raw WFI frames (already in the public domain) with ESO-MVM in an automated fashion. An approximate bias subtraction and flat fielding is applied to the raw frames using master calibrations obtained once a month. A rough de-fringing for the *I*- and *z*-band exposures is applied by building fringing maps from science frames taken over several nights, as intra-night, widely dithered, science frames are not available for most of these observations. As a result, the fringing correction is often not satisfactory. The resulting images are then rebinned by a factor of 10 and compressed using a loss-less algorithm. Notably, the FITS ver-

sion of these previews contains recalibrated positional (WCS) information with an accuracy ≤ 1 arcsec.

In addition to the main ESO archive query form, the archive also offers its users the possibility to query by instrument-specific parameters, via the so-called instrument-specific query forms. The latest one released was the CRIRES query form

in October 2007. The APEX query form has been updated to be able to retrieve observing logs and CLASS files for the APEX-2A/FLASH data. Finally HAWK-I science verification data packages have been released.

For the latest information about the ESO archive, or to subscribe to the archive RSS feed, please see <http://archive.eso.org/>.

For any questions or comments on the ESO archive, please contact us at archive@eso.org.

References

- Aigrain S. et al. 2007, *The Messenger* 130, 36
 Tacconi-Garman L. E. 2007, *The Messenger* 130, 54
 Warmels R. and Zech G. 2007, *The Messenger* 128, 73

ALMA Science: the ESO-Garching Astronomers View

Leonardo Testi (ESO)

At the Garching Science Day 2007, proposals for observations with ALMA were presented. A comparison is presented with the ALMA Design Reference Science Plan. The comparison shows that ALMA can be exploited by the wider community for a variety of different science projects, many of which are beyond the expectations of the current community of millimetre astronomers.

ALMA has been designed and is being built to allow the astronomical community to achieve transformational science. To reach this ambitious goal, all ALMA components are scrutinised to ensure that they meet stringent scientific requirements. Together with the top-level science goals, the ALMA Design Reference Science Plan (DRSP)¹ has been created (see Hogerheijde 2006). The DRSP is a collection of science programmes that are used as reference for the scientific capabilities of the instrument. The DRSP has gone through a major revision (version 2.0) during 2007, in order to update its scientific content and to take into account the new ALMA capabilities made acces-

sible through the East Asian contribution. Even though the DRSP contains a number of projects prepared by non-millimetre specialists, the bulk of it has been prepared by the millimetre community.

For the annual Science Day, held on 6 December 2007, the ESO Garching astronomers were invited to prepare potential programmes to be carried out with ALMA. Most of the science staff of ESO-Garching has profound experience in optical/infrared astronomy, therefore the Science Day was then a unique opportunity to receive input from a community base quite different from that of the DRSP, and possibly more similar to the future ALMA users.

The 147 programmes in the DRSP 2.0 and the 43 Science Day presentations were analysed in a homogeneous way to compare the distribution of programmes and the total requested time in the four ESO-OPC categories, with the addition of a new category for observations of the Sun, which will be possible with ALMA. The requests for observing time in each of the ALMA frequency bands were also compared.

The results of this analysis are shown as ring charts in Figure 1. In the DRSP, almost 60 % of the programmes are in four large scientific areas that are contained in the OPC-C category: Interstellar Me-

dium, Star Formation, Circumstellar Matter and Solar System. Most of the remaining programmes target Galaxies (B) or Cosmology (A) with a minor fraction in Stellar Evolution (D) and Solar Physics (S).

The distribution of requested time reveals that the relatively few Cosmology programmes actually require a large investment of telescope time, while only a small fraction of time is needed to complete the Stellar Evolution and Solar Physics part of the programmes (less than 5 %).

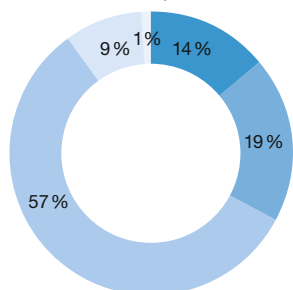
The Science Day programmes offer a significantly different view, in that there is a much lower fraction of programmes in the C category and higher fractions in the other areas, especially the Stellar Evolution (D) and Solar Physics (S). This is also reflected in the fraction of requested time, where these latter two categories combined approach 10 % of the total time needed.

The analysis of the time requested in each of the ALMA receiver bands shows that the request for the highest frequency bands, B8 and B9, is similar (around 15 %). The lowest frequencies (B3 and B4) add up to about 25 % in the DRSP, but to almost 37 % in the Science Day programmes. The intermediate frequencies (B5, B6 and B7 – see Haupt and Rykaczewski 2007) are confirmed to be the workhorse of ALMA with 60 % in

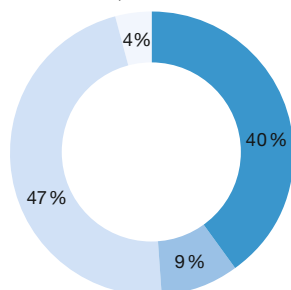
¹ See <http://www.strw.leidenuniv.nl/~alma/drsp.shtml>.

ALMA DRSP 2.0

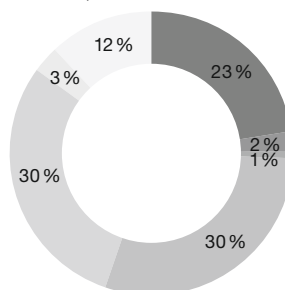
a – Number of Proposals



b – Time Requested

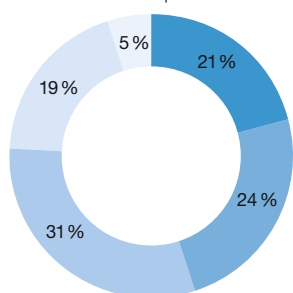


c – Time per Receiver Band

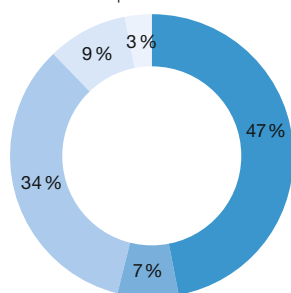


ESO Garching Science Day 2007

d – Number of Proposals



e – Time Requested



f – Time per Receiver Band

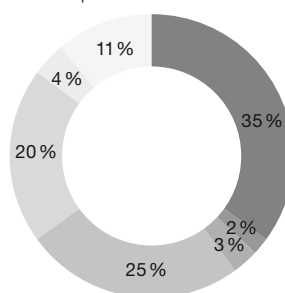


Figure 1: Ring charts show the distributions of the number of proposals and total time requested in the various ESO-OPC categories (A-Cosmology; B-Galaxies and Galactic Nuclei; C-Interstellar Medium, Star Formation and Planetary Systems; D-Stellar Evolution, with the addition of S-Solar

Physics), and the distribution of the requested time for the various ALMA frequency bands (see Haupt and Rykaczewski 2007). The top diagrams relate to the ALMA DRSP 2.0 while the bottom ones derive from the ESO Garching Science Day 2007 presentations.

the DRSP and almost 50% in the Science Day programmes.

While the differences between the DRSP and the ESO Science Day programmes may, in part, reflect the large fraction of scientists among the ESO staff interested in stars, galaxies and cosmology, it is important to point out that several ALMA applications in these areas, that are not covered in the DRSP 2.0, were presented. These new programmes will be incorporated in the next revision of the DRSP. The Science Day is thus a strong and positive indication that astronomers coming from outside the traditional millimetre community want to use the unique ALMA potential to attack problems that are completely out of reach with current millimetre instruments.

References

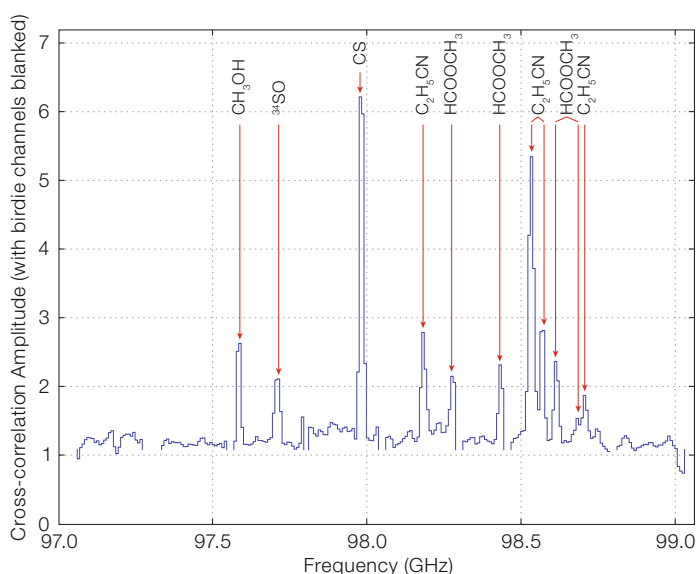
- Hogerheijde M. 2006, *The Messenger* 123, 20
 Haupt C. and Rykaczewski H. 2007, *The Messenger* 128, 25

Key to a, b, d, e:	Key to c, f:
OPC Categories	ALMA Receiver Bands
A B C D S	B3 B4 B5 B6 B7 B8 B9
■ ■ ■ ■ ■	■ ■ ■ ■ ■ ■ ■ ■ ■

News from the ALMA Test Facility

Todd Hunter (NRAO), Robert Laing (ESO)

A major milestone was achieved at the ALMA Test Facility (ATF) on 19 January 2008 when the first interferometric spectrum of an astronomical source was obtained. The spectrum, shown right, was of the hot molecular core of the Orion Nebula. The two ALMA prototype antennas at the ATF were used, along with evaluation front-end receivers and production back-end equipment controlled by a combination of ALMA software and ad hoc scripts and procedures. This milestone follows the ability of obtaining stable dynamical fringes on bright quasars, which was achieved in the second half of 2007. The baseline length at ATF is 35 metres and the spectral resolution used is 7.8 MHz (24 km/s) which is one of the low-resolution configurations of the correlator.



Report on the

2007 ESO Fellowship Symposium

held at ESO, Vitacura, Chile, 12–14 November 2007

Michael West, Bruno Leibundgut (ESO)

The third ESO Fellowship Symposium took place in Santiago from 12–14 November 2007. These symposia, held every two years, bring together ESO Fellows from Chile and Germany for several days of scientific discussion and camaraderie. This year's symposium was framed by an earthquake and visits to the ESO observatories.

Separated by an ocean, ESO Fellows usually have few opportunities to interact with their colleagues on the other site. The goal of the ESO Fellowship symposia is to bring the ESO Fellows from Chile and Germany together to discuss science, build personal connections, stimulate new research collaborations, and discuss strengths and weaknesses of the Fellowship programme. The symposia are held every second year alternating between Santiago and Garching.

Thirty Fellows from Santiago and Garching participated in this year's event, which was also attended by many ESO Chile staff astronomers and students (see

lower picture of the Astronomical News section page, page 35). Each Fellow gave a 30-minute presentation about his or her current research and plans for the near future. The presentations covered nearly all topics of modern astrophysics, such as extrasolar planets, gravitational lensing, starspots, and galaxies at low and high redshifts, as well as observations spanning the electromagnetic spectrum from gamma ray to radio. Interested readers can view and download the Fellows' science presentations at <http://www.eso.org/sci/meetings/fellowsymp2007/>.

After the three-day symposium in Santiago, Fellows were given an opportunity to visit the APEX and ALMA sites on the Chajnantor plain or the VLT on Cerro Paranal. This was an exciting experience for all, combining spectacular views of the beautiful northern Chilean landscape with a behind-the-scenes look at the astronomical facilities. The upper picture on page 35 shows fifteen of the ESO Fellows, accompanied by the Head of the Office for Science in Chile, who had travelled to Chajnantor. They are seen in front of the Atacama Pathfinder Experiment (APEX) telescope at an altitude of 5 100 metres. As one Fellow said be-

tween whiffs of canned oxygen at the 5 000-metre future site of ALMA: "This is amazing, like no place I've ever been." An earthquake measuring 7.7 on the Richter scale struck northern Chile the day before the Fellows arrived there, and occasional minor aftershocks continued to be felt during their stay in the small village of San Pedro de Atacama.

The next ESO Fellowship Symposium will take place in Garching in 2009.



Photo: A. Triat, ESO

No gathering in Chile would be complete without a traditional Chilean *asado* or barbecue.

Report on the

ESO Chile Science Days

held at ESO, Vitacura, Chile, 20 November and 5 December 2007

Michael West (ESO)

Science Days in Santiago are an annual gathering of ESO's geographically dispersed team in Chile to learn more about each other's research, to celebrate scientific achievements of the past year and to encourage new collaborations.

More than 50 ESO staff astronomers, fellows and students based in Chile participated in this year's Science Days, which were held in ESO's Santiago offices. Each

participant gave a five- to ten-minute presentation about his or her current research activities and plans for the near future. Because of the turno schedule for ESO scientific staff with duty stations on Paranal, La Silla and Sequitor, the talks were spread over two days, 20 November and 5 December 2007, to allow as many people as possible to participate.

The research presented by ESO staff during Science Days in Santiago covered a broad range of topics and included collaborators from every ESO member state. As active researchers, ESO staff con-

tribute not only to the advancement of astronomy through their scientific explorations, but also their expert knowledge of ESO telescopes, instrumentation and data processing, gained from first-hand experience. The latter is an important component of ESO's mission to provide the highest quality data in service to the ESO user community.

More information about the research interests and biographies of ESO science staff in Chile can be found on the ESO website at <http://www.eso.org/sci/activities/santiago/personnel/index.html>.

Astronomical Observatories and the Republic of Chile Pave the Way for Future Projects

Gonzalo Argandoña, Félix Mirabel (ESO)

For the very first time after more than four decades of operations of several astronomical observatories in the country, the Chilean Ministry of Foreign Affairs hosted an international workshop, held on 4 and 5 December 2007. The event, called "Chile: A Window into the Universe", was jointly organised by the Ministry and all international observatories currently installed in Chile – including ESO, SOCHIAS (the Chilean Astronomical Society) and CONICYT (the National Commission of Science and Technology).

The workshop offered the unique opportunity of bringing together a wide range of institutions essential for the success of astronomical operations in the country, including local universities, mayors and representatives of local governments, members of industry, officers dealing with legal affairs, and Chilean national agencies in charge of key issues, such as environment, light pollution control, mining and administration of the electromagnetic spectrum.

"Astronomy is a fascinating discipline that captivates not only the interest of experts, but also of those who are impressed every day by the advancements of this science in the understanding of the origin of our planet and the Universe", said the Vice Minister of Foreign Affairs, Ambassador Carlos Portales, during the inauguration of the event. The president of SOCHIAS, Dr. Andreas Reisenegger, commented that "having this international workshop at the Ministry of Foreign Affairs implies a very important recognition of astronomy by the government of Chile. Besides, this initiative confirms the importance of astronomy for the promotion of science in Chile, given the great interest in astronomy by young people".

On behalf of ESO, two presentations were made. Félix Mirabel, Representative in Chile, introduced the main ESO operations in the country, including the La Silla Paranal Observatory, APEX and ALMA, as well as several cooperation agreements with the government and local communities. Michael Sterzik, Deputy Director of the La Silla Paranal Observatory, presented plans for the future

E-ELT (European Extremely Large Telescope), where Chile is one of a few candidates in the world to host this new giant foreseen for the next decade.

Astronomers from Chilean universities presented the main science contributions of recent years undertaken by global teams of scientists, thanks to the international telescopes installed in the country. Topics included the use of supernovae for the determination of the acceleration rate of the expansion of the Universe, the detailed study of a massive black hole at the centre of the Milky Way, and the detection of dozens of new exoplanets, including the first direct image of one of these objects (obtained at Paranal) and the discovery from La Silla of the first rocky exoplanet in the habitable zone.

On behalf of all international observatories in the country, Félix Mirabel also gave a short talk on the general impact of astronomy in Chile, in addition to science

and education. In the same round table session, Sandra Berna, mayor of San Pedro de Atacama (the closest village to the ALMA construction site) emphasised the benefits for the Andean local communities arising from the recent arrival of a series of radio astronomy projects, including ALMA.

The final session of the workshop inspired a rich, lively discussion on future challenges for astronomical activities in the country, including the protection of the sky and the possible installation of new international facilities in the next decades.

Figure 1 (below): Round table on the impact of international astronomical activities for Chile as host country, being chaired by Ambassador Juan Eduardo Eguiguren, Director of Special Policies of the Ministry of Foreign Affairs. From left to right: Félix Mirabel, ESO Representative in Chile; Juan Alcayaga, Tourism National Service; Roberto Guarini, SOFOFA (association representing industry); Fernando Mercado, Intendencia of Coquimbo Region; and Sandra Berna, mayor of San Pedro de Atacama.

Photos: A. Figueras



Figure 2: The ESO interactive stand explaining the principles of interferometry attracted the interest of many secondary school students visiting a parallel exhibition on astronomy at the Chilean Ministry of Foreign Affairs.

Report on the ELSA School on

The Science of Gaia

held at the Lorentz Center, Leiden, the Netherlands, 19–28 November 2007

Anthony Brown¹
Lennart Lindegren²
Mary Kontizas³
Catherine Turon⁴
Karri Muinonen⁵

¹ Leiden University, the Netherlands

² Lund University, Sweden

³ National and Kapodistrian University of Athens, Greece

⁴ Observatoire de Paris, France

⁵ University of Helsinki, Finland

From 19–28 November 2007, the ELSA school on the science of Gaia was held at the Lorentz Center. Gaia is the European Space Agency mission which will provide a stereoscopic census of our Galaxy through the measurement of high-accuracy astrometry, radial velocities and multi-colour photometry. Gaia is scheduled for launch in late 2011 and over the course of its five-year mission will measure parallaxes and proper motions for every object in the sky brighter than magnitude 20 – amounting to about 1 billion stars, galaxies, quasars and Solar System objects. It will achieve an astrometric accuracy of 12–25 micro-arcseconds, depending on colour, at 15th magnitude and 100–300 micro-arcseconds at 20th magnitude. Multi-colour photometry will be obtained for all objects by means of low-resolution spectrophotometry between 330 and 1000 nm. In addition, radial velocities with a precision of 1–15 km/s will be measured for all objects to 17th magnitude.

ELSA (European Leadership in Space Astrometry) is a Marie-Curie research training network which brings together world-leading expertise in space astrometry, the use of space platforms for mapping the three-dimensional structure of our Galaxy, with specialists on numerical algorithms and software engineering for the double purpose of: (1) preparing for the scientific exploitation of data from the Gaia mission; and (2) training the next generation of researchers in this uniquely European specialty to maintain and extend European leadership in space astrometry.

The primary goal of ELSA is to develop a new theoretical understanding of the conceptual, physical, and numerical aspects of space astrometry and turn this understanding into practical analysis tools which will form an essential contribution towards the Gaia data processing system. The organisers of the school felt that it is important from the outset that the young researchers in this network have a solid understanding of the science goals of the Gaia mission in order to provide them with the proper background and motivation for the specific research they will undertake. Further, bringing the potential ‘end-users’ of the Gaia data together with the community involved in preparing for and running the mission, would foster very valuable contacts and mutual understanding.

The lecture programme was of general interest to anyone interested in the Gaia mission and the school was also open to participants from outside the ELSA network. 25 students participated in the school which was also attended by the scientists in charge of the network nodes. Including the lecturers there was a total of 54 participants.

The programme in the first week consisted of two 90-minute lectures in the morning followed in the afternoon by exercises that the students had to carry out in groups. The lectures covered the following topics: stellar evolution; stellar atmospheres; structure and dynamics of the Galaxy and the Local Group; formation and evolution of the Galaxy in a cosmological context; chemical enrichment history of the Galaxy as encoded in its stars; binaries; exoplanets; fundamental physics; and dynamics and physical properties of small Solar System bodies.

The afternoon exercises were intended to let the students actually work actively on some of the topics discussed during the lectures and so create a more workshop-like atmosphere. The exercises were designed by the lecturers together with the ELSA scientists in charge. The students were divided into groups of two to four people and they worked on exercises covering for example: population synthesis and stellar content of galaxies; estimating the photocentre-barycentre discrepancy for observations of Solar System objects; computing a relativistic astrometric model; and working with SDSS data to detect the Sagittarius stream. The results of the exercises were presented by the students and discussed on the last afternoon of the first week. In addition all the students brought posters on their work which they presented during a mid-week afternoon session.

The lectures in the second week were devoted to more ELSA-specific issues. An introduction to GRID computing was given by a representative from Dutch Space BV through a very interesting role-playing game in which the participants had to take on the roles of the various components in a GRID architecture. There were three lectures on how space projects are realised by ESA and its industrial partners and the final two lectures concentrated on the interpretation of astrometric data and the Gaia mission in the context of other large surveys. This rounded out the lecture programme which, in combination with the exercises, was very successful in providing the students with a broad introduction to the science of Gaia and fostered a real sense of being together in a large and exciting project.

Photo: A. Brown, Leiden University



Introduction to GRID computing: Participants taking on the roles of various components in a GRID architecture.

The Lorentz Center

The Lorentz Center in Leiden is an international centre that coordinates and hosts high-visibility workshops in the sciences, in particular physics, astronomy, mathematics, computer science and the

life sciences. The focus is on new collaborations and interactions between scientists from different countries, fields, and levels of seniority. The Center offers substantial logistic as well as financial support for such workshops. Astronomers who are planning an international work-

shop or group meeting are invited to consider the Lorentz Center; more information can be found at www.lorentzcenter.nl.

Fellows at ESO



Lise Christensen

Growing up in a city, I never saw the Milky Way with my own eyes until the age of 16, and I could never identify more than two constellations. I was not at all certain that astronomy was the most interesting field of natural sciences that one could study until an observing trip to La Silla during my undergraduate studies finally convinced me.

After obtaining my Masters degree from the University of Copenhagen, where I studied images of the host galaxies of Gamma-ray bursts, I wanted to gain experience with spectroscopy. In 2002 the instrumentation division in the Potsdam Astrophysical Institute had recently commissioned a new integral-field unit (IFU) for the 3.5-m telescope at Calar Alto. Data from this instrument (PMAS) were to form the basis for my Ph.D. thesis, and it turned out to be quite a challenge to find the faint Lyman-alpha emitting galaxies that are responsible for strong absorption lines in the spectra of background quasars. After finishing my thesis in 2005, I immediately started as a fellow on Paranal, and having knowledge about

IFU data naturally led me to the position as a VIMOS instrument fellow.

My scientific interests are inclined towards galaxies in the high-redshift Universe. Instead of using traditional large surveys with flux-limited samples of galaxies, I have used other selection criteria in order to locate and study either the more common or unusual galaxies that existed in the early Universe. The experience with IFU data has allowed me to gain insight into different types of scientific projects that can be done with the same data sets, such as searching for field Lyman-alpha emitters or looking at quasar environments. Besides, working at ESO has given me the freedom and opportunity to work with several people on various projects that are outside my main scientific path.



Sune Toft

I did my Masters and Ph.D. studies at the Niels Bohr Institute, University of Copenhagen. During my first years of studying physics, I became very interested in

the philosophical aspects of physics, and discovered that astronomy, in particular cosmology, was a natural framework to pursue this interest. I was fascinated by cosmologist's attempts to develop a model for the entire Universe, despite the limited amount of observational constraints available at the time.

One of the best ways to constrain cosmology is to study the build-up of mass as a function of cosmic time. Observations of high-redshift galaxies provide the strongest constraints. For my Ph.D. thesis I used deep near-infrared (NIR) observations obtained with the VLT to study galaxy evolution in high-redshift clusters of galaxies. I spent seven months at the Institute of Astronomy in Hawaii, where I had the opportunity to observe with several of the big telescopes on Mauna Kea. I also had prolonged collaborative visits to ESO and Leiden.

In 2003 I received my Ph.D. and moved to the United States where I took up a postdoc position at Yale University. There I started working on a newly discovered population of NIR-selected massive, high-redshift galaxies. Working in the U.S. was very interesting, and I seriously considered staying for a second postdoc, but when in 2006 I had the opportunity to return to Europe for an ESO fellowship, I didn't hesitate. I have been very happy with this decision. ESO is a stimulating place to work, with lots of stuff going on (talks, workshops, etc). For my functional work I have become involved in the planning of the ELT, a project with great momentum which is exciting to be part of, and besides that I have plenty of time to pursue my own independent research programme.

New Staff at ESO



Suzanne Ramsay

Since accepting my new job in ESO's Instrumentation Division, I have been telling friends and family that this post makes me 'poacher turned gamekeeper'. I'm not sure how well this phrase translates into the many languages spoken at ESO – I think it might prove a challenge to Google Translation or Babelfish! Basically, until December I had spent a very happy career developing instruments at the UK Astronomy Technology Centre/Royal Observatory in Edinburgh for delivery to UKIRT, Gemini and, latterly, ESO, as instrument scientist on the KMOS project. However, the lure of a post which would bring me closer to the European ELT project was great, and so after 18 years it was time to leave ROE and to enjoy a new perspective – that of the observatory staff.

As well as my involvement with ELT and VLT instrumentation projects, I aim to maintain my research interests. These are in the area of star formation, more specifically in exploring the role that observations of molecular hydrogen can play in helping us to understand the environment of young stars. The chance to participate in the E-ELT project coupled with the exciting and positive working environment at ESO are just two of the many reasons I am delighted with my move. For years I had stated a desire to live and work in a country where the spoken language is other than English. I do have to keep reminding myself of this as I wrestle with the day-to-day issues of banking, telephony and apartment rental armed only with school-level German, but so far I'm really enjoying the challenge.

Michael West

I joined ESO in August 2007 as the new Head of the Office for Science in Chile.

As a young high school student, reading Carl Sagan's book *The Cosmic Connection* changed my life and motivated me to become an astronomer. After obtaining my Ph.D. in astronomy from Yale University in 1987 I held various research and teaching positions around the world, most recently as Head of Science Operations at Gemini South and before that as a professor of astronomy at the University of Hawaii for eight years. My research interests include globular clusters as probes of galaxy formation and evolution, clusters of galaxies at low and high redshifts, and the large-scale structure of the Universe. I began my research career as a theorist but gradually moved into observational work.

As professional astronomers we are very fortunate to be able to do what we do for a living. For this reason I am active in astronomy education and outreach, as a way of giving something back to the public whose taxes fund our astronomical explorations. I currently head a newly formed IAU working group on New Ways of Communicating Astronomy with the Public. I also had the pleasure of serving as chief astronomy content advisor for the Imiloa Astronomy Center of Hawaii, a 28 million USD NASA-funded museum

that weaves together astronomy and Hawaiian culture into a unique story of human exploration. In addition, I am author of a general interest book titled *A Gentle Rain of Starlight: The Story of Astronomy on Mauna Kea*.

I am delighted to be part of ESO and enjoy my new position very much. It is hard to imagine a more exciting time to be doing astronomy and to be working at ESO. I see my role as that of a 'science enabler' whose most important duty is to help ESO Chile astronomers, fellows, students and visitors succeed in their research. The opportunity to mentor younger astronomers and to be an advocate for more senior ones is very gratifying. I also enjoy helping to build bridges between ESO and the Chilean astronomical community as well as with the other international observatories in Chile.

I look forward to meeting the many members of ESO's diverse community. If you are passing through Santiago sometime, please stop by to say hello!



Announcement of

ESO Large Programmes on the Gran Telescopio Canarias

The accession agreement of Spain into ESO includes the allocation of 122 clear nights with the new 10.4-m Gran Telescopio Canarias (GTC) to proposals by PI's from ESO member countries (including Spain).

The ESO/GTC programmes must satisfy the following conditions: (1) each programme should request a minimum of 20 nights; (2) the observations will be conducted either in Service or in Visitor Mode by the ESO/GTC PI teams according to the standard GTC operational procedures.

The mechanism for submission and evaluation of ESO/GTC proposals, and the duration of the programmes will be the

same as that for ESO Large Programmes. There will be two calls for proposals for the first year of operations with deadlines 21 April 2008 for observations starting in March 2009, and 16 October 2008 for observations starting in September 2009. For the first (this) call, the available instruments will be the optical imager and multi-object spectrograph OSIRIS and the mid-IR imager-spectro-polarimeter CanariCam, which will be commissioned during 2008. Proposals should be prepared using the information available on the web, which includes exposure-time calculators. Technical information about the telescope and the instruments OSIRIS and CanariCam is available through the GTC web pages, <http://www.gtc.es/>.

The ESO rules for Guaranteed Time Observations (GTO) will apply to the ESO/GTC programmes recommended by the OPC. Please refer to the ESO Call for Proposals for Period 82 and to the ESO web pages <http://www.eso.org/sci/> for additional information on this call.



Announcement of the

ASTRONET Infrastructure Roadmap Symposium: An Opportunity to Contribute to the European Astrophysical Strategy for the Next 20 Years

16–19 June 2008, Liverpool, United Kingdom

Faithful readers of the ESO Messenger might experience here a slight feeling of *déjà vu*. A year or so after the Astronet Poitiers Symposium, where the community at large provided precious feedback on the European astronomical Science Vision, it is time for another call for arms ... and brains. This second and last time is to invite every European researcher in the scientific, technical, educational

and communicating astronomy fields to help in the building of an Infrastructure Roadmap for the next 20 years. You are strongly encouraged to participate in the 16–19 June 2008 Astronet Infrastructure Roadmap Symposium in Liverpool, United Kingdom. Please note also that, in preparation for the Symposium, a web-based discussion of the Infrastructure Roadmap draft document will open by the end of April 2008 and your input is eagerly sought as well.

Establishing a Science Vision was the first segment of the process conducted by ASTRONET (<http://www.astronet-eu.org/>), the consortium created by a group of European funding agencies, and financed by the European Commission, in order to establish a comprehensive long-term planning for the development of European astronomy. The Science Vision was released at the end of September 2007 (<http://www.strw.leidenuniv.nl/sciencevision/>). It covers all wavelengths

and observing means from ground and space and provides a set of prioritised science goals as well as an analysis of the generic facilities needed to attain them.

The next and last phase is the building of a prioritised 'Infrastructure Roadmap', elucidating the ways and means to implement the Vision. This process (<http://www.astronet-eu.org/-Infrastructure-Roadmap->) started in March 2007. Thematic panels drawn from the astronomical community have since addressed the whole astronomical 'food chain' from infrastructure and technology development to observation, data access, modelling, theory, education, training and public communication. Their input is currently being distilled by the Infrastructure Roadmap Working Group, which is composed of the panel chairs and co-chairs plus external experts, with the release of the draft roadmap on the Astronet web pages, expected by the end of April 2008.



Your contributions, via a forum discussion of the draft document, will be incorporated by the panels and the Working Group in the presentation of their preliminary conclusions at the 16–19 June 2008 Astronet Infrastructure Roadmap Symposium in Liverpool, United Kingdom. The Symposium will provide a live – and hope-fully lively – platform to refine the

roadmap. Through this two-step process, for which your participation is essential, ASTRONET will finally deliver its full bi-decadal, long-term plan to the European Commission and its funding agencies by the end of 2008.

Do not miss this golden opportunity to contribute to this crucial milestone.

Please join us in Liverpool next June to help ensuring a vibrant future for astronomy in Europe.

For further information and to register for the Symposium, please visit <http://www.astro.livjm.ac.uk/~airs2008/>.

Announcement of the MPA/ESO/MPE/USM 2008 Joint Astronomy Conference on

Chemical Evolution of Dwarf Galaxies and Stellar Clusters

21–25 July 2008, ESO Headquarters, Garching, Germany

Small stellar systems, like dwarf galaxies and globular clusters, may be well suited in order to study galactic nucleosynthesis and chemical evolution as, to a first approximation, they can be treated as simple, homogeneous one-component objects.

Currently there is intensive work on determining stellar abundances in Galactic stellar systems (notably globular clusters) and in local-group dwarf galaxies. Many of these projects are actually pursued with the latest instruments, and have revealed surprising results.

Stars in globular clusters, on the one hand, are characterised by a well-defined iron abundance with a small spread, which indicates that they formed from gas that has been pre-enriched. This narrow spread in iron abundance, on the other hand, is in contrast with the widespread abundance anomalies in light elements which are preferentially explained by 'primordial pollution' scenarios. The latter may imply, at least to some degree, internal chemical evolution, where presently observed stars formed out of cluster matter polluted by earlier generations of stars, or at least by the more massive objects of the same generation. There are also scenarios which claim that this pollution was due to external field stars in the surroundings

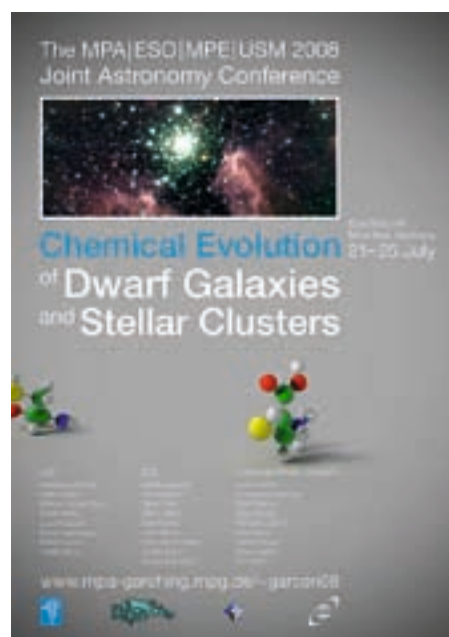
of the proto-globular cluster cloud which was part of a small, dwarf-galaxy-like substructure of the Galaxy. This host galaxy was later disrupted by the Milky Way, while its globular clusters survived and are now part of the Milky Way system.

Dwarf galaxies are likely to have formed, as is typical for galaxies, through infall of primordial gas onto a dark-matter halo. They therefore have their own chemical evolution, which, however, is different from that of large galaxies due to the shallower potential wells, thus leading to more efficient mixing and a stronger influence of galactic tides causing harassment and tidal disruption. In addition, outflows of enriched hot gas in galactic winds are very likely to affect these systems. Dwarf galaxies are also investigated in integrated light to derive their star-formation history and age-metallicity relations. Some globular clusters are thought to be cores of former dwarf galaxies, in particular those where multiple populations of stars have been found (such as Omega Cen and NGC 2808).

As globular clusters and dwarf galaxies form a mass sequence and as there are the above-mentioned possible connections between the two classes of stellar systems, the topic of the conference is a confrontation and comparison of cluster

and dwarf galaxy chemical evolution, which should be helpful in understanding the origin of the abundances in both classes of object.

For registration and more information, please visit <http://www.mpa-garching.mpg.de/~garcon08/>. The deadline for preliminary registration and abstract submission is 15 April 2008; final registration closes on 15 May 2008.



Announcement of the Joint ESO/INAF-Arcetri Workshop on

Future Ground-based Solar System Research: Synergies with Space Probes and Space Telescopes

8–12 September 2008, Portoferraio, Isola d'Elba, Livorno, Italy

In the coming years fundamentally new observing platforms and space probes will become available for Solar System research. This workshop will provide a forum to review the state of the field and to discuss the use of these future facilities, especially to optimise and establish synergies.

The idea for this workshop came from the group of scientists who participated in the worldwide ground-based support and follow-up for NASA's Deep Impact experiment (c.f. Käufel et al. 2005, *The Messenger* 121, 11; Käufel and Sterken 2006, *The Messenger* 126, 48).

In order to further improve communication between the ground-based observers, the spacecraft experimenters and astrophysicists interested in star formation, planetary system formation as well as astrobiology, a set of invited reviews on the state of research as well as on the available present and future facilities is planned. To highlight what 'fundamentally new' means in this context for space

missions, reference is made as an example to ESA's Rosetta mission, *en route* for a *rendezvous* with 67P/Churyumov-Gerasimenko in 2014. The spacecraft will stay orbiting the comet throughout its perihelion passage while dispatching a lander module. Previous missions to comets were of fly-by type with relative velocities of 15–75 km/s. In a similar sense JWST will provide precious observing capabilities not only for cosmology, but especially also for our own Solar System. The next generation of 30–40-m-class ground-based extremely large telescopes (ELTs) – including the Large Binocular Telescope as a stepping stone towards the ELTs – will not only allow for unique observing capabilities within our own Solar System, but will also for the first time enable systematic searches – and hopefully detections – of direct radiation from representative extrasolar planets.

From the ESO point of view, particularly interesting is to develop a coherent set of large or key-project science cases for the European Extremely Large Telescope

(E-ELT) and to ensure that the planned suite of instrumentation allows for optimum synergies between future space missions and the E-ELT.

We envisage a highly interactive meeting in a very pleasant historical setting within the 16th-century fortress of Portoferraio, built in Renaissance style as *Cosmopoli* on the initiative of Cosimo I. de' Medici. There is ample space for poster presentations. Proceedings of this workshop will be published in *Memorie della Societa Astronomica Italiana*.

The deadline for registration and receipt of abstracts is 1 July 2008.

Limited funds are available under the OPTICON programme for contributions in the context of the use of E-ELTs (for details see the conference web page).

For registration and more information please visit <http://www.eso.org/sci/meetings/elba2008> or <http://www.arcetri.astro.it/elba2008>.

Personnel Movements

Arrivals (1 January–31 March 2008)

Europe	
Bruton, Andrew (GB)	Mechanical Technician
da Rocha, Cristiano (BR)	Fellow
Karovicova, Iva (CZ)	Student
Kurz, Richard (USA)	Project Manager ALMA
Mallaband, Stephen (GB)	Senior Contract Officer
Santangelo, Gina (I)	Student
Schimpelsberger, Johannes (A)	Contract Officer
Specht, Alexandra (D)	Administrative Assistant
Stöckl, Josef (A)	Student
Szyszk, Cezary (PL)	Student
Zwaan, Martin A. (NL)	Astronomer
Chile	
Almeida, Pedro Viana (P)	Student
Caceres, Claudio (RCH)	Student
Fuenteseca, Eloy (RCH)	Mechanical Engineer
Jockel, Karl (D)	Chief Procurement Officer
Montironi, Katia (I)	Secretary/Assistant
Planesas, Pere (E)	Test Scientist
Ruppert, Jan (D)	Student
Salinas, Ricardo (RCH)	Student
Schmidt, Heidi (N)	Human Resources Officer
Ventura, Laura (I)	Education and Outreach Officer
Whyborn, Nicholas (GB)	Engineer

Departures (1 January–31 March 2008)

Europe	
Cesarsky, Catherine (F)	Senior Astronomer
de Jong, Jeroen (NL)	Applied Scientist
Esteves, Raul (P)	Electronics Engineer
Gobat, Raphaël (CH)	Student
Marx, Beate (D)	Database Administrator
Oberti, Sylvain (F)	Optical Engineer
Rite, Charles (BR)	Software Engineer
Saitta, Francesco (I)	Student
Sierra González, María del Mar (E)	Software Engineer
Thillerup, Jesper (DK)	Electronics Technician
Chile	
Ageorges, Nancy (F)	Operations Astronomer
Bergman, Per Mikael (S)	Operations Astronomer
Carrasco, Cecilia (RCH)	Administrative Officer
Ederoclite, Alessandro (I)	Operations Astronomer
Harding, George (RCH)	Electrical Engineer
Jullo, Eric (F)	Student
Lopez, Ariel (RCH)	Telescope Instruments Operator
Morell, Merilio (RCH)	Telescope Instruments Operator
Naef, Dominique (CH)	Fellow
Parra, Jose (RCH)	Data Handling Administrator
Rahoui, Farid (F)	Student
Torres, Soraya (RCH)	Secretary

Annual Index 2007 (Nos. 127–130)

Subject Index

The Organisation

- Editorial; Cesarsky, C.; 127, 2
Tim de Zeeuw to Become the Next Director General of ESO; 127, 3
Astronomy in Spain; Barcons, X.; 127, 4
The Czech Republic Joins ESO; Cesarsky, C.; 128, 2
Astronomy in the Czech Republic; Palouš, J.; Hadrava, P.; 128, 3
A Science Vision for European Astronomy in the Next 20 Years; Monnet, G.; Molster, F.; Melnick, J.; 130, 2

Telescopes and Instrumentation

- The European Extremely Large Telescope (E-ELT); Gilmozzi, R.; Spyromilio, J.; 127, 11
Reports on the Conference "Towards the European Extremely Large Telescope"; Monnet, G.; Hook, I.; Cuby, J.-G.; 127, 20
ESO Public Surveys with the VST and VISTA; Arnaboldi, M.; Neeser, M. J.; Parker, L. C.; Rosati, P.; Lombardi, M.; Dietrich, J. P.; Hummel, W.; 127, 28
AMBER, the Near-Infrared Instrument of the VLT; Malbet, F.; Petrov, R.; Rantakyro, F.; and the AMBER consortium; 127, 33
First AMBER/VLT Science; Malbet, F.; Petrov, R.; Weigelt, G.; Chesneau, O.; Domiciano de Souza, A.; Meilland, A.; Millour, F.; Tatulli, E.; and the AMBER consortium; 127, 37
ULTRASPEC: High-speed Spectroscopy with Zero Read-out Noise; Dhillon, V.; Marsh, T.; Copperwheat, C.; Bezawada, N.; Ives, D.; Vick, A.; O'Brien, K.; 127, 41
FORS1 is getting Blue: New Blue Optimised Detectors and High Throughput Filters; Szeifert, T.; Reiss, R.; Baksai, P.; Deiries, S.; Izzo, C.; Jehin, E.; Kiekebusch, M.; Moehler, S.; O'Brien, K.; Pompei, E.; Riquelme, M.; Rupprecht, G.; Shen, T.-C.; 128, 9
Towards Precision Photometry with FORS: A Status Report; Freudling, W.; Moller, P.; Patat, F.; Moehler, S.; Romaniello, M.; Jehin, E.; O'Brien, K.; Izzo, C.; Depagne, E.; Pompei, E.; Naef, D.; Rupprecht, G.; Järvinen, A.; 128, 13
Exploring the Near-Infrared at High Spatial and Spectral Resolution: First Results from CRIFES Science Verification; Siebenmorgen, R.; Smette, A.; Käufel, H. U.; Seifahrt, A.; Uttenthaler, S.; Bik, A.; Casali, M.; Hubrig, S.; Jung, Y.; Kerber, F.; Melnick, J.; Moorwood, A.; Pirard, J.-F.; Sana, H.; Valenti, E.; Tacconi-Garman, L. E.; Hilker, M.; Primas, F.; Amado, P. J.; Carmona, A.; van Dishoeck, E. F.; Foellmi, C.; Goto, M.; Gredel, R.; Günther, E.; Gustaffson, B.; Kurtz, D.; Lidman, C.; Linz, H.; Martins, F.; Menten, K.; Moutou, C.; Nissen, P. E.; Nürnberger, D.; Reiners, A.; 128, 17

- The First Active Segmented Mirror at ESO; Gonté, F.; Dupuy, C.; Frank, C.; Araujo-Hauck, C.; Brast, R.; Frahm, R.; Karban, R.; Andolfato, L.; Esteves, R.; Nylund, M.; Sedghi, B.; Fischer, G.; Noethe, L.; Derie, F.; 128, 23
Progress of the ALMA Project; Haupt, C.; Rykaczewski, H.; 128, 25
ALMA European Project Scientist Appointed; Wilson, T.; 128, 31
A New Era in Submillimetre Continuum Astronomy has Begun: LABOCA Starts Operation on APEX; Siringo, G.; Weiss, A.; Kreysa, E.; Schuller, F.; Kovacs, A.; Beelen, A.; Esch, W.; Gemünd, H.-P.; Jethava, N.; Lundershausen, G.; Menten, K. M.; Güsten, R.; Bertoldi, F.; De Breuck, C.; Nyman, L.-Å.; Haller, E.; Beeman, J.; 129, 2
On-sky Testing of the Multi-Conjugate Adaptive Optics Demonstrator; Marchetti, E.; Brast, R.; Delabre, B.; Donaldson, R.; Fedrigo, E.; Frank, C.; Hubin, N.; Kolb, J.; Lizon, J.-L.; Marchesi, M.; Oberti, S.; Reiss, R.; Santos, J.; Soenke, C.; Tordo, S.; Baruffolo, A.; Bagnara, P.; The CAMCAO consortium; 129, 8
Circular Polarimetry Now Offered at EFOOSC2; Saviane, I.; Piirola, V.; Bagnulo, S.; Monaco, L.; Hutsemekers, D.; Katajainen, S.; Lehto, H.; Vornanen, T.; Berdyugin, A.; Hakala, P.; 129, 14
The 3.6-m Dome: 30 Years After; Ihle, G.; Montano, N.; Tamai, R.; 129, 18
Calibration Sources for the Near-IR Arm of X-shooter; Kerber, F.; Saitta, F.; Bristow, P.; 129, 21
Future Wavelength Calibration Standards at ESO: the Laser Frequency Comb; Araujo-Hauck, C.; Pasquini, L.; Manescau, A.; Udem, T.; Hänsch, T. W.; Holzwarth, R.; Sizmman, A.; Dekker, H.; D'Odorico, S.; Murphy, M. T.; 129, 24
ESO's Next Generation Archive System in Full Operation; Wicenec, A.; Knudstrup, J.; 129, 27
Coming Soon on Stage: X-shooter; Vernet, J.; Dekker, H.; D'Odorico, S.; Pallavicini, R.; Rasmussen, P. K.; Kaper, L.; Hammer, F.; Groot, P.; and the X-shooter team; 130, 5
Peering into the Dust: News from VISIR; Käufel, H. U.; Nürnberger, D.; Vanzi, L.; Baksai, P.; Dobrzycka, D.; Jimenez, J.; Leiva, A.; Lundin, L.; Marchesi, M.; Mardones, P.; Mehrgan, L.; Pirard, J.-F.; Rojas, C.; Salazar, D.; Siebenmorgen, R.; Silber, A.; van den Ancker, M.; Weilenmann, U.; Durand, G.; Pantin, E.; Moerchen, M.; 130, 8

- GROND Commissioned at the 2.2-m MPI Telescope on La Silla; Greiner, J.; Bornemann, W.; Clemens, C.; Deuter, M.; Hasinger, G.; Honsberg, M.; Huber, H.; Huber, S.; Krauss, M.; Krühler, T.; Yoldaş, A. K.; Mayer-Hasselwander, H.; Mican, B.; Primak, N.; Schrey, F.; Steiner, I.; Szokoly, G.; Thöne, C. C.; Yoldaş, A.; Klose, S.; Laux, U.; Winkler, J.; 130, 12
Status of the ALMA Antenna Production; Stanghellini, S.; 130, 15

Astronomical Science

- Twenty Years of Supernova 1987A; Fransson, C.; Gilmozzi, R.; Gröningsson, P.; Hanuschik, R.; Kjær, K.; Leibundgut, B.; Spyromilio, J.; 127, 44
SN 1987A at La Silla: The Early Days; Danziger, J.; Bouchet, P.; 127, 49
Integral-field Spectroscopy of Galactic Planetary Nebulae with VLT FLAMES; Tsamis, Y. G.; Walsh, J. R.; Péquignot, D.; Barlow, M. J.; Liu, X.-W.; Danziger, J.; 127, 53
Hunting for Frozen Super-Earths via Microlensing; Beaulieu, J.-P.; Albrow, M.; Bennett, D.; Brilliant, S.; Caldwell, J. A. R.; Calitz, J. J.; Cassan, A.; Cook, K. H.; Coutures, C.; Dieters, S.; Dominik, M.; Dominis-Prestre, D.; Donatowicz, J.; Fouqué, P.; Greenhill, J.; Hill, K.; Hoffman, M.; Jørgensen, U. G.; Kane, S.; Kubas, D.; Marquette, J.-B.; Martin, R.; Meintjes, P.; Menzies, J.; Pollard, K.; Sahu, K.; Vinter, C.; Wambsganss, J.; Williams, A.; Woller, K.; Zub, M.; Horne, K.; Allan, A.; Bode, M.; Bramich, D. M.; Burgdorf, M.; Fraser, S.; Mottram, C.; Rattenbury, N.; Snodgrass, C.; Steele, I.; Tsapras, Y.; 128, 33
Sulphur Abundances in Metal-Poor Stars – First Result from CRIFES Science Verification; Nissen, P. E.; Asplund, M.; Fabbian, D.; Kerber, F.; Käufel, H. U.; Pettini, M.; 128, 38
Using Globular Clusters to Test Gravity in the Weak Acceleration Regime; Scarpa, R.; Marconi, G.; Gilmozzi, R.; Carraro, G.; 128, 41
Dissecting the Nuclear Environment of Mrk 609 with SINFONI – the Starburst-AGN Connection; Zuther, J.; Fischer, S.; Pott, J.-U.; Bertram, T.; Eckart, A.; Straubmeier, C.; Iserlohe, C.; Voges, W.; Hasinger, G.; 128, 44
GHostS – Gamma-Ray Burst Host Studies; Savaglio, S.; Budavári, T.; Glazebrook, K.; Le Borgne, D.; Le Floch, E.; Chen, H.-W.; Greiner, J.; Yoldaş, A. K.; 128, 47
The Puzzle of the Ly α Galaxies: New Results from the VLT; Tapken, C.; Appenzeller, I.; Gabasch, A.; Heidt, J.; Hopp, U.; Bender, R.; Noll, S.; Seitz, S.; Richling, S.; 128, 51
Status and Perspectives of Astroparticle Physics in Europe; Spiering, C.; 129, 33
Hot Gas in High-Redshift Protogalaxies: Observations of High-Ion Absorption in Damped Lyman-Alpha Systems; Fox, A. J.; Petitjean, P.; Ledoux, C.; Srianand, R.; 129, 38

- The Redshift of BL Lacertae Objects from High Signal-to-Noise VLT Spectra; Falomo, R.; Treves, A.; 129, 42
- Results from the Multiwavelength Survey by Yale-Chile (MUSYC); Treister, E.; Gawiser, E.; Van Dokkum, P.; Lira, P.; Urry, M.; and the MUSYC Collaboration; 129, 45
- Weighing Ultracompact Dwarf Galaxies in the Fornax Cluster; Hilker, M.; Baumgardt, H.; Infante, L.; Drinkwater, M.; Evstigneeva, E.; Gregg, M.; 129, 49
- VLT/FORS Surveys of Wolf-Rayet Stars beyond the Local Group: Type Ib/c Supernova Progenitors?; Crowther, P. A.; Hadfield, L. J.; 129, 53
- Surface Ice Spectroscopy of Pluto, Charon and Triton; Protopapa, S.; Herbst, T.; Bönnhardt, H.; 129, 58
- First Thermal IR Images of Neptune: Evidence for Southern Polar Heating and Methane Escape; Encrenaz, T.; Orton, G. S.; Leyrat, C.; Puetter, R. C.; Friedson, A. J.; Pantin, E.; 130, 23
- Polarimetry of Solar System Gaseous Planets; Joos, F.; Schmid, H. M.; 130, 27
- η Carinae 2009.0: One of the Most Remarkable Stars in the Sky; Sterken, C.; van Genderen, A.; Weigelt, G.; Kaufer, A.; 130, 32
- The Monitor Project: Tracking the Evolution of Low-Mass and Pre-Main-Sequence Stars; Aigrain, S.; Irwin, J.; Hebb, L.; Hodgkin, S.; Miller, A.; Moraux, E.; Stassun, K.; 130, 36
- Star-Forming Nuclear Rings in Spiral Galaxies; Falcón-Barroso, J.; Böker, T.; Schinnerer, E.; Knapen, J. H.; Ryder, S.; 130, 40
- Gamma-Ray Bursts as Cosmological Probes: from Concept to Reality; Fynbo, J.; Vreeswijk, P.; Jakobsson, P.; Jaunsen, A.; Ledoux, C.; Malesani, D.; Thöne, C.; Ellison, S.; Gorosabel, J.; Hjorth, J.; Jensen, B.; Kouveliotou, C.; Leván, A.; Møller, P.; Rol, E.; Smette, A.; Sollerman, J.; Starling, R.; Tanvir, N.; Watson, D.; Wiersema, K.; Wijers, R.; Xu, D.; 130, 43
- [Astronomical News](#)
- Nature Around the ALMA Site – Part 1; Grenon, M.; 127, 59
- Research Project “Safety and Health in High-altitude Observatories”; Böcker, M.; Vogt, J.; 127, 64
- First Report on the 2007 ESO Instrument Calibration Workshop; Kaufer, A.; Kerber, F.; Hanuschik, R.; Patat, F.; Peron, M.; Romaniello, M.; Sterzik, M.; Tacconi-Garman, L. E.; 127, 66
- Report on the Fourth Advanced Chilean School of Astrophysics: Interferometry in the Epoch of ALMA and VLTI; Barrientos, F.; Nagar, N.; Mirabel, F.; 127, 67
- Report on the Third Advanced Chilean School of Astrophysics; Gieren, W.; Zoccali, M.; Saviane, I.; Méndez, R.; Pietrzynski, G.; 127, 68
- ESO at the AAS, the AAAS and in Dublin; Boffin, H.; Madsen, C.; 127, 69
- Announcement of the ESO Workshop “12 Questions on Star and Massive Star Cluster Formation”; 127, 70
- Announcement of ONTHEFRINGE: The Very Large Telescope Interferometer Training Schools; 127, 71
- ESO Studentship Programme; 127, 72
- Fellows at ESO: Andrés Jordán, Paul Lynam; 127, 73
- ESO Vacancies: Engineer for Cryogenic Systems, System Engineer; 127, 74
- Personnel Movements; 127, 75
- List of Proceedings from the ESO Astrophysics Symposia; 127, 75
- New Editor; 127, 75
- Nature Around the ALMA Site – Part 2; Grenon, M.; 128, 57
- Using the *h*-index to Explore the Scientific Impact of the VLT; Grothkopf, U.; Melo, C.; Erdmann, C.; Kaufer, A.; Leibundgut, B.; 128, 62
- Status of Women at ESO: a Pilot Study on ESO Staff Gender Distribution; Primas, F.; 128, 67
- Report on the International Workshop on Observing Planetary Systems; Sterzik, M.; Dumas, C.; 128, 72
- The Re-launch of the ESO Web; Warmels, R.; Zech, G.; 128, 73
- Fellows at ESO: Maria Messineo, Laura Parker; 128, 75
- Personnel Movements; 128, 76
- ESO Fellowship Programme 2007/2008; 128, 77
- Announcement of ALMA Community Meeting and Surveys for ALMA Workshop; 128, 78
- Announcement of the MPA/ESO/MPE/USM 2007 Joint Astronomy Conference on Gas Accretion and Star Formation in Galaxies; 128, 78
- BACHES – A Compact Light-Weight Echelle Spectrograph for Amateur Astronomy; Avila, G.; Burwitz, V.; Guirao, C.; Rodriguez, J.; Shida, R.; Baade, D.; 129, 62
- Report on the ESO Workshop on Obscured AGN across Cosmic Time; Fosbury, R. A. E.; De Breuck, C.; Mainieri, V.; Robertson, G.; Vernet, J.; 129, 64
- Report on the ESO Workshop on “12 Questions on Star and Massive Star Cluster Formation”; Kissler-Patig, M.; Wilson, T.; Bastian, N.; D’Antona, F.; de Grijs, R.; Froebrich, D.; Galliano, E.; Grosbøl, P.; Johnson, K.; Keto, E.; Klessen, R.; Megeath, T.; Rejkuba, M.; Steinacker, J.; Zinnecker, H.; 129, 69
- Announcement of a Workshop on Science from UKIDSS; 129, 72
- Observing at ESO: a New Procedure for Target and Instrument Set-up Changes; Primas, F.; Nass, P.; Hainaut, O.; Sterzik, M.; 129, 73
- Personnel Movements; 129, 73
- Scisoft VII – with Virtual Observatory Support; Hook, R.; on behalf of the Scisoft Team; 129, 74
- Gruber Prize in Cosmology Awarded for the Discovery of the Accelerated Expansion of the Universe; 129, 74
- Fellows at ESO: Steffen Mieske, Julia Scharwächter; 129, 75
- Report on the Conference “Science with the VLT in the ELT Era”; Moorwood, A.; on behalf of the Scientific Organising Committee; 130, 48
- Report on ALMA Community Days; Testi, L.; De Breuck, C.; 130, 51
- Report on the Workshop “Surveys for ALMA”; Testi, L.; De Breuck, C.; 130, 53
- Announcement of the Launch of the New ESO User Portal; Tacconi-Garman, L. E.; on behalf of the User Portal Project Team; 130, 54
- Announcement of the ESO Workshop on Star Formation across the Milky Way Galaxy; 130, 55
- Announcement of a Practical Workshop on IFU Observations and Data Reduction; 130, 55
- Announcement of the Workshop on Gas and Stars in Galaxies – a Multi-Wavelength 3D Perspective; 130, 56
- Announcement of ONTHEFRINGE: the Very Large Telescope Interferometer Training Schools; 130, 56
- Announcement of the NEON Observing Schools; 130, 57
- Personnel Movements; 130, 57
- Fellows at ESO: Gaël James, Lorenzo Monaco; 130, 58
- A Long Night for ESO; Boffin, H.; Madsen, C.; 130, 59
- Report on the First ESO-EAAE Astronomy Summer School; Pierce-Price, D.; Ros, R. M.; Madsen, C.; 130, 60
- A String of Exhibitions; Janssen, E.; Calçada, L.; Heyer, H. H.; 130, 61
- Distinguished Visitors to Paranal; Boffin, H.; Madsen, C.; 130, 62

Author Index

A

- Aigrain, S.; Irwin, J.; Hebb, L.; Hodgkin, S.; Miller, A.; Moraux, E.; Stassun, K.; The Monitor Project: Tracking the Evolution of Low-Mass and Pre-Main-Sequence Stars; 130, 36
- Araujo-Hauck, C.; Pasquini, L.; Manescau, A.; Udem, T.; Hänsch, T. W.; Holzwarth, R.; Sizmman, A.; Dekker, H.; D'Odorico, S.; Murphy, M. T.; Future Wavelength Calibration Standards at ESO: the Laser Frequency Comb; 129, 24
- Arnaboldi, M.; Neeser, M. J.; Parker, L. C.; Rosati, P.; Lombardi, M.; Dietrich, J. P.; Hummel, W.; ESO Public Surveys with the VST and VISTA; 127, 28
- Avila, G.; Burwitz, V.; Guirao, C.; Rodriguez, J.; Shida, R.; Baade, D.; BACHES – A Compact Light-Weight Echelle Spectrograph for Amateur Astronomy; 129, 62

B

- Barcons, X.; Astronomy in Spain; 127, 4
- Barrientos, F.; Nagar, N.; Mirabel, F.; Report on the Fourth Advanced Chilean School of Astrophysics: Interferometry in the Epoch of ALMA and VLTI; 127, 67
- Beaulieu, J.-P.; Albrow, M.; Bennett, D.; Brillant, S.; Caldwell, J. A. R.; Calitz, J. J.; Cassan, A.; Cook, K. H.; Coutures, C.; Dieters, S.; Dominik, M.; Dominis-Prestre, D.; Donatowicz, J.; Fouqué, P.; Greenhill, J.; Hill, K.; Hoffman, M.; Jørgensen, U. G.; Kane, S.; Kubas, D.; Marquette, J.-B.; Martin, R.; Meintjes, P.; Menzies, J.; Pollard, K.; Sahu, K.; Vinter, C.; Wambsganss, J.; Williams, A.; Woller, K.; Zub, M.; Horne, K.; Allan, A.; Bode, M.; Bramich, D. M.; Burgdorf, M.; Fraser, S.; Mottram, C.; Rattenbury, N.; Snodgrass, C.; Steele, I.; Tsapras, Y.; Hunting for Frozen Super-Earths via Microlensing; 128, 33
- Böcker, M.; Vogt, J.; Research Project "Safety and Health in High-altitude Observatories"; 127, 64
- Boffin, H.; Madsen, C.; ESO at the AAS, the AAAS and in Dublin; 127, 69
- Boffin, H.; Madsen, C.; A Long Night for ESO; 130, 59
- Boffin, H.; Madsen, C.; Distinguished Visitors to Paranal; 130, 62

C

- Cesarsky, C.; Editorial; 127, 2
- Cesarsky, C.; The Czech Republic Joins ESO; 128, 2
- Crowther, P. A.; Hadfield, L. J.; VLT/FORS Surveys of Wolf-Rayet Stars beyond the Local Group: Type Ib/c Supernova Progenitors?; 129, 53

D

- Danziger, J.; Bouchet, P.; SN 1987A at La Silla: The Early Days; 127, 49
- Dhillon, V.; Marsh, T.; Copperwheat, C.; Bezawada, N.; Ives, D.; Vick, A.; O'Brien, K.; ULTRASPEC: High-speed Spectroscopy with Zero Read-out Noise; 127, 41

E

- Encrenaz, T.; Orton, G. S.; Leyrat, C.; Puetter, R. C.; Friedson, A. J.; Pantin, E.; First Thermal IR Images of Neptune: Evidence for Southern Polar Heating and Methane Escape; 130, 23

F

- Falcón-Barroso, J.; Böker, T.; Schinnerer, E.; Knapen, J. H.; Ryder, S.; Star-Forming Nuclear Rings in Spiral Galaxies; 130, 40
- Falomo, R.; Treves, A.; The Redshift of BL Lacertae Objects from High Signal-to-Noise VLT Spectra; 129, 42
- Fosbury, R. A. E.; De Breuck, C.; Mainieri, V.; Robertson, G.; Vernet, J.; Report on the ESO Workshop on Obscured AGN across Cosmic Time; 129, 64
- Fox, A. J.; Petitjean, P.; Ledoux, C.; Srianand, R.; Hot Gas in High-Redshift Protogalaxies: Observations of High-Ion Absorption in Damped Lyman-Alpha Systems; 129, 38
- Fransson, C.; Gilmozzi, R.; Gröningsson, P.; Hanuschik, R.; Kjær, K.; Leibundgut, B.; Spyromilio, J.; Twenty Years of Supernova 1987A; 127, 44
- Freudling, W.; Møller, P.; Patat, F.; Moehler, S.; Romaniello, M.; Jehin, E.; O'Brien, K.; Izzo, C.; Depagne, E.; Pompei, E.; Naef, D.; Rupprecht, G.; Järvinen, A.; Towards Precision Photometry with FORS: A Status Report; 128, 13
- Fynbo, J.; Vreeswijk, P.; Jakobsson, P.; Jaunsen, A.; Ledoux, C.; Malesani, D.; Thöne, C.; Ellison, S.; Gorosabel, J.; Hjorth, J.; Jensen, B.; Kouveliotou, C.; Levan, A.; Møller, P.; Rol, E.; Smette, A.; Sollerman, J.; Starling, R.; Tanvir, N.; Watson, D.; Wiersema, K.; Wijers, R.; Xu, D.; Gamma-Ray Bursts as Cosmological Probes: from Concept to Reality; 130, 43

G

- Gieren, W.; Zoccali, M.; Saviane, I.; Méndez, R.; Pietrzynski, G.; Report on the Third Advanced Chilean School of Astrophysics; 127, 68

- Gilmozzi, R.; Spyromilio, J.; The European Extremely Large Telescope (E-ELT); 127, 11
- Gonté, F.; Dupuy, C.; Frank, C.; Araujo-Hauck, C.; Brast, R.; Frahm, R.; Karban, R.; Andolfato, L.; Esteves, R.; Nylund, M.; Sedghi, B.; Fischer, G.; Noethe, L.; Derie, F.; The First Active Segmented Mirror at ESO; 128, 23
- Greiner, J.; Bornemann, W.; Clemens, C.; Deuter, M.; Hasinger, G.; Honsberg, M.; Huber, H.; Huber, S.; Krauss, M.; Krühler, T.; Yoldaş, A. K.; Mayer-Hasselwander, H.; Mican, B.; Primak, N.; Schrey, F.; Steiner, I.; Szokoly, G.; Thöne, C. C.; Yoldaş, A.; Klose, S.; Laux, U.; Winkler, J.; GROND Commissioned at the 2.2-m MPI Telescope on La Silla; 130, 12
- Grenon, M.; Nature Around the ALMA Site – Part 1; 127, 59
- Grenon, M.; Nature Around the ALMA Site – Part 2; 128, 57
- Grothkopf, U.; Melo, C.; Erdmann, C.; Kaufer, A.; Leibundgut, B.; Using the *h*-index to Explore the Scientific Impact of the VLT; 128, 62

H

- Haupt, C.; Rykaczewski, H.; Progress of the ALMA Project; 128, 25
- Hilker, M.; Baumgardt, H.; Infante, L.; Drinkwater, M.; Evstigneeva, E.; Gregg, M.; Weighing Ultracompact Dwarf Galaxies in the Fornax Cluster; 129, 49
- Hook, R.; on behalf of the Scisoft Team; Scisoft VII – with Virtual Observatory Support; 129, 74

I

- Ihle, G.; Montano, N.; Tamai, R.; The 3.6-m Dome: 30 Years After; 129, 18

J

- Janssen, E.; Calçada, L.; Heyer, H. H.; A String of Exhibitions; 130, 61
- Joos, F.; Schmid, H. M.; Polarimetry of Solar System Gaseous Planets; 130, 27

K

- Kaufer, A.; Kerber, F.; Hanuschik, R.; Patat, F.; Peron, M.; Romaniello, M.; Sterzik, M.; Tacconi-Garman, L. E.; First Report on the 2007 ESO Instrument Calibration Workshop; 127, 66
- Käuffl, H. U.; Nürnberger, D.; Vanzi, L.; Baksai, P.; Dobrzycka, D.; Jimenez, J.; Leiva, A.; Lundin, L.; Marchesi, M.; Mardones, P.; Mehrgan, L.; Pirard, J.-F.; Rojas, C.; Salazar, D.; Siebenmorgen, R.; Silber, A.; van den Ancker, M.; Weilenmann, U.; Durand, G.; Pantin, E.; Moerchen, M.; Peering into the Dust: News from VISIR; 130, 8
- Kerber, F.; Saitta, F.; Bristow, P.; Calibration Sources for the Near-IR Arm of X-shooter; 129, 21
- Kissler-Patig, M.; Wilson, T.; Bastian, N.; D'Antona, F.; de Grijs, R.; Froebrich, D.; Galliano, E.; Grosbøl, P.; Johnson, K.; Keto, E.; Klessen, R.; Megeath, T.; Rejkuba, M.; Steinacker, J.; Zinnecker, H.; Report on the ESO Workshop on "12 Questions on Star and Massive Star Cluster Formation"; 129, 69

M

- Malbet, F.; Petrov, R.; Rantakyro, F.; and the AMBER consortium; AMBER, the Near-Infrared Instrument of the VLTI; 127, 33
- Malbet, F.; Petrov, R.; Weigelt, G.; Chesneau, O.; Domiciano de Souza, A.; Meilland, A.; Millour, F.; Tatulli, E.; and the AMBER consortium; First AMBER/VLTI Science; 127, 37
- Marchetti, E.; Brast, R.; Delabre, B.; Donaldson, R.; Fedrigo, E.; Frank, C.; Hubin, N.; Kolb, J.; Lizon, J.-L.; Marchesi, M.; Oberti, S.; Reiss, R.; Santos, J.; Soenke, C.; Tordo, S.; Baruffolo, A.; Bagnara, P.; The CAMCAO consortium; On-sky Testing of the Multi-Conjugate Adaptive Optics Demonstrator; 129, 8
- Monnet, G.; Hook, I.; Cuby, J.-G.; Reports on the Conference "Towards the European Extremely Large Telescope"; 127, 20
- Monnet, G.; Molster, F.; Melnick, J.; A Science Vision for European Astronomy in the Next 20 Years; 130, 2
- Moorwood, A.; on behalf of the Scientific Organising Committee; Report on the Conference "Science with the VLT in the ELT Era"; 130, 48

N

- Nissen, P. E.; Asplund, M.; Fabbian, D.; Kerber, F.; Käuffl, H. U.; Pettini, M.; Sulphur Abundances in Metal-Poor Stars – First Result from CRIRES Science Verification; 128, 38

P

- Palouš, J.; Hadrava, P.; Astronomy in the Czech Republic; 128, 3
- Pierce-Price, D.; Ros, R. M.; Madsen, C.; Report on the First ESO-EAAE Astronomy Summer School; 130, 60
- Primas, F.; Status of Women at ESO: a Pilot Study on ESO Staff Gender Distribution; 128, 67
- Primas, F.; Nass, P.; Hainaut, O.; Sterzik, M.; Observing at ESO: a New Procedure for Target and Instrument Set-up Changes; 129, 73
- Protopapa, S.; Herbst, T.; Bönnhardt, H.; Surface Ice Spectroscopy of Pluto, Charon and Triton; 129, 58

S

- Savaglio, S.; Budavári, T.; Glazebrook, K.; Le Borgne, D.; Le Floch, E.; Chen, H.-W.; Greiner, J.; Yoldaş, A. K.; GHostS – Gamma-Ray Burst Host Studies; 128, 47
- Saviane, I.; Piirola, V.; Bagnulo, S.; Monaco, L.; Hutsemekers, D.; Katajainen, S.; Lehto, H.; Vornanen, T.; Berdyugin, A.; Hakala, P.; Circular Polarimetry Now Offered at EFOSC2; 129, 14
- Scarpa, R.; Marconi, G.; Gilmozzi, R.; Carraro, G.; Using Globular Clusters to Test Gravity in the Weak Acceleration Regime; 128, 41
- Siebenmorgen, R.; Smette, A.; Käuffl, H. U.; Seifahrt, A.; Uttenthaler, S.; Bik, A.; Casali, M.; Hubrig, S.; Jung, Y.; Kerber, F.; Melnick, J.; Moorwood, A.; Pirard, J.-F.; Sana, H.; Valenti, E.; Tacconi-Garman, L. E.; Hilker, M.; Primas, F.; Amado, P. J.; Carmona, A.; van Dishoeck, E. F.; Foellmi, C.; Goto, M.; Gredel, R.; Günther, E.; Gustaffson, B.; Kurtz, D.; Lidman, C.; Linz, H.; Martins, F.; Menten, K.; Moutou, C.; Nissen, P. E.; Nürnberger, D.; Reiners, A.; Exploring the Near-Infrared at High Spatial and Spectral Resolution: First Results from CRIRES Science Verification; 128, 17
- Siringo, G.; Weiss, A.; Kreysa, E.; Schuller, F.; Kovacs, A.; Beelen, A.; Esch, W.; Gemünd, H.-P.; Jethava, N.; Lundershausen, G.; Menten, K. M.; Güsten, R.; Bertoldi, F.; De Breuck, C.; Nyman, L.-Å.; Haller, E.; Beeman, J.; A New Era in Submillimetre Continuum Astronomy has Begun: LABOCA Starts Operation on APEX; 129, 2

- Spiering, C.; Status and Perspectives of Astroparticle Physics in Europe; 129, 33
- Stanghellini, S.; Status of the ALMA Antenna Production; 130, 15
- Sterken, C.; van Genderen, A.; Weigelt, G.; Kaufer, A.; η Carinae 2009.0: One of the Most Remarkable Stars in the Sky; 130, 32
- Sterzik, M.; Dumas, C.; Report on the International Workshop on Observing Planetary Systems; 128, 72
- Szeifert, T.; Reiss, R.; Baksai, P.; Deiries, S.; Izzo, C.; Jehin, E.; Kiekebusch, M.; Moehler, S.; O'Brien, K.; Pompei, E.; Riquelme, M.; Rupprecht, G.; Shen, T.-C.; FORS1 is getting Blue: New Blue Optimised Detectors and High Throughput Filters; 128, 9

T

- Tacconi-Garman, L. E.; on behalf of the User Portal Project Team; Announcement of the Launch of the New ESO User Portal; 130, 54
- Tapken, C.; Appenzeller, I.; Gabasch, A.; Heidt, J.; Hopp, U.; Bender, R.; Noll, S.; Seitz, S.; Richling, S.; The Puzzle of the Ly α Galaxies: New Results from the VLT; 128, 51
- Testi, L.; De Breuck, C.; Report on ALMA Community Days; 130, 51
- Testi, L.; De Breuck, C.; Report on the Workshop "Surveys for ALMA"; 130, 53
- Treister, E.; Gawiser, E.; Van Dokkum, P.; Lira, P.; Urry, M.; and the MUSYC Collaboration; Results from the Multiwavelength Survey by Yale-Chile (MUSYC); 129, 45
- Tsamis, Y. G.; Walsh, J. R.; Péquignot, D.; Barlow, M. J.; Liu, X.-W.; Danziger, J.; Integral-field Spectroscopy of Galactic Planetary Nebulae with VLT FLAMES; 127, 53

V

- Vernet, J.; Dekker, H.; D'Odorico, S.; Pallavicini, R.; Rasmussen, P. K.; Kaper, L.; Hammer, F.; Groot, P.; and the X-shooter team; Coming Soon on Stage: X-shooter; 130, 5

W

- Warmels, R.; Zech, G.; The Re-launch of the ESO Web; 128, 73
- Wicenec, A.; Knudstrup, J.; ESO's Next Generation Archive System in Full Operation; 129, 27
- Wilson, T.; ALMA European Project Scientist Appointed; 128, 31

Z

- Zuther, J.; Fischer, S.; Pott, J.-U.; Bertram, T.; Eckart, A.; Straubmeier, C.; Iserlohe, C.; Voges, W.; Hasinger, G.; Dissecting the Nuclear Environment of Mrk 609 with SINFONI – the Starburst-AGN Connection; 128, 44

ESO is the European Organisation for Astronomical Research in the Southern Hemisphere. Whilst the Headquarters (comprising the scientific, technical and administrative centre of the organisation) are located in Garching near Munich, Germany, ESO operates three observational sites in the Chilean Atacama desert. The Very Large Telescope (VLT), is located on Paranal, a 2 600 m high mountain south of Antofagasta. At La Silla, 600 km north of Santiago de Chile at 2 400 m altitude, ESO operates several medium-sized optical telescopes. The third site is the 5 000 m high Llano de Chajnantor, near San Pedro de Atacama. Here a new submillimetre telescope (APEX) is in operation, and a giant array of 12-m submillimetre antennas (ALMA) is under development. Over 2 000 proposals are made each year for the use of the ESO telescopes.

The ESO Messenger is published four times a year: normally in March, June, September and December. ESO also publishes Conference Proceedings and other material connected to its activities. Press Releases inform the media about particular events. For further information, contact the ESO Public Affairs Department at the following address:

ESO Headquarters
Karl-Schwarzschild-Straße 2
85748 Garching bei München
Germany
Phone +49 89 320 06-0
Fax +49 89 320 23 62
information@eso.org
www.eso.org

The ESO Messenger:
Editor: Jeremy R. Walsh
Technical editor: Jutta Boxheimer
Technical assistant: Mafalda Martins
www.eso.org/messenger/

Printed by
Peschke Druck
Schatzbogen 35
81805 München
Germany

© ESO 2008
ISSN 0722-6691

Contents

Telescopes and Instrumentation

P. Bristow, F. Kerber, M. R. Rosa – Advanced Calibration Techniques for Astronomical Spectrographs	2
R. Davies et al. – Laser Guide Star Adaptive Optics without Tip-tilt	7
R. McMahon et al. – DAZLE on the VLT	11
B. Nikolic et al. – Phase Correction for ALMA: Adaptive Optics in the Submillimetre	14

Astronomical Science

M. van den Ancker et al. – A Multi-Wavelength Study of the 2003–2006 Outburst of V1647 Orionis	20
C. Evans et al. – The VLT-FLAMES Survey of Massive Stars	25
F. Patat et al. – Seeking for the Progenitors of Type Ia Supernovae	30

Astronomical News

F. Primas et al. – The 2007 Users Feedback Campaign	36
R. Hook et al. – ESO Reflex: A Graphical Workflow Engine for Astronomical Data Reduction	42
N. Delmotte – News from the ESO Science Archive Facility	45
L. Testi – ALMA Science: the ESO-Garching Astronomers View	46
T. Hunter, R. Laing – News from the ALMA Test Facility	47
M. West, B. Leibundgut – Report on the 2007 ESO Fellowship Symposium	48
M. West – Report on the ESO Chile Science Days	48
G. Argandoña, F. Mirabel – Astronomical Observatories and the Republic of Chile Pave the Way for Future Projects	49
A. Brown et al. – Report on the ELSA School on the Science of Gaia	50
Fellows at ESO – L. Christensen, S. Toft	51
New Staff at ESO – S. Ramsay, M. West	52

Announcement of ESO Large Programmes on the Gran Telescopio Canarias	53
Announcement of the ASTRONET Infrastructure Roadmap Symposium: An Opportunity to Contribute to the European Astrophysical Strategy for the Next 20 Years	53
Announcement of the MPA/ESO/MPE/USM 2008 Joint Astronomy Conference on Chemical Evolution of Dwarf Galaxies and Stellar Clusters	54
Announcement of the Joint ESO/INAF-Arcetri Workshop on Future Ground-based Solar System Research: Synergies with Space Probes and Space Telescopes	55
Personnel Movements	55
Annual Index 2007	56

Front Cover Picture: The central region of the Orion Nebula (M42, NGC 1976) is shown in the near-infrared from three HAWK-I images taken during Science Verification. Three exposures of 600 s on a continuum filter centred at 1.58 μm (CH_4 band), on the H Brackett- γ emission line at 2.17 μm and on the rotational-vibrational H_2 line at 2.12 μm were combined (as blue, green and red respectively) to form the colour image. The bright star in the upper right corner is θ^1 Ori D, one of the Trapezium ionising cluster. Image processing by Monika Petr-Gotzens and Hans-Hermann Heyer (ESO).